Development of an Optimization Framework for the Design of High Speed Planing Craft

Author:
Mohamad Ayob, Ahmad Faisal

Publication Date:
2011

DOI:
https://doi.org/10.26190/unsworks/15702

DEVELOPMENT OF AN OPTIMIZATION FRAMEWORK FOR THE DESIGN OF HIGH SPEED PLANING CRAFT

Ahmad Faisal Mohamad Ayob

A thesis submitted in fulfilment
of the requirements for the degree of
Doctor of Philosophy

School of Engineering and Information Technology
University College
University of New South Wales
Australian Defence Force Academy

July 2011

COPYRIGHT STATEMENT

'I hereby grant the University of New South Wales or its agents the right to archive and to make available my thesis or dissertation in whole or part in the University libraries in all forms of media, now or here after known, subject to the provisions of the Copyright Act 1968. I retain all proprietary rights, such as patent rights. I also retain the right to use in future works (such as articles or books) all or part of this thesis or dissertation.
I also authorise University Microfilms to use the 350 word abstract of my thesis in Dissertation Abstract International (this is applicable to doctoral theses only).
I have either used no substantial portions of copyright material in my thesis or I have obtained permission to use copyright material; where permission has not been granted I have applied/will apply for a partial restriction of the digital copy of my thesis or dissertation.'

Signed ....

Date ......14/11/2011..

AUTHENTICITY STATEMENT

'I certify that the Library deposit digital copy is a direct equivalent of the final officially approved version of my thesis. No emendation of content has occurred and if there are any minor variations in formatting, they are the result of the conversion to digital format.'

Signed ....

Date ......14/11/2011..

ORIGINALITY STATEMENT

I hereby declare that this submission is my own work and to the best of my knowledge it contains no material previously published or written by another person, or substantial portions of material which have been accepted for the award of any other degree or diploma at UNSW or any other educational institute, except where due acknowledgment is made in the thesis. Any contribution made to the research by others, with whom I have worked at UNSW or elsewhere, is explicitly acknowledged in the thesis. I also declare that the intellectual content of this thesis is the product of my own work, except to the extent that assistance from others in the project's design and conception or in style, presentation and linguistic expression is acknowledged.

Signed ....

Date 13/11/2011

Abstract

High speed planing craft play key roles in supporting several critical maritime activities, such as coastal surveillance, reconnaissance, life-saving operations, passenger and high value cargo transport. Despite their significant use, formal optimization frameworks have rarely been proposed to deal with their design challenges. In this thesis, an optimization framework for the preliminary design of high speed planing craft is presented. Several case studies of single and multi-objective formulations of the high speed planing craft design problem are solved using state-of-the-art optimization algorithms. The notion of *scenario-based* design optimization and *innovization*, i.e. a means to uncover design relations are also discussed.

Traditionally, ship design activity took the form of an iterative process called *design spiral*. The iterative steps in the ship design spiral provided the ship designers with a method for obtaining *feasible* candidate designs. However it failed to guarantee identification of near *optimum* candidate designs. Later, with the availability of efficient optimization methods, designers had an option to identify near optimum designs, rather than simply feasible designs. Since then, the development of design optimization frameworks for displacement craft have received a significant amount of attention among researchers due to the availability of standard naval architectural tools and the demand to produce designs that minimize the use of resources in competitive environments. However, despite the significant importance of high speed planing craft, there has been little advancement towards the development of such optimization frameworks for the design of high speed craft. Therefore, the development of an optimization framework for the design of high speed planing craft is set as the core of this thesis.

A modular, extensible state-of-the art design optimization framework for use

in concept and preliminary design stage is proposed in this thesis. This is to ensure that the analysis tools can be extended or replaced with the desired level of complexity or with the state-of-the-art analysis tools when it is available. A 3D hull form representation combined with empirical estimates for analysis is used in this work. The use of global parametric transformation that preserves surface fairness and allows for the presence of curve discontinuities (i.e. hard chines or knuckles) is incorporated. A suite of three state-of-the-art optimization algorithms, namely Non-dominated Sorting Genetic Algorithm (NSGA-II), Infeasibility Driven Evolutionary Algorithm (IDEA) and Surrogate Assisted Evolutionary Algorithm (SA-EA) is incorporated within the framework. The performance of the algorithms are compared using the case studies.

Several case studies consisting of single- and multi-objective hull form resistance minimization problems are discussed. Starting with a basis ship, solutions to single-objective calm water resistance minimization, minimization of resistance in a seaway and multi-objective formulations considering minimization of total resistance, minimization of vertical impact acceleration and minimization of steady turning diameter have been presented in this thesis. In this thesis, the capability of the proposed framework to capture design trade-offs is illustrated. In addition, the case studies are extended to provide for *scenario-based* hydrodynamic design optimization in order to demonstrate the capability of the proposed framework to solve optimization problems based on the ship's operational profile and operating conditions.

Finally, a concept of *innovization* is introduced. It allows for the automatic discovery of design rules governing optimum hull forms. Furthermore, the relationship gathered through the process of innovization is applied as a cheap *pseudo-performance* indicator within an optimization formulation. The results compare favourably between the relationship derived from innovization and the empirical estimate obtained from experimental data. Such extensions are new contributions to the ship design discipline, which enable fast distillation of design rationales from a pool of optimized candidate ship designs. This finding opens up the possibility of the development of optimum design rules for any particular ship class.

Acknowledgments

Design is not what it looks like. Design is how it works.

~ Steve Jobs (1955-2011)

I must thank many people. This research would have not been possible without their support and encouragements.

Dr. Andrew Mason, Dr. Patrick Couser and Mr. Phillip Christensen from Formsys for allowing me to use Maxsurf as the platform for my PhD research; and for their great encouragements throughout the project.

My main supervisor, Dr. Tapabrata Ray, for his experience; for stimulating discussions and comments; for answering a million questions; for his exceptional pursuit for excellence; and for his patience on guiding me throughout the research. My co-supervisor, Dr. Warren Smith, for pointing me to the overlooked spots in the work; for his fine eye for details; and for his contagious optimism to the people around him (especially his students). Mrs. Danica Robinson, for her satire and great company during the ups and downs of the life as a post-graduate student. Also thanks to Mrs. Denise Russell for her comments on the earlier manuscript.

To Amitay, Mahendra, Abhi, Khin, Khairul, Asaf, Sharif, Liu Min, Arif, Priyanka, Zaman, Baki, Vishal, Hawa, Miza, Shirly and others (you know who you are) for being such wonderful friends in ADFA. Special mentions are due to Hemant and Amit, we drank tea, fight fire (alarms) together with Vera, that later spun a memorable quote, 'you can be a distinguished professor, or a fire extinguisher'.

This thesis is dedicated to my wife, Dr. Siti Addis. We dream, plan and execute our plans together which means everything to me. My life is complete wherever, whenever I'm accompanied by her. I thank my parents, Mr. Mohamad Ayob Ahmad and Mrs. Asmah Harun for their love and blessings, and the loyal Brotherhood members for always being there for me.

List of Publications

Journal Papers

1. **Mohamad Ayob, A.F.**, Ray, T. and Smith, W.F., Beyond Hydrodynamic Design Optimization of Planing Craft. *Journal of Ship Production and Design*, Vol. 27, No. 1, February 2011, pp. 1–13.

2. **Mohamad Ayob, A.F.**, Ray, T. and Smith, W.F., Uncovering Secrets Behind Low-resistance Planing Craft Hull Forms Through Optimization. *Engineering Optimization*, Vol. 43, No. 11, November 2011, pp. 1161–1173.

3. **Mohamad Ayob, A.F.**, Ray, T. and Smith, W.F., A Hydrodynamic Preliminary Design Optimization Framework for High Speed Planing Craft. *Journal of Ship Research*, in press.

4. Khan, M.S., **Mohamad Ayob, A.F.**, Isaacs, A. and Ray, T., A Smart Repair Embedded Memetic Algorithm for 2D Shape Matching Problems. *Engineering Optimization*, in press.

Conference Papers

1. **Mohamad Ayob, A.F.**, Ray, T. and Smith, W.F., The Quest for Optimum High Speed Planing Craft Design. *Pacific 2012 International Maritime Conference (Pacific 2012)*, accepted.

2. Khan, M.S., **Mohamad Ayob, A.F.**, Isaacs, A. and Ray, T., A Novel Evolutionary Approach for 2-D Shape Matching Based on B-Spline Modelling. *IEEE Congress on Evolutionary Computation 2011 (CEC 2011)*, 2011.

3. **Mohamad Ayob, A.F.**, Ray, T. and Smith, W.F., Scenario-based Hydrodynamic Design Optimization of High Speed Planing Craft for Coastal Surveillance. *IEEE Congress on Evolutionary Computation 2011 (CEC 2011)*, 2011.

4. **Mohamad Ayob, A.F.**, Ray, T. and Smith, W.F., A Framework for Scenario- Based Hydrodynamic Design Optimization of Hard Chine Planing Craft. *9th International Conference in Computer and IT Applications in the Maritime Industries (COMPIT'10)*, 2010.

5. **Mohamad Ayob, A.F.**, Ray, T. and Smith, W.F., Hydrodynamic Design Optimization of a Hard Chine Planing Craft for Coastal Surveillance. *Pacific 2010 International Maritime Conference (Pacific 2010)*, 2010.

6. **Mohamad Ayob, A.F.**, Ray, T. and Smith, W.F., An Optimization Framework for the Design of Planing Craft. *International Conference on Computer Applications in Shipbuilding 2009 (ICCAS09)*, 2009.

Contents

List of Figures

List of Tables

List of Algorithms

Nomenclature

3D	Three Dimensional
API	Application Programming Interface
B	Beam
b_{ij}	Corresponding powers of the design rules, ϕ_j
c_b	Block coefficient
c_i	Proportionality constant
c_p	Prismatic coefficient
c_m	Midship coefficient
c_wp	Waterplane coefficient
c_v	Speed coefficient
c_δ	Static beam-loading coefficient
BC	Before Century
CAD	Computer Aided Design
CFD	Computational Fluid Dynamics
COM	Component Object Model
DACE	Design and Analysis of Computer Experiments
Δ	Displacement (kg)
δ	Deadrise angle (^{o})
δ_r	Rudder deflection angle (^{o})
DPSO	Deterministic Particle Swarm Optimization
DGL	Design Geometry Library
η	Vertical impact acceleration (g above static)
FC	Fuel Consumption
FEA	Finite Element Analysis
FFD	Free-Form Deformation
Fn	Froude number
F_∇	Volumetric Froude number
g	Gravitational Acceleration (ms^{-2})
GM	Metacentric height (m)
$H_{1/3}$	Significant wave height (m)
IDEA	Infeasibility Driven Evolutionary Algorithm
Ie	Half angle of entrance at bow (^{o})

IFC	Indian Fast Craft
L	Length
LCB	Longitudinal Center of Buoyancy
LCG	Longitudinal Center of Gravity
MSE	Mean Squared Error
NAVSEA	Naval Sea Systems Command, United States Navy
NSGA-II	Non-dominated Sorting Genetic Algorithm II
NURBS	Non-Uniform Rational B-splines
NPVI	Net Present Value Index
OPV	Offshore Patrol Vessel
P_E	Effective Power
P_T	Thrust Power
PT	Patrol Torpedo
USCG	United States Coast Guard
WPB	W (designation code) Patrol Boat
RPO	Resistance Prediction and Optimization
ϕ_j	Design rule for innovization
R_A	Added resistance in a seaway
R_C	Calm water resistance
R_L	Total resistance in a lifetime operation
R_T	Total resistance in a seaway
r_{LB}	Length-Beam relationship
r_{LT}	Length-Draft relationship
r_{BT}	Beam-Draft relationship
r_{LBT}	Length-Beam-Draft relationship
RSM	Response Surface Method
$ORSM$	Ordinary Response Surface Method
RBF	Radial Basis Function
$ORBF$	Ordinary Radial Basis Function
SA-EA	Surrogate Assisted Evolutionary Algorithm
SD	Standard Deviation
sfc	Specific Fuel Consumption
SRB	Surf Rescue Boat
STD	Steady Turning Diameter (m)
SUMT	Sequential Unconstrained Optimization Technique
SWATH	Small Waterplane Area Twin Hull
T	Draft
τ	Running trim angle (^{o})
VCG	Vertical Center of Gravity

VESPA	Virtual Evolution based Sailing Performance Analysis
∇	Volumetric displacement (m^3)
V	Speed (ms^{-1})
V_k	Speed (knots)
VBA	Visual Basic for Application
w	Water density
WSA	Wetted Surface Area (m^2)
XML	Extensible Markup Language

Chapter 1

Introduction

1.1 Evolution of Ship Design

More than 70% of the Earth is covered by water. Ever since humans uncovered the principles of buoyancy, moving from place to place using flotation attracted serious attention and exploitation. More than 10,000 years ago, humans found ways to refine the shapes of floating logs which resulted in the construction of canoes. Later, rafts were created by joining a number of logs together which allowed for a greater payload. The design of vessels using the assembly of wooden planks to construct a hull form was perfected by the ancient Egyptians around 3000 BC. The Greeks, Swahilis and Chinese made use of their uniquely designed ships to discover new lands, engage in trade and establish dominance. Ship design and building activities have spanned time with unique designs evolving in different parts of the world. The Romans, Vikings, English, Spanish and Japanese built different styles of fleets. Their various designs evolved slowly and characterized as being more an art, than a science.

Today, the ship design process has evolved to a well structured science-based discipline. Evans [3] introduced a formal model of the ship design process i.e.

the ship *design spiral* in 1959, which captured the basic principles in designing a ship using an iterative process. It follows that ships are designed based on providing functional capability (e.g. transport, military, recreation, etc.) while satisfying the set of constraints arising from statutory requirements, physical laws etc. Several enhancements have been introduced to the spiral, including the inclusion of time and economic dimensions. However, the ship design spiral approach results in a feasible design and not necessarily an *optimum*[1]. A shift from *sequential and iterative* (i.e. design spiral) to *simultaneous* considerations of the performance indicators was proposed by Lyon and Mistree [4] through the incorporation of optimization techniques. Such a shift in design practice provided an opportunity for ship designers to produce near *optimum*, rather than simply feasible designs.

While the mathematical models are inexact even with the best/most appropriate performance indicators, their combination with good optimization solvers offer the potential of identifying designs that are of great use in the concept and preliminary design stage.

1.2 Existing Problems (Motivation of Work in Thesis)

Ship types can be generalized by their operational mode, with one such classification being the way in which vessels are physically supported. The categories include the displacement craft and planing craft as shown in Figure 1.1. The majority of ships at sea are of the displacement type, in which the full load

[1]The words 'optimum design', used in this thesis refer to 'the best final design' relevant to the mathematical model and its variables and constraints in the optimization formulation.

is balanced by buoyancy forces (e.g. cargo ships, landing craft and transport ferries). In contrast, planing craft operation is made possible by a combination of buoyancy and hydrodynamic lift. In the literature, planing craft are sometimes perceived as 'flying craft' due to their ability to plane on the water's surface [5]. Colloquial names for planing craft include 'Mosquito Fleet' and 'Devil Boats' due to their ability to move fast, maneuver quickly and maintain speed in various sea conditions. Since the 1930s, there has been significant interest in building planing craft and, in particular Patrol Torpedo (PT) boats [6] and fast recreational craft. However, rigorous research into planing craft design only occurred in the 1970s [7].

(a) Typical Container Vessel

(b) USS PT-105 Patrol Torpedo Craft

FIGURE 1.1: EXAMPLES OF DISPLACEMENT CONTAINER SHIP AND HIGH SPEED PLANING VESSELS

The development of design optimization frameworks for displacement craft has received a significant amount of attention among researchers. Factors contributing towards such efforts include the availability of standard naval architectural tools and the demand for producing designs that minimize the use of resources in competitive environments (e.g. fuel and building costs etc.). Although significant literature has been produced on displacement craft designs, there is a lack of it in the domain of high speed planing craft. High speed planing vessels such as the

United States Coast Guard patrol craft and surf rescue boats are important for protecting coastal waters and performing life-saving operations. In contributing to this area, the key questions addressed in this work are: (i) how to develop an optimization framework for the design of high speed planing craft using the available naval architectural tools?; (ii) with the potential of such a design optimization framework, how can various forms of the optimization problem be modeled and explored (e.g. for different operational profiles)?; and (iii) finally, what is there beyond hydrodynamic design optimization of high speed planing craft, i.e. how can the results of optimization be used for the generation of new design rules?

Presented in this thesis is an optimization framework for the design of high speed planing craft. Unlike past attempts which tend to optimize the principal dimensions and form coefficients, complete geometry is modeled in this work. Experimentally derived empirical relationships are incorporated to identify the high speed planing craft designs with good performance. Such an approach allows for the generation of valid candidate designs. The underlying geometry of the vessel is optimized using state-of-the-art optimization methods that allow for the solution of problems involving highly non-linear constraints and objectives.

Placing this work in context, an inquest into the incident off Christmas Island, Australia that resulted in the deaths of 30 asylum seekers in December 2010, concluded that 'the life-saving rescue vessels designed are not capable of being operated in adverse weather' [8]. This incident sparked the initiative to investigate whether the design of high speed planing craft should be optimized with operational scenarios in mind, rather than only optimizing for calm water and single-speed operation. Therefore, the development of a design optimization framework capable of handling various analysis with varying fidelity is valuable and timely for the high speed craft design domain.

1.3 Scope of Research

The aim of this research is to present an optimization framework for the design of high speed planing craft. The following four aspects define its scope.

1. The research is focused on the design of high speed planing craft in the concept or preliminary design stages.

2. The study covers a class of planing craft with hard chines and transom sterns.

3. Validation ranges are enforced, in terms of several principal parameter ratios relevant to the applied performance prediction algorithms in order to ensure the optimized candidate designs are valid.

4. The proposed framework allows for analysis modules to be included using a component object model (COM[2]) interface. Higher fidelity analysis such as structural finite element analysis (FEA) or computational fluid dynamics (CFD) could be included to extend the framework's capabilities.

1.4 Contributions of Thesis

In this thesis, the following five significant contributions are made.

1. A three-dimensional mathematical model to represent the complete geometry of a high speed planing craft using B-spline method and experimentally

[2]Details of the COM interface are elaborated in Chapter 3

derived naval architectural tools is introduced. This model compares favorably with data published in the literature.

2. The proposal incorporates a COM interface within the design framework. A workflow example is demonstrated using a number of analysis tools seamlessly coupled within the proposed optimization framework. Furthermore, the framework allows for the extension of analysis modules of varying fidelity on top of a standard interface.

3. The possible uses of optimization for high speed planing craft design is thoroughly explored in this thesis. Optimization problems based on operational scenarios are explored, referred to as *scenario-based* hydrodynamic design optimization. Such provisions provide unlimited possibilities for creating innovative designs for specialized missions of high speed planing craft.

4. The next contribution relates to the comparison of performance of different optimization algorithms in solving ship design optimization problems. Since it is known that there is no 'one-size-fits-all' algorithm for solving optimization problems [9], a real-coded evolutionary algorithm, an infeasibility-driven evolutionary algorithm and a surrogate-assisted evolutionary algorithm are utilized and the performance of the candidate designs obtained from them are compared within the proposed framework.

5. Finally, the proposed framework contributes to the search for optimum high speed planing craft designs. The work contributes to both single-objective and multi-objective design optimization. Furthermore, a preliminary investigation into what is beyond hydrodynamic design optimization using the *innovization*[3] principle is presented. The usage of innovization helps

[3] The principle of innovization is introduced in Chapter 6.

to uncover the secrets behind optimum planing craft designs and opens a possibility of the development of optimum design rules for any particular class of ship.

1.5 Organization of Thesis

In this introductory chapter, the background to, motivation for, scope of research and contributions of this research are established. Following this chapter, the thesis is divided into six further chapters.

Chapter 2 is dedicated to a literature review. The literature review identified a few significant gaps in the existing works. Hull form representation and form variational approaches adopted by several ship design optimization frameworks are discussed. An observation regarding scenario considerations (e.g. operational profile) in design optimization is made. Finally, features of several existing naval architectural tools are discussed. In each following chapter, additional related literature is referenced to supply readers with further relevant knowledge.

In Chapter 3, an optimization framework for the design of high speed planing craft is proposed. Shape representation and surface information retrieval using a B-spline method are presented followed by some demonstrations using several various hull shapes. Thereafter, the mathematical model of the hydrodynamic design of a high speed planing craft is presented. Later, the solution methodology using a library of optimization algorithms is elaborated. The module-based approach incorporated in this proposed framework is described, followed by a discussion of the limitations that exist within the scope of this research.

In Chapter 4, resistance minimization case studies involving two planing craft are presented. The vessels used for the case studies are a 10m planing craft known as the Indian Fast Craft (IFC) and a 32m United States Coast Guard WPB-110ft (WPB-110ft)[4] craft. The capability of the proposed framework to solve calm water resistance minimization is discussed. Then, minimization of resistance in a seaway for both craft are presented.

In Chapter 5, a scenario-based hydrodynamic design optimization of high speed planing craft is introduced. Unique scenarios with respect to the vessel's responsibilities are presented using the example of IFC and WPB-110ft craft. Hydrodynamic design optimization using varying operational profiles, high speed intercepts and fast rescue missions are demonstrated to highlight the capability of the proposed framework to handle such formulations.

In Chapter 6, the topic of what is beyond hydrodynamic design optimization is discussed. A concept called *innovization* is introduced. Using a pool of optimized candidate designs, a pseudo-performance relationship is derived and incorporated in an optimization formulation. Analysis of the optimized candidate designs are performed to provide some indicators of the factors that drive the process towards an optimized candidate design.

Finally in Chapter 7, a summary and outcomes of the thesis are presented. Its achievements, together with several potential areas for further research in this domain, are listed.

[4] Based on the Coast Guard history record [10], in 1940's the USCG adopted the Navy's ship classification system whereby a vessel was designated with a two-letter abbreviation based on the type of ship and its hull number. While "PB" stands for Patrol Boat, no one knows for sure why the Navy and Coast Guard picked the letter "W" to designate a Coast Guard vessel although rumors abound. In any case, the practice stuck and each cutter still bears the "W".

1.6 Related Publications

Parts of this thesis work have been published in A-ranked Excellence in Research for Australia (ERA) journal publications and major refereed-conferences on ship design and maritime research. Below are some related publications:
Related publications for Chapter 3 and Chapter 4 include:

- Mohamad Ayob, A.F., Ray, T. and Smith, W.F., A Hydrodynamic Preliminary Design Optimization Framework for High Speed Planing Craft. *Journal of Ship Research*, 2011, in press.

- Mohamad Ayob, A.F., Ray, T. and Smith, W.F., Hydrodynamic Design Optimization of a Hard Chine Planing Craft for Coastal Surveillance. *Pacific 2010 International Maritime Conference (Pacific 2010)*, 2010.

- Mohamad Ayob, A.F., Ray, T. and Smith, W.F., An Optimization Framework for the Design of Planing Craft. *International Conference on Computer Applications in Shipbuilding 2009 (ICCAS09)*, 2009.

Related publications for Chapter 5 include:

- Mohamad Ayob, A.F., Ray, T. and Smith, W.F., Scenario-based Hydrodynamic Design Optimization of High Speed Planing Craft for Coastal Surveillance. *IEEE Congress on Evolutionary Computation 2011 (CEC 2011)*, 2011.

- Mohamad Ayob, A.F., Ray, T. and Smith, W.F., A Framework for Scenario-Based Hydrodynamic Design Optimization of Hard Chine Planing Craft. *9th International Conference in Computer and IT Applications in the Maritime Industries (COMPIT'10)*, 2010.

Related publications for Chapter 6 include:

- Mohamad Ayob, A.F., Ray, T. and Smith, W.F., Beyond Hydrodynamic Design Optimization of Planing Craft. *Journal of Ship Production and Design*, Vol. 27, No. 1, February 2011, pp. 1–13.
- Mohamad Ayob, A.F., Ray, T. and Smith, W.F., Uncovering Secrets Behind Low-resistance Planing Craft Hull Forms Through Optimization. *Engineering Optimization*, Vol. 43, No. 11, November 2011, pp. 1161–1173.

Chapter 2

Literature review

Abstract

The state-of-the-art in ship design optimization is reviewed in this chapter. Through the discussion, the reader will be exposed to the available shape representation and modeling approaches available in computer aided ship hull design, ship design optimization, operational scenario modeling in optimization and the existing performance prediction tools in ship design. Drawn from this study, a few important gaps in the literature are addressed, leading to a set of problem formulations that motivated the research work reported in this thesis.

2.1 3D Shape Representation in Computer Aided Ship Hull Design

2.1.1 Hull Form Representation and Design

Before the introduction of desktop computers and computer-aided design (CAD) tools, *mathematical representation* methods for generating a hull form surface geometry were not popular among ship designers [11]. Practical drafting methods using a batten and weights to physically construct the shape of a line was the dominant approach. However, some work on virtual (as opposed to physical) representations of hull forms dates back to the 1770's with Fredrik Henrik af Chapman [12]. Nevertheless, the importance of a mathematical representation of a hull form lies in its capability to analyze the hydrostatic and hydrodynamic characteristics data required prior to shipbuilding. In 1915 Taylor [13] published a series of hull forms based on a parent ship using a polynomial approach. His work, commonly known as the Taylor Series Hull, allowed resistance estimations to be carried out using different form parameters, such as the slenderness ratio, beam to draft ratio and prismatic coefficient. Interest in extending this polynomial technique [14] and conformal mapping [15] began to increase due to their capabilities to evaluate the resistance and seakeeping performance of a ship while, at the same time, being able to define and represent the hull form itself. Similarly, the growth in visualization and computational capabilities have made computer graphics valuable in aiding ship designers to manipulate the surface geometry of a candidate ship [11].

Benson's [14] work on the polynomial representation of hull form geometry appeared in the 1940s at about the same time as interest in the mathematical representation of surface geometry in the automotive industry, initiated by de Casteljau [16] and later extended by Bézier [17, 18] (now known as the Bézier curves and surfaces), emerged. Gordon and Riesenfield [19] showed that B-spline curves are a generalization of the Bézier curves. B-spline curves overcome the stability limitations in terms of the local control and the degree of curves [20]. Both representation methods (Bézier and B-spline) contribute to high flexibility in free-form design through the use of *control polygon nets/control points*. Using them, the application of weights and battens could be virtually emulated in the design of ship geometries. Later computer aided design (CAD) tools incorporating Bézier and B-splines curves and surfaces were quickly adapted in the ship design domain. The implementation of interactive designs and modifications of ship hulls, which were analogous to using battens and weights was demonstrated by Rogers and Satterfield [21] in the 1980s using control dials and a computer terminal. Their work showed that the B-spline curves and surfaces are convenient and intuitive when applied to performance evaluations, practical ship design and the modeling of an automated manufacturing process [22].

Harries *et al.* [23] and Abt and Harries [24] highlighted that the capability to design and modify ship hulls in the preliminary design stage using CAD tools can be generalized to three types, namely, conventional CAD modeling, full parametric modeling and partial parametric modeling. While conventional and full parametric modeling are two different methods, partial parametric modeling overlaps both, as visualized in Figure 2.1. The advantages and limitations of these modeling approaches are discussed in the following sections.

2.1.2 Conventional CAD Modeling

Traditionally, ship designers used weights and a batten to generate a 2D curve. With the advent of computers, the analogy of weights and a batten are used through the manipulation of 2D control points, to generate a virtual hull form's curve. A collection of 2D control point sets results in a 3D control polygon net that can be used to control the surface deformation of a hull form. Rogers and Satterfield [21] and Rogers *et al.* [22] used a control polygon net to manipulate a single surface to represent a hull form using the B-spline method. Starting from a rectangular surface, a ship-like hull form was constructed by moving the control points manually in the 3D design space.

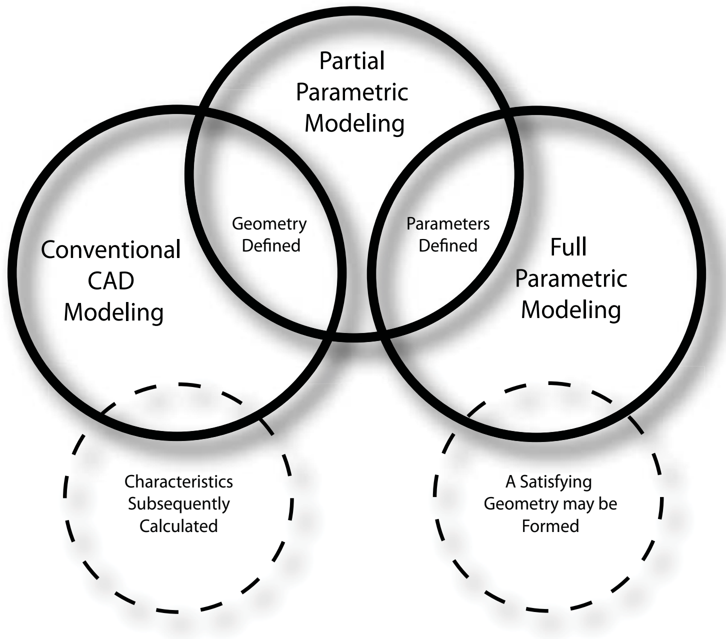

Figure 2.1: 3D CAD ship hull form modeling approach

Conventional manual modeling of surface data offers a high degree of freedom for ship designers to manipulate a hull shape. However, this process is tedious as surface fairness problems (e.g. waviness or irregularities) are easily introduced with irregular locations of control points, especially when handled by a non-experienced ship designer. It requires considerable effort to reflect surface fairness, and specific know-how on various shapes and characteristics of hull forms [24]. Consequently, this renders the method to be time-expensive and hard to apply when many alternative designs are to be considered.

2.1.3 Full Parametric CAD Modeling

In contrast to conventional 3D CAD modeling, full parametric CAD modeling allows ship designers to create new candidate geometries without manually manipulating the control points of the 3D ship hull form geometry. This paradigm comes from the desire to generate a model based on a set of parameters and form coefficients (e.g. L, B c_b and c_p of a hull form) associated with, but not controlled by the geometry. Consequently, a family of objects or *primitives* is defined. The advantage of full parametric CAD modeling is that it allows for the *automatic design* of engineering artifacts [25]. For the design of destroyer-type hulls, Taggart and Magnusson highlighted that the full parametric modeling method offers a direct relation between the functional characteristics and the hull geometry [26]. Several other implementations of full parametric CAD modeling can be seen in the works of [27, 11, 28] on yacht and Ro-Ro, fleet tanker [29] and frigate [28] designs.

However, the full parametric CAD modeling method is unfavorable to ship designers due to its associated complex mathematics involved [30] and the difficulty of writing algorithms to represent different hull type geometries [31]. A considerable amount of family-specific information/rulings has to be built into the algorithms [32]. Each generic primitive must be treated as a special case, with no uniform overall treatment allowed.

2.1.4 Partial Parametric Modeling

Partial parametric modeling combines a set of defining points (e.g. control points or offsets) and parametric information to represent a ship hull [33]. It serves as an ideal method in a situation in which new candidate designs are derived from a parent hull. It has a parallel with a 'basis ship approach', in which by using both the parent ship's hull shape and the parametric information, an 'adaptive/variant'[1] design can be produced.

[1]Mistree *et al.* [34] identified three different types of design, namely, original, adaptive and variant. The distinction among them is based on the amount of originality exercised during the design phase.

Innovative new designs within a class can emerge from the usage of partial parametric modeling as this method simultaneously considers both the parametric information and the 3D surface geometry of a candidate design in the early design stage. Creautz [35] and Bardis and Vafiadou [36] demonstrated the creation of new designs through the combination of form parameters and interactive manipulations of B-spline surfaces. Campana *et al.* [37] and Pinto *et al.* [38] used a number of Bézier patches on an available target surface data set to generate a basis hull complemented by its parent hull's form parameters. Partial parametric modeling also allows for the reverse-engineering of a well-performing parent hull form as a design starting point or *basis ship*, which can be used as a setting stone towards the generation of superior candidate designs by further virtual modification in the design space.

The knowledge on reverse-engineering a hull form using partial parametric modeling is much more useful when combined with a method for developing new variants based on the basis hull. Doctors [39] proposed a *hull blending* technique for creating new hull variants. The method involves the application of a library of previously designed hulls to generate new candidate hulls through a merging process. A new hull can be obtained by linearly superimposing a pair of parent hulls using a *blending factor* which serves as the weight of inheritance between the distinct characteristics of the parent hulls. However, the shape of the resulting candidate hull is not easy to determine or control. Lackenby [40] proposed the use of a linear parametric transformation method for modifying the lines plan while matching the required values of the longitudinal center of buoyancy, LCB and the prismatic coefficient, c_p using a set of known offsets to generate a new variant hull. Söding and Rabien [41] presented a method for creating hull variations using transformation functions that can be controlled using cubic splines and piecewise polynomials of various degrees. Hoekstra and Raven [42] used global and local volume deformation methods by defining a box around the part of the hull that was to be interactively modified. Mason [43] combined Lackenby's [40] approach with a Free-Form Deformation (FFD) technique [44] and B-spline surfaces to parametrically transform the basis ship to achieve the desired principal parameters and form coefficients. Other than linear transformation, manipulation of the control polygon net to create new hull variants based on the desired parametric changes has also been demonstrated in the literature. Peri and Campana [45] presented a control points perturbation of Bézier patches that defines a naval surface combatant in a design optimization problem. Realistic hull shape deformation can be achieved at a computational cost by introducing additional variables and boundary constraints in this formulation.

The combination of the ship's geometry representation and the form parameter variation method is powerful in terms of generating new designs based on a basis ship. It allows for progression of improvements where the ship designers are given a set of parametric information for comparison [33], rather than continuously generating new hulls with no previous reference. Improvements in candidate design's performance can be achieved iteratively or concurrently.

2.2 Towards Ship Design Optimization

2.2.1 Ship Design Spiral

In conventional ship design, the process takes a form that was earlier called the *general design diagram* and is now known as the *design spiral* – an iterative ship design process that allows for an increase in complexity and precision across the design cycle. Significant contributions through the visualization and modeling of this process can be found in the work of Evans [3]. The ship design spiral combines synthesis (e.g. hull geometry and arrangement) and analysis (e.g. resistance, stability and seakeeping) in its sequential process. Its generic form is shown in Figure 2.2. The definition of mission requirements starts the sequential process and is followed by determination of the generic proportions (e.g. the principal dimensions of the hull and its ratios), preliminary powering, determination of suitable hull geometry/preliminary lines, hydrostatics and bonjeans. Further analysis follows. As the cycle is completed, the design step/stage is incremented to a more detailed form (e.g. from the concept to preliminary design stage).

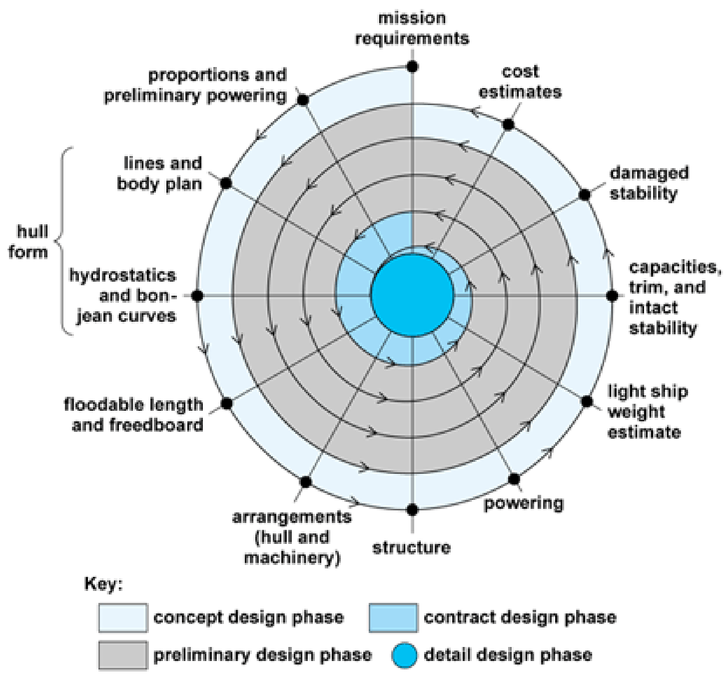

FIGURE 2.2: A GENERIC SHIP DESIGN SPIRAL DIAGRAM [1]

Refinements have been made to the design spiral, such as economic aspects being introduced into it by Buxton [46]. Andrews [47] introduced time aspects in the design spiral and his model became known as a helical ‘corkscrew’. The design spiral provides a *safe template* for producing a satisfactory hull for which the designs *evolve* over time. Although the Evans-Buxton-Andrews ship design spiral is able to capture the iterative practice and necessary elements in the ship design discipline, it is inefficient for handling complex simultaneous design changes, especially when later variable changes affect the ship's performance characteristics evaluated in earlier stages [48]. Mistree *et al.* [34] commented that, although the spiral approach may result in *satisfactory* designs, it does not promote the identification of *superior* solutions. The distinction here is between a design that is feasible and one that approaches optimality.

2.2.2 Ship Design Optimization

Prior to 1990, a significant amount of work conducted on ship design optimization was documented. Lyon and Mistree [4] and Smith and Woodhead [49] incorporated linear programming (LP) to solve ship design optimization that included structural problems. The use of non-linear programming was demonstrated by Moe and Gisvold [50], Moe and Lund [51], Nowacki *et al.* [52], Pal [53] and Lutkus *et al.* [54] using sequential unconstrained optimization technique (SUMT). Other optimization methods include Hooke and Jeeves [55] with penalty function [56], parametric study [57], simulated annealing [58, 59] and convergent random search technique [60]. The ship design optimization problems presented include structural optimization, transportation system optimization, construction cost and minimization of drag. Ship design optimization works before 1990 successfully demonstrated the use of empirical relations in which the full form surface geometry of the ship remained unknown, except for the principal parameters, form coefficients and performance characteristics information obtained following optimization.

In the early 1990s, the development of ship design optimization methods that combined analytical estimates, such as computational fluid dynamics (CFD), with full hull form geometry are observed. Motivation towards the inclusion of full hull geometry was driven by the advancements of CFD in the domain of ship design optimization. Janson [61] and Janson *et al.* [62] demonstrated calm water resistance minimization using standard Wigley and Series 60 hulls, where the offset data were treated as free variables. Maisonneuve [63] presented a small waterplane area twin hull (SWATH) optimization using sequential quadratic programming (SQP), in which the offset data of the ship was represented by spline curves. Although CFD requires the full geometry of a ship , using it within an optimization algorithm comes at a high computational cost and the final hull generated might be impractical due to substantial waviness [33]. However, utilizing full hull geometry in optimization is not limited to CFD as empirical relations can also be incorporated. Ganesan [64] proposed an optimization framework for a container ship using a hull blending technique following the work of Doctors [39].

The majority of the work discussed above is focused on the design of container ships, transport ferries, surface combatants, etc., which are displacement ships. However, the use of both empirical relations/analytical methods and optimization algorithms could be beneficial for the design of both *displacement vessels* and high speed *planing craft*. In the following paragraphs, these observations are further elaborated.

The displacement ship is a widely used type of vessel in applications such as bulk transportation, passenger ferries, fishing vessels and recreational craft. Due to its extensive application, there are a significant number of optimization frameworks for the design of such vessels such as the works of Ray [59] and Ganesan [64] on container ships, Smith [65] on destroyer frigates, Peacock [30] on Offshore Patrol Vessel (OPV) and Gammon [66] and Majumder *et al.* [67] on fishing vessels. The application of genetic algorithms for fast displacement craft resistance minimization with a first principle parameters technique and Mitchell thin ship theory has been demonstrated by Day and Doctors [68]. Examples of the application of genetic algorithms for displacement craft optimization can be seen in the work of Dejhalla [69, 70]. Also, more recent studies from 2000 until 2010, on displacement craft optimization can be found in the literature, e.g. [71, 72, 73, 43, 74, 75, 76, 42, 77].

In contrast, although high speed planing vessels are popular as commercial and recreational craft, and widely used for life-saving, coastal patrol and surveillance missions, much information about them has been kept proprietary. As a result, there is only a small number of case studies available in the literature[2]. Some earlier research includes the work of Almeter [78], in which resistance optimization of the Soviet's BK and MBK planing hulls was performed using Resistance Prediction and Optimization (RPO) software via a database of varied planing hulls. Jons *et al.* [79] presented an integrated CAD process that employed a comprehensive design geometry library (DGL) to satisfy the design goals required by the customer. Although using a database of various hulls is helpful, it can be argued that, given a parent hull as a starting point for resistance minimization, a comprehensive database is not necessarily important if the parametric transformation method driven by an optimization algorithm is applied. Bearing in mind such a paradigm, a high speed planing craft optimization framework was proposed by Mohamad *et al.*[3] [80, 81, 82] that include the use of Savitsky's [83]

[2] Clark *et al.* [7] highlighted that the aggressive and successful planing hull research program initiated in the early 1970s subsided in the late 1970s when the US Navy decided to concentrate on the acquisition of large combatants capable of transiting the world's oceans.

[3] The literatures cited are the works of the author, conducted in the University of New South Wales at the Australian Defence Force Academy, Australia.

equation. Bertram [84] argued that, although the classical Savitsky's empirical resistance estimation method remains popular, real planing hull geometries violate the inherent assumptions of Savitky's approach, e.g. that concerning constant deadrise over the length of the hull. However, it has been shown in Chapter 3 of this thesis that, through the use of such empirical relations, very small discrepancies ($\leq 5\%$) between the modeled hull and the real ship (USCG WPB-110ft) in terms of resistance values are observed. Nagai and Yoshida [85] demonstrated the minimization of calm water resistance of a planing hull using a SUMT method while restricting the maximum trim angle change. Using the same algorithm, Herrington and Latorre [86] performed structural optimization with the reduction in weight of a 40m length high speed planing craft that operated at 35 to 40 knots.

2.2.3 Seakeeping Considerations in Ship Design Optimization

Success in minimizing resistance using optimization algorithms has brought forward attempts to include seakeeping estimations in optimization problem formulations. Pinto *et al.* [38] incorporated a deterministic particle swarm optimization (DPSO) technique in solving shape optimization problem to reduce the heave and pitch motion peaks of the response amplitude operator of a container ship. Grigoropoulos [72] presented seakeeping optimization of a modern destroyer and a reefer followed by manual local modifications of the candidate hulls to reduce calm water resistance. Grigoropoulos and Chalkias [71] later extended this work (in 2010) to include dual-objective optimization of wave loads and vertical acceleration at bow.

The seakeeping optimization of displacement craft presented above uses strip theory [87, 88] to predict ship motions in the concept or preliminary design stages. This method has been widely used in estimations of the seakeeping performance for displacement craft. However, despite its wide application for various craft designs, results gathered by White and Savitsky [89] on a tank test of two United States Coast Guard planing craft suggested that the seakeeping results obtained from displacement craft estimation tools should not be used to compare between a pool of competing high speed planing craft designs. This was further supported by Lahtiharju *et al.* [90] and Barry *et al.* [91] where Zarnick's [92, 93] strip theory is used. They concluded that, with a lack of tank test data, approximations of some important coefficients in the analytical equation need to be further justified. Savitsky and Brown [94] derived reliable regression equations to evaluate planing craft seakeeping performance following the experimental work of Fridsma [95]. An elaboration on these procedures in terms of designing a planing craft with superior performance in a seaway operation are further discussed in the work of Savitsky and Koelbel [2].

2.2.4 Operational Profile Inclusion in Ship Design Optimization

A ship is designed to be operated based on its required operational profile. Several operational scenarios that include seaway conditions, survivability, energy consumptions and emergency events can be simulated in the early design stage. There are a small number of articles in the literature that include operational scenario considerations in optimization apart from the advancements in resistance and seakeeping optimization research. The operating scenarios are derived from the required operational profile combined with the performance measure of the ship such as survivability [96, 97], fuel consumption [98] and electrical generation [99]. Scenario consideration based on required operational profile in optimization is referred to in this thesis as *scenario-based optimization*.

Boulougouris and Papanikolaou [96] proposed an optimization of the survivability of naval ships with respect to their operational profiles using a genetic algorithm. Akhil *et al.* [97] formulated an optimization problem for evading a hostile torpedo in order to enhance ship survivability, using several maneuvering strategies combined with single or multiple decoy deployments to increase the time at which the torpedo intercepts the ship.

Radan *et al.* [98] presented the minimization of diesel fuel consumption with respect to efficient use of power generation systems in a North Atlantic operation. This optimization suggested savings of up to 3.9% of fuel usage due to efficient start-stop criteria of prime movers. The Naval Sea Systems Command, United States Navy (NAVSEA) [99] demonstrated a considerable variance in performance of different power system options when endurance was measured in operationally different ways. Later, Doerry [100] extended the work of NAVSEA [99] and proposed a design process for optimizing the performance of an electrical warship in various wind and wave conditions.

Although increasing interest in including operational profiles in ship design optimization has been observed, these studies have been limited to minimizing fuel consumption and increasing the probability of survival. There is though a lack of consideration for changes in hull form geometry in these studies.

2.2.5 Existing Ship Design Software Tools

There are several standard naval architectural tools available to support hull form design activities as presented in Table 2.1. It can be observed that most of the ship design tools support B-spline or non-uniform rational B-splines (NURBS) modeling as the standard. In the scope of ship design optimization, there are two tools that are heavily incorporated in frameworks that aim to provide optimum designs namely; FRIENDSHIP-Framework and Maxsurf, which are capable of handling multiple integrations between in-house and/or commercial codes. Furthermore, both tools were developed with parametric variation and optimization in mind. Development of the prototype of FRIENDSHIP-framework can be seen in the work of Harries [33]. Mason and Thomas [43] developed the prototype Virtual Evolution based Sailing Performance Analysis (VESPA) that brought an integrated parametric transformation capability tightly into the Maxsurf suite. Koh *et al.* [76] and Grigoropoulos and Chalkias [71] took advantage of the FRIENDSHIP-Modeller (available in the FRIENDSHIP-Framework) and combined it with an optimization algorithm to solve displacement craft design optimization. Mohamad *et al.* [80, 82, 81] combined a library of optimization algorithms developed in the Matlab environment with Maxsurf to solve planing craft resistance optimization through the use of the Component Object Model (COM[4]) interface.

[4]The component object model (COM) is an interface standard that allows different softwares to communicate with each other. Its concept and implementation in this thesis are elaborated in Chapter 3.

TABLE 2.1: CAPABILITY COMPARISON BETWEEN SOME AVAILABLE TOOLS

Tools	License	Geometry Rep.	Para. transform	Integration	Built-in Opt. Algo.	Planing craft estimates
Aveva Marine	Fee	B-spline	√	×	×	×
FRIENDSHIP - framework	Fee	B-spline and NURBS	√	COM, XML, generic	√	CFD
Polycad	Free	B-spline and NURBS	√	×	×	×
Delftship	Free / Fee	Subdivision surface	√	×	×	×
Maxsurf	Free / Fee	B-spline and NURBS	√	COM	×	Savitsky, Savitsky - Mercier, Lahtiharju

2.3 SUMMARY

With the advent of computers, the use of weights and a batten to produce a physical model of a ship line has been replaced by mathematical representation methods that emulate physical tools. Therefore, a ship geometry can be constructed with varying levels of complexity in virtual environments. In general, there are three methods applied in computer-aided ship hull design, namely, conventional CAD modeling, full parametric CAD hull generation, and partial parametric modeling. The direct manipulation of surface geometry in conventional CAD modeling is time-expensive and requires a ship designer to have specific know-how (e.g. unique design features, hull surface properties etc.), where such knowledge are rare for an entry-level ship designer. A full parametric design relies on defining the principal parameters and form coefficients from which a matching ship hull geometry is then generated automatically. However, it requires a great deal of algorithmic work (e.g. introducing specific rulings, constraints, mathematical definitions) before an automated hull design process can be found. This is due to the non-uniqueness of the set of parameter values involved. In addition, a full parametric method does not allow for the inheritance of successive designs as it introduce only new hull form in each iteration. In contrast, partial parametric modeling provides a head start for ship designers by using a basis ship and its supplementary information. Then, the performance characteristics of the modeled and basis ship can be measured and compared.

Design optimization has been shown to be an efficient method in the search for *superior* designs, in contrast to the ship design spiral method that is capable of providing in principle only *satisfactory* (feasible) designs. Although the ship design spiral is able to capture the tenets and discipline involved for designing a ship, it offers only a sequential iterative method during the process. Therefore, as the design stage move to the next level, later modifications (e.g. to improve seakeeping performance) will likely affect the previous performance (e.g. worsen the resistance performance) of the craft. However, through the incorporation of optimization, the resistance and seakeeping considerations can be considered simultaneously.

Use of optimization methods for design of ships is now a well accepted norm. A significant number of works on the available optimization methods, case studies and frameworks have been observed. However, most of the effort displayed in the literature are focused on the design of displacement vessels. Although there are tools available that can be incorporated in the development of a high speed planing craft optimization framework, holistic models have not been created. Therefore, it is of interest in the context of this thesis to present a framework for hull form design optimization of high speed planing craft.

There is also significant amount of interest in incorporating scenario considerations in ship design optimization. Given a set of operational profile requirements, scenario-based design optimizations in the literature include those of electric generation and usage, survivability and war situation strategy. In terms of planing craft, the impact of implementing scenario-based design optimization has never been investigated. With the application of such knowledge one can improve the working condition of the people and equipment on-board of the ship.

Chapter 3

Planing Craft Optimization Framework

Abstract

In this chapter, an optimization framework for the design of high speed planing craft is described. It consists of a surface geometry information retrieval module, a geometry manipulation module, several accepted naval architectural performance estimation methods and a suite of optimization algorithms. It represents an *automation* scheme to assist ship designers in searching for optimized candidate designs and is capable of handling both single- or multi-objective optimization formulations of high speed planing craft design problems. The development of a mathematical model suitable for the preliminary design of planing craft is presented, followed by a validation study using a well known planing craft, the USCG WPB-110ft patrol boat as documented in [2].

3.1 Overview

In this chapter, an optimization framework for the preliminary design of planing craft with resistance, stability, seakeeping and maneuvering considerations is presented. This *modular*[1] design framework, facilitates a ship designer to effectively execute design optimization exercises with his/her desired level of complexity. The proposed framework incorporates an *automation*[2] scheme that allows single- and multi-objective optimization formulations to be executed utilizing commercial and in-house codes without user intervention. The flowchart of the developed framework is presented in Figure 3.1 and the details of each of its components are described in the following sections.

Presented in Section 3.2 is a brief background to the B-spline curve and surface representation methods. The motivation behind the use of a basis ship approach is established by close inspection of the available hull form generation techniques. Later, mathematical definitions of a B-spline curve and surface are elaborated.

Discussed in Section 3.3 is the hull form geometry representation and its variation using a B-spline method. Proposals for surface representation methods that include one- and multi-surface approaches are presented, followed by examples of hull forms generated using the proposed approach. Later, the hull geometry variational method adopted in the proposed framework is discussed.

Described in Section 3.5 is the development of the mathematical model capable of representing a high speed planing vessel forms. Initially, design parameter identification is discussed followed by descriptions of several performance indicators, e.g. calm water resistance, maneuvering and seakeeping response. Then,

[1] In software engineering, a modular framework is composed by integrating relatively independent units of functionality (e.g those used to measure resistance, stability etc.) [101].

[2] Automation is an application platform that allows one application to manipulate objects implemented in another application, or to expose objects so they can be manipulated [102].

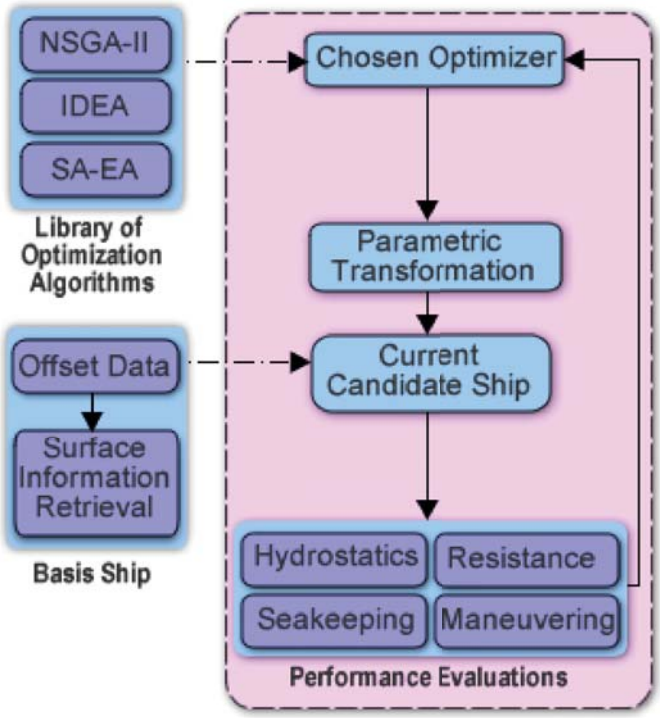

FIGURE 3.1: OPTIMIZATION FRAMEWORK FLOWCHART

the objective function, for which a few assumptions catering for limitations in the information available in the preliminary design stage, are identified. Finally, validation of the mathematical model, by comparing the numerical results with the experimentally measured data published in the literature, is provided.

Presented in Section 3.6 are the optimization algorithms incorporated in the proposed framework. The solution methodologies elaborated in this text consist of three optimization algorithms namely; Non-dominated Sorting Genetic Algorithm (NSGA-II), Infeasibility Driven Evolutionary Algorithm (IDEA) and Surrogate Assisted Evolutionary Algorithm (SA-EA).

After each component of the framework is introduced and described, the common ground, or the relationships between the modules are discussed in Section 3.7. Also, the inter-process communications between the commercial and in-house codes embedded in the framework are explained, giving the reader a full picture of the proposed framework.

After a thorough discussion of the capabilities and limitations offered by the proposed framework, its advantages are highlighted in Section 3.8.

Finally, Section 3.9 concludes the chapter.

3.2 Curve and Surface Representations

3.2.1 Available Hull Form Generation Techniques

There are three standard approaches applied in computer-aided ship hull design, namely, (1) manual generation of hull geometry using surface coordinate data, (2) generation of hull geometry using only form parameter values and (3) partial parametric modeling which is a combination of methods (1) and (2) [103].

1. **Manual/Interactive Generation of Hull Surface in CAD.** The surface geometry of a ship hull can be defined by the x, y and z coordinates in Cartesian space. Since there can be a substantial amount of data defining a particular ship's hull, several curve approximation techniques can be used to better control the surface data, e.g. spline interpolation, conformal mapping, Bézier and B-spline methods. Ultimately, the aim is to provide a small number of *control points* to approximate the full form. An arbitrary B-spline control polygon net defines a surface in Cartesian space which allows a ship designer to form a surface geometry. By interactively moving the control points, the surface can be refined until a satisfactory hull form design is generated. This method offers the most flexible and intuitive method for the design of a new hull form geometry. Fundamentally, if a ship designer is

not overly concerned with the form coefficients, unconventional designs can be allowed to emerge. The design process is highly interactive where specific features (e.g hard chine, transom stern) can be added/removed using clever manipulation of additional surfaces/control points. Although this approach offers a high level of freedom, the final designs are normally a product of iteration and extensive knowledge [33].

2. **Generation of Hull Geometry using Form Parameters' Definitions in CAD.** A ship's hull can be represented using a set of principal parameters (e.g. length, beam, draft, depth, etc.) and form coefficients (e.g. prismatic coefficient, block coefficient, midship coefficient etc.). Additional features for refining the hull definition include the deadrise angle, half angle of entrance, and the presence of hard chines and/or a bulbous bow. Through a set of comprehensive mathematical definitions, a specific hull can be generated automatically [30]. At times, a ship designer may have to manually override the mathematical definitions to finally resolve an acceptable hull shape [103], which requires a fair level of expertise regarding the type of hull. Having established a mathematical definition which may be a tedious process, an algorithm can be formed to define a family of hull forms. This method then provides direct relationships among the functional characteristics. However, a considerable amount of family-specific information must be built into the algorithms and each unique geometry (e.g. trawler, planing craft and naval combatant) must be treated as a special case as a general 'one model fits all' solution is not achievable.

3. **Partial Parametric Modeling in CAD.** Conceptually, both the above methods (**1** and **2**) separate the hull form surface geometry and form pa-

rameters during early generation of the candidate ship hull form geometry. In contrast, when designing a hull form, a naval architect is simultaneously concerned with the principal particulars, form coefficients and shape defined by the coordinates (offset data) of the hull geometry. Partial parametric modeling combines the best of both methods by integrating the surface geometry data and the hull form's principal particulars and form coefficients. A starting hull, the performance characteristics of which can be modified and tailored based on its intended operations, can be generated and is named the parent or basis ship. Variations of a ship hull's geometry while maintaining several principal particulars, form coefficients and hull surface features can be achieved using this approach.

In the present study, the partial parametric modeling approach was chosen due to its balanced level of flexibility and its capability to incorporate the available knowledge of a basis ship, especially in the preliminary design stage. It allows ship designers to understand and derive new candidate designs based on an existing hull form. This basis ship approach is highly suitable for the proposed optimization framework because it permits comparisons among the generated hull's parent form geometry and performance characteristics in the early design stage.

The optimization framework presented in this thesis allows for full geometry representation using a B-spline method, as detailed in the following sections.

3.2.2 B-spline Curves and Surfaces

Classic explanations of a B-spline can be found in [104, 22, 20]. A brief summary, accompanied by several examples based on the work of Rogers and Adams [104] and Piegl and Tiller [20], are presented in the following.

Curve generation

A B-spline curve or function, $P(t)$, is generated using a set of position vectors (control points), B, and a set of mathematical relationships called the B-spline basis, $N_{i,k}(t)$, the function of which allows the control points to affect the shape of a curve only over a range of parameter values for which its associated basis function is nonzero. The B-spline basis function also allows the order of the curve (and its degree) to be changed without changing the number of control points.

Letting $P(t)$ be the curves (e.g. hull form coordinate data) as a function of parameter t, a B-spline curve is given by

$$P(t) = \sum_{i=1}^{n+1} B_i N_{i,k}(t) \qquad 0 \leq t \leq 1 \tag{3.1}$$

where B_i is the position vector of the $n+1$ defining control points and $N_{i,k}$ the kth-degree normalized B-spline basis function. The B-spline basis functions are defined recursively and requires a selection of a sequence of scalars, t. Each t_i is referred to as a knot at which the total sequence forms a knot vector. The values of t_i are elements of a knot vector satisfying the non-decreasing relation. Parameter t varies from t_{min} to t_{max} along the curve, $P(t)$. The basis function that starts the recursive definition is

$$N_{i,1}(u) = \begin{cases} 1 & \text{if} \quad t_i \leq t \leq t_{i+1} \\ 0 & \text{otherwise} \end{cases} \tag{3.2}$$

$$N_{i,k}(t) = \frac{(t - t_i)N_{i,k-1}(t)}{t_{i+k-1} - t_i} + \frac{(t_{i+k} - t)N_{i+1,k-1}(t)}{t_{i+k} - t_{i+1}} \tag{3.3}$$

The non-periodic, non-uniform knot vector, t, is defined by

$$t = \{ \underbrace{0, \ldots, 0}_{k}, t_{k+1}, \ldots, t_{\alpha-k}, \underbrace{1, \ldots, 1}_{k} \} \tag{3.4}$$

where k is the degree of the curve ($k = 3$ in the case of a cubic curve), α is the total number of knots ($\alpha = CP + k + 1$), and CP is the number of control points. The term t_{k+1} and $t_{\alpha-k}$ is equal to 0 and 1 respectively. In order to produce a closed B-spline curve, the initial and the final knots are repeated $k+1$ times [104] [20]. Shown in Figure 3.2 is a set of cubic B-spline curves generated using a different number of control points (CP) with the respective knot vectors, t, enumerated.

Surface generation

A B-spline surface, $Q(u, w)$, is defined using a bi-directional net of control points and two sets of knot vectors, as expressed in Equation (3.5). The bi-directional net in B-spline is akin to the station- and waterline-direction arrangements in a ship's offset data.

$$Q(u, w) = \sum_{i=1}^{n+1} \sum_{j=1}^{m+1} N_{i,k}(u) N_{j,l}(w) B_{i,j} \tag{3.5}$$

where $CP_u = n+1$ and $CP_w = m+1$ are the number of control points in the u and w directions respectively, and k and l are the degree of the curve, respectively. A similar definition of the knot vector, as presented previously for a curve, is

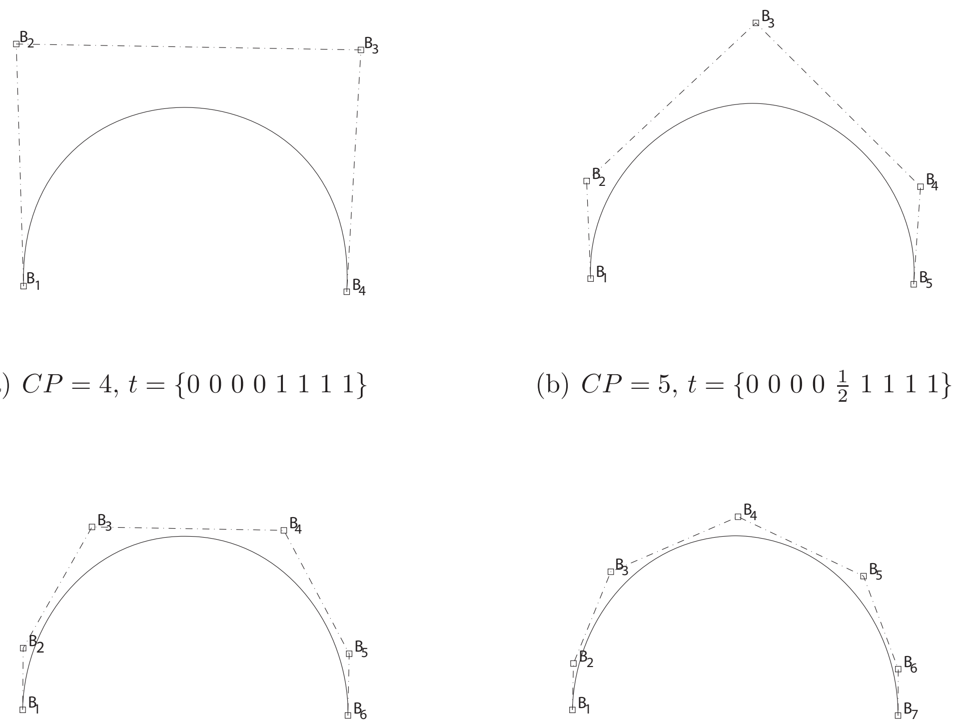

(a) $CP = 4$, $t = \{0\ 0\ 0\ 0\ 1\ 1\ 1\ 1\}$

(b) $CP = 5$, $t = \{0\ 0\ 0\ 0\ \frac{1}{2}\ 1\ 1\ 1\ 1\}$

(c) $CP = 6$, $t = \{0\ 0\ 0\ 0\ \frac{1}{3}\ \frac{2}{3}\ 1\ 1\ 1\ 1\}$

(d) $CP = 7$, $t = \{0\ 0\ 0\ 0\ \frac{1}{4}\ \frac{2}{4}\ \frac{3}{4}\ 1\ 1\ 1\ 1\}$

FIGURE 3.2: CUBIC B-SPLINE CURVE WITH DIFFERENT NUMBERS OF CONTROL POINTS WITH RESPECTIVE KNOT VECTORS

applied in the form

$$u = \{\ \underbrace{0, \ldots, 0}_{k}, t_{k+1}, \ldots, t_{\alpha-k}, \underbrace{1, \ldots, 1}_{k}\ \}$$

$$w = \{\ \underbrace{0, \ldots, 0}_{l}, t_{l+1}, \ldots, t_{\beta-l}, \underbrace{1, \ldots, 1}_{l}\ \}$$

$$\alpha = CP_u + k + 1 \text{ and } \beta = CP_w + l + 1$$

where CP_u and α are the number of control points and number of knots in the u-direction respectively. Similarly, CP_w and β are the number of control points and number of knots respectively in the w-direction.

Shown in Figure 3.3 is a set of cubic B-spline surfaces generated using a different number of control points (CP) in u- and w-direction with the respective knot vectors enumerated.

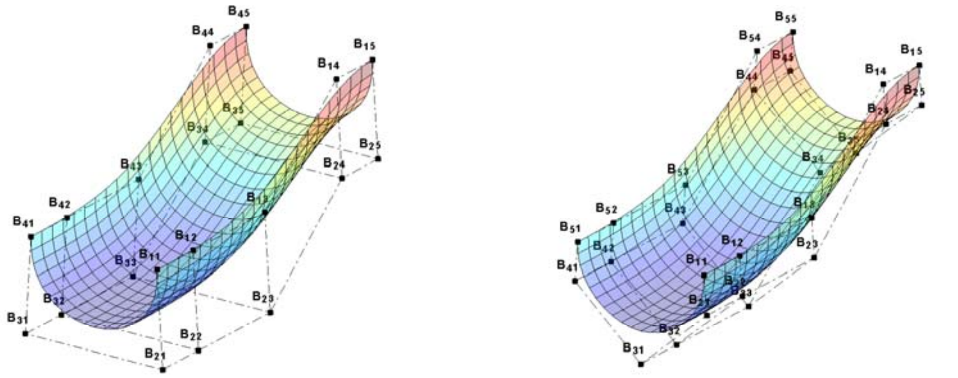

(a) $CP_u = 4$, $\alpha = 8$, $u = \{0\ 0\ 0\ 0\ 1\ 1\ 1\ 1\}$; $CP_w = 5$, $\beta = 9$, $w = \{0\ 0\ 0\ 0\ \frac{1}{2}\ 1\ 1\ 1\ 1\}$

(b) $CP_u = 5$, $\alpha = 9$, $u = \{0\ 0\ 0\ 0\ \frac{1}{2}\ 1\ 1\ 1\ 1\}$; $CP_w = 5$, $\beta = 9$, $w = \{0\ 0\ 0\ 0\ \frac{1}{2}\ 1\ 1\ 1\ 1\}$

FIGURE 3.3: BI-CUBIC ($k = 3$; $l = 3$) B-SPLINE SURFACE WITH DIFFERENT NUMBERS OF CONTROL POINTS AND RESPECTIVE KNOT VECTORS

CURVE FITTING

The previous section discussed the generation of a B-spline curve from its defining polygon. In this section, determining the defining polygon that generates a B-spline curve for a known set of data points is considered.

If a known data point, $D_j(t)$, lies on the B-spline curve, it must satisfy Equation (3.1) which for each j data point with Q_i as the unknown control points, yields

$$
\begin{aligned}
D_1(t_1) &= N_{1,k}(t_1)Q_1 + N_{2,k}(t_1)Q_2 + \ldots + N_{n+1,k}(t_1)Q_{n+1} \\
D_2(t_2) &= N_{1,k}(t_2)Q_1 + N_{2,k}(t_2)Q_2 + \ldots + N_{n+1,k}(t_2)Q_{n+1} \\
&\vdots \\
D_j(t_j) &= N_{1,k}(t_j)Q_1 + N_{2,k}(t_j)Q_2 + \ldots + N_{n+1,k}(t_j)Q_{n+1}
\end{aligned}
$$

where $2 \leq k \leq n+1 \leq j$, where $n+1$ is the maximum number of control points and k is the degree of the curve. This system of equations can be compactly written in matrix form as

$$[D] = [N]\,[Q] \tag{3.6}$$

where

$$
\begin{aligned}
[D]^T &= [D_1(t_1)\ D_2(t_2)\ \ldots\ D_j(t_j)] \\
[Q]^T &= [Q_1\ Q_2\ \ldots\ Q_{n+1}] \\
[N] &= \begin{bmatrix} N_{1,k} & \ldots & \ldots & N_{n+1,k}(t_1) \\ \vdots & \ddots & & \vdots \\ \vdots & & \ddots & \vdots \\ N_{1,j} & \ldots & \ldots & N_{n+1,k}(t_j) \end{bmatrix}
\end{aligned}
$$

If $2 \leq k \leq n+1 = j$, the matrix, $[N]$, is square and the control points can be obtained directly by matrix inversion, i.e.,

$$[Q] = [N]^{-1}\,[D] \tag{3.7}$$

In this case, the resulting B-spline curve passes through each data point, i.e., a curve fit is obtained. However, since in this case the numbers of control points and data points are the same, the fitted curve may develop unwanted wiggles and undulations [22].

A fairer or smoother curve is obtained by specifying fewer defining control points than data points, i.e. $2 \leq k \leq n+1 \leq j$. Here, $[N]$ is no longer square, and the matrix problem can be solved using the least squares approximation [104] method. As the matrix times its transpose is square, the defining control points, Q, for a B-spline curve that fairs or smooths the data is given by

$$\begin{aligned} [D] &= [N]\,[Q] \\ [N]^T\,[D] &= [N]^T\,[N]\,[Q] \\ [Q] &= \left[[N]^T\,[N]\right]^{-1}[N]^T\,[D] \end{aligned}$$

The fitting error, ϵ, between the 2D curve data points P, and D, can be calculated using the Euclidean distance method that yields

$$\epsilon = \sqrt{(P_x - D_x)^2 + (P_y - D_y)^2}$$

These techniques assume that the matrix $[N]$ is known. Provided the degree of the B-spline basis, k, the number of polygon points, $n+1$, and the parameter values along the curve are known, the basis functions, $N_{i,k}(t_j)$, and the matrix, $[N]$, can be obtained. However, as implied earlier, for good fitting it is worth noting that the number of control points should be less than the number of sample data points to be fitted [20].

Surface fitting

Extending the discussion to surface fitting, given a known set of data on a surface, the problem is to determine the defining polygon net for a B-spline surface that best interpolates or fits the data. In this case, the $S_{r,s}(u, w)$'s are the data points that lie on a known B-spline surface, Q. The $N_{i,k}(u)$ and $M_{j,l}(w)$ basis functions can be determined for: (i) a known degree of curve; (ii) a known number of defining polygon net vertices in each parametric direction; and (iii) the known parametric values, u and w at the surface data points. Thus, for each known surface data point, Equation (3.5) provides a linear equation in the unknown defining polygon net vertices, $R_{i,j}$ and, for a single surface data point, yields

$$\begin{aligned} S_{1,1}(u_1, w_1) = N_{1,k}(u_1)[M_{1,l}(w_1)R_{1,1} + M_{2,l}(w_1)R_{1,2} + \ldots + \\ M_{m+1,l}R_{1,m+1}] + N_{n+1,k}(u_1)[M_{1,l}(w_1)R_{n+1,1} + \\ M_{2,l}(w_1)R_{n+1,2} + \ldots + M_{m+1,l}R_{n+1,m+1}] \end{aligned}$$

for an $r \times s$ topologically rectangular set of data, $2 \leq k \leq n+1 \leq r$ and $2 \leq k \leq m+1 \leq s$, where $n+1$ and $m+1$ are the maximum number of control points in u and w direction respectively, and r and s are the maximum number of surface data points in u and w respectively. Writing an equation of this form for each data point yields a system of simultaneous equations. In matrix form, the result is

$$[S] = [C][R] \tag{3.8}$$

where $C_{i,j} = N_{i,k}M_{j,l}$. If $[C]$ is square, the defining polygon net is obtained directly by matrix inversion, i.e.,

$$[R] = [C]^{-1}[S]. \tag{3.9}$$

As shown in Equation (3.9), the resulting surface passes through each data point and, since the number of control points is equal to the number of data points, oscillation is again likely to occur. To obtain a number of control points that is fewer than the number of data points, Equation (3.9) is solved using the least squares approximation [104]. The solution is given by

$$[R] = \left[[C]^T[C]\right]^{-1}[C]^T[S]. \tag{3.10}$$

The fitting error, ϵ, between the 3D curve data points, Q and S, can be calculated using Euclidean distance method that yields

$$\epsilon = \sqrt{(Q_x - S_x)^2 + (Q_y - S_y)^2 + (Q_z - S_z)^2}$$

The curve and surface fittings are demonstrated using hull form examples in the next section.

3.3 Hull Form Representation and Variation

In this section, the hull form geometry representation using a B-spline approach is discussed. A *one-surface* hull geometry representation method is presented to inform the reader of general practice in hull form geometry design. Later, a *multi-surface* hull geometry approach is proposed as a suitable method of representing the C^0 curve discontinuity[3] (non-differentiable edge) that better represents a 'knuckle' or hard chine of a planing hull form. Other hull form examples that are generated and presented using the proposed method are a Series 60 cargo ship, the U.S. Navy Combatant DTMB 5415 craft, a trawler and a wave-piercing catamaran. Finally, the hull variational processes involved in the proposed framework are discussed.

3.3.1 Suitable Hull Representation in B-spline

Hull form data may be represented using standard offset data. However, with the vast amount of CAD software available in the market, the ship hull data might be represented using a non-standard 3D array (x, y and z) of data points expressed in Cartesian coordinates. In such a form, the coordinates can be in any sequence in the Cartesian space. Although the data can be viewed through a conventional 3D plot, it is inconvenient/unsuitable for a B-spline representation that is dependent on the sequence and arrangement of the data points [33]. However, a suitable representation of B-spline hull fitting and curve generation is in the form of a station-wise or waterline-wise coordinate arrangement. Hence, to counter this problem, a mechanism for converting the initial arrangement of unordered x, y and z data points to a suitable representation is developed. As shown graphically in Figure 3.4, given un-arranged x, y and z data points of the parent hull, the `Station Sorter` function automatically sorts the coordinates in a station-wise arrangement. The processed coordinates are then passed to the `B-spline Inverse` function that results in a set of control points that collectively define a polygon net. Thereafter, the B-spline surface that approximates the

[3] Recall from calculus that a function of class C^n has continuous derivatives up to order n. The C^0 discontinuity is usually called the *step edge* [105]. In the context of hull form design, the C^0 discontinuity can be used to represent knuckles or hard chines.

parent hull is generated using the obtained control polygon net.

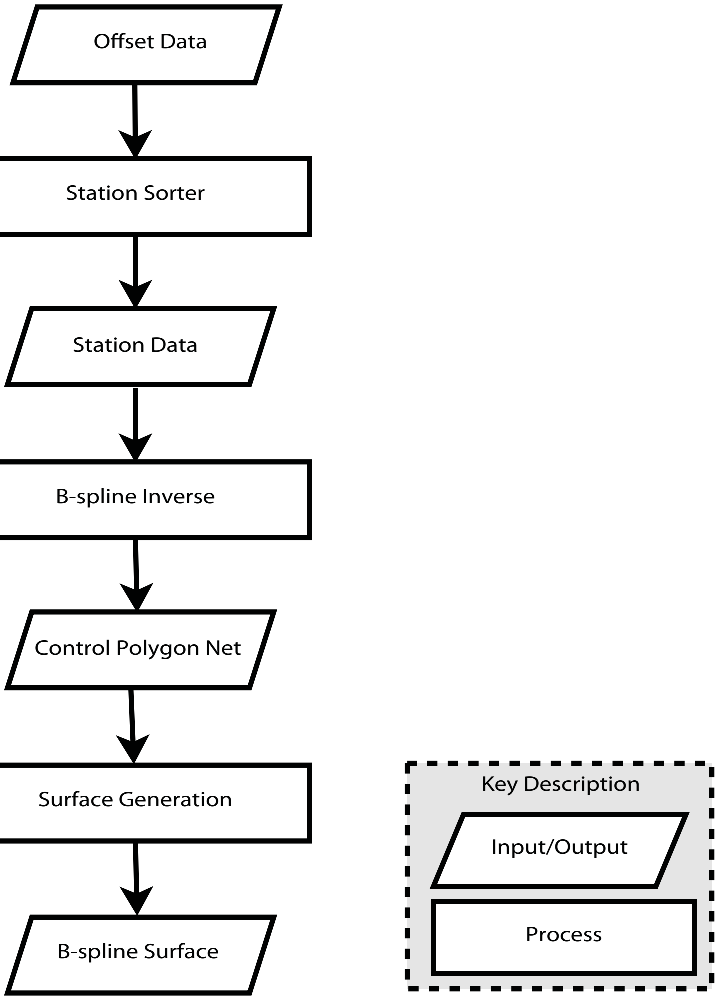

Figure 3.4: Process flowchart of surface information retrieval module

3.3.2 One-Surface Hull Approach

A one-surface hull form geometry representation approach is the simplest embodiment of a three-dimensional hull form representation method. It is assumed that a hull can be approximated using a set of *continuous* data points located on its surface. This means that the method eliminates several characteristics of the hull, such as knuckles (hard chines) or other forms of C^0 discontinuities. The topology of the hull (e.g. keel, stations, deck) is assumed to be correct when the resulting surface matches the shape desired by the ship designer. Complementary works in the literature that discuss one-surface hull geometry representation are Rogers *et al.* [22], Bole [27] and Harries [33].

A one-surface hull approach is best for a simple hull form (e.g. no bulbous bow, no hard chine, etc.). A fair hull surface can be generated using a minimal number of control points, which prevent unwanted wiggles and undulations. Shown in Figure 3.5 are the steps taken to fit a one-surface hull using a simple yacht. The original definition of the yacht consisted of 1282 three-dimensional data points of the x, y and z coordinates.

1. The original coordinate data that defined the parent hull was arranged station-wise, from aft to forward (Figure 3.5(a)). The stations are numbered for clarity (in this case, stern to bow).

2. For each station, the data points were fitted to obtain the station-wise control points. Shown in Figure 3.5(b) are the fitted/extrapolated lines together with the corresponding control points. A good fitting error was obtained with a mean error, $\bar{\epsilon}$, of 0.34×10^{-2}.

3. The station-wise control points were then fitted to obtain the control points in the longitudinal direction. Shown in Figure 3.5(c) are the longitudinal control points obtained with respect to the station-wise control points. The number of longitudinal control points was independent of the number of station-wise control points. It could be increased providing the desired number of longitudinal control points was less than the number of stations.

4. Finally, the control polygon net that defines the whole hull surface was

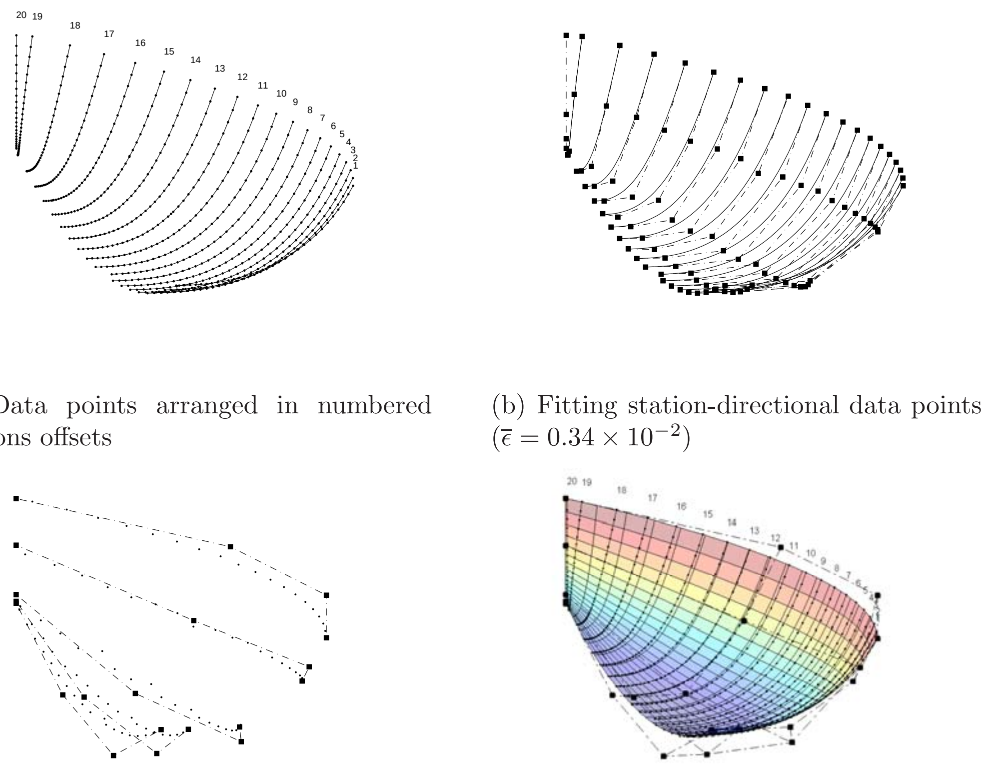

(a) Data points arranged in numbered stations offsets

(b) Fitting station-directional data points ($\overline{\epsilon} = 0.34 \times 10^{-2}$)

(c) Fitting longitudinal direction through control points of station-directional control points ($\overline{\epsilon} = 0.15$)

(d) Surface defined from B-spline fitting process

FIGURE 3.5: EXAMPLE OF ONE-SURFACE HULL FITTING

obtained, as shown in Figure 3.5(d). In this example, 5 × 4 control points were employed to approximate the whole surface of the yacht.

3.3.3 Multi-Surface Hull Approach

In real-world design, a hull form geometry may contain several complex features, such as surface discontinuities (e.g. a planing craft's hard chine) and a bulbous bow. For planing craft, a one-surface fitting approach was attempted by Rogers *et al.* [22]. Their implementation involved interactive manipulation of the control vertices to produce knuckles/hard chines of the planing craft. Although it is possible to manually relocate the control points to represent a hard chine, there are two problems: firstly, the initial approximations of the hull are poorly faired, especially on the hard edges; and secondly, allowing the designer to interactively modify the location of the control points interferes with the fairness of the B-spline surfaces.

It can be argued that a one-surface hull representation method is only useful for simple hull shapes whereas using a multi-surface hull representation approach allows ship designers to define the discontinuity characteristics of a hull's shape. Complex features can be generated by 'stitching' multiple surfaces at the shared points and edges, e.g. hard chines and bulbous bow. Non-differentiable edges can be defined with a minimal number of control points using a B-spline method. The work reported in this thesis proposes the splitting of surface data points at the edge of the surface for the design of a planing craft; for example, a ship designer identifies the knuckle positions and feeds the coordinate data points to a module that defines the control points of the surface data that fit the parent ship. The steps taken to approximate a three-surface hull are demonstrated using the basic planing craft shown in Figure 3.6. The original planing craft example was defined by 6066 discrete x, y and z data points.

1. The coordinates of the parent hull were partitioned into three segments and, for clarity, labeled 'top offset data', 'middle offset data' and 'bottom offset data' respectively (Figure 3.6(a)). Each set of offset data had common points representing the hard edges/discontinuities on the planing hull form surface.

2. The three segments of the offset data were fitted station-wise independently, as shown in Figure 3.6(b). The top, middle and bottom offset data are

fitted using 4 control points respectively, which were sufficient to cater for the minimal curvature of such planing craft forms. The mean fitting errors, $\overline{\epsilon}$, for the top, middle and bottom segments were 0.92×10^{-2}, 0.78×10^{-9} and 0.95×10^{-8}.

3. Longitudinal control points were fitted using the station-wise control points (Figure 3.6(c)). This second fitting process produced a set of global control points that was independent of the number of control points in the station-wise direction.

4. Shown in Figure 3.6(d) is the final form of the parent planing vessel. The three surfaces, each with a 4×4 control polygon net with appropriate matching of the edges on the hull form, are illustrated.

3.4 Additional Hull Examples

The benefit of using the proposed multi-surface hull representation is not limited to planing craft hull forms. Although its aim is to better represent the hull form for a hard chine planing vessel, it can be used to fit and represent any hull form type. Several examples that demonstrate its versatility are a Series 60 cargo ship, a US Navy Combatant DTMB 5415 craft, a trawler and a wave-piercing catamaran. The offset data in the forms of x, y and z coordinates of the typical hull forms listed above were generated from several example designs obtained from Maxsurf [106] and post-processed using the proposed approach. Descriptions of each are given below.

A Series 60 cargo ship represented using one B-spline surface fitted using a polygon net consisting of 7×14 control points is shown in Figure 3.7. The control

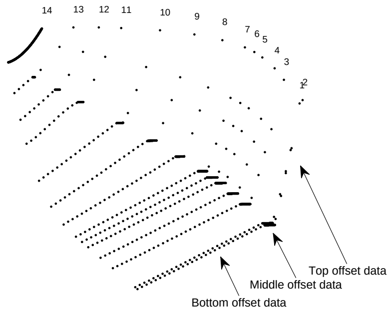

(a) Original station-based data points

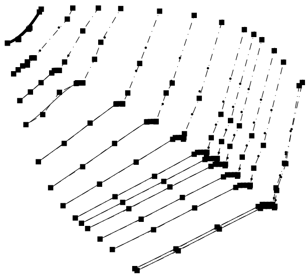

(b) Fitting station-directional data points ($\overline{\epsilon}_{\text{top}} = 0.92 \times 10^{-2}$, $\overline{\epsilon}_{\text{middle}} = 0.78 \times 10^{-9}$, $\overline{\epsilon}_{\text{bottom}} = 0.95 \times 10^{-8}$)

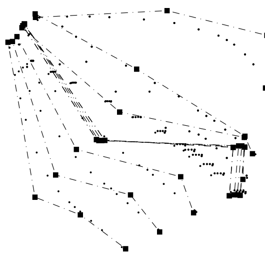

(c) Longitudinal control points and corresponding B-spline ($\overline{\epsilon}_{\text{top}} = 0.67$, $\overline{\epsilon}_{\text{middle}} = 0.67$, $\overline{\epsilon}_{\text{bottom}} = 0.48$)

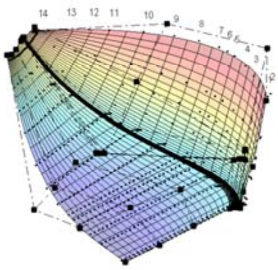

(d) Surface defined from longitudinal net

Figure 3.6: Example of multi-surface hull fitting

polygon net was obtained by fitting a set of offset coordinates consisting of 441 x, y and z data points. The fitting errors station-wise and longitudinally were $\overline{\epsilon}_{\text{station}} = 1.38 \times 10^{-2}$, $\overline{\epsilon}_{\text{longitudinal}} = 2.77 \times 10^{-7}$ respectively.

A typical trawler hull form represented using a one-surface B-spline formed using a polygon net consisting of 7×15 control points is shown in Figure 3.8. The offset data that defined the parent hull form consists of 441 data points. The fitting errors station-wise and longitudinally were $\overline{\epsilon}_{\text{station}} = 3.2 \times 10^{-7}$, $\overline{\epsilon}_{\text{longitudinal}} = 3.10 \times 10^{-7}$ respectively.

A US Navy Combatant, DTMB 5415, represented using three B-spline surfaces segmented at the bow, middle body and transom is shown in Figure 3.9. The three polygon nets at these surfaces consisted of 8×10, 8×7 and 8×5 control points respectively. The original parent hull was defined by 1323 data

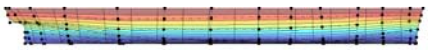

(a) Profile View

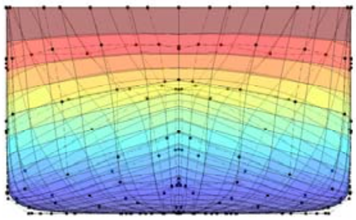

(b) Body Plan View

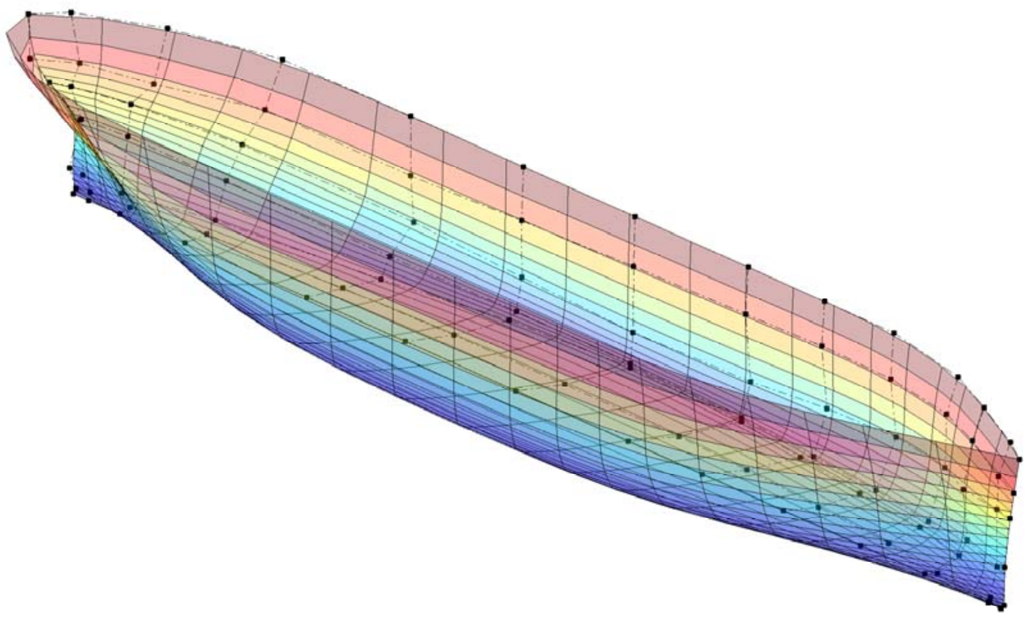

(c) Perspective View

FIGURE 3.7: SERIES 60 CARGO SHIP

points. The respective error values for each segment are reported in Table 3.1

A multi-hull example, represented using a typical wave-piercing catamaran is shown in Figure 3.10. This vessel was fitted using four B-spline surfaces, with 6×7 control points for both the outer- and inner-bottoms of the hull and 5×7

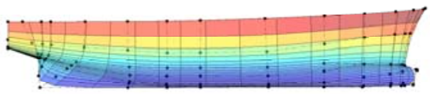

(a) Profile View

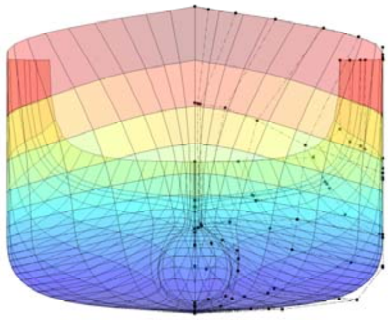

(b) Body Plan View

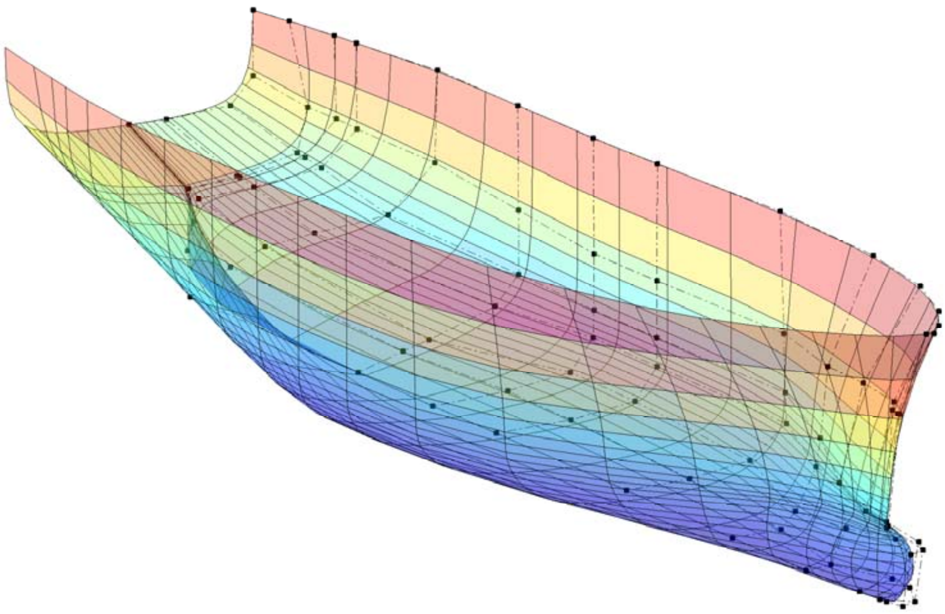

(c) Perspective View

FIGURE 3.8: TRAWLER/FISHING VESSEL

control points for bot its top sides (inner and outer). The parent hull was defined by 1764 x, y and z coordinates. The ‘exploded’ surfaces in the body plan view are shown in Figure 3.11. The respective error values for each segment are reported in Table 3.2.

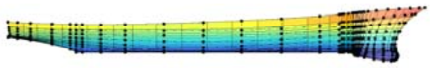

(a) Profile View

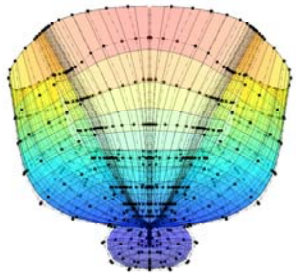

(b) Body Plan View

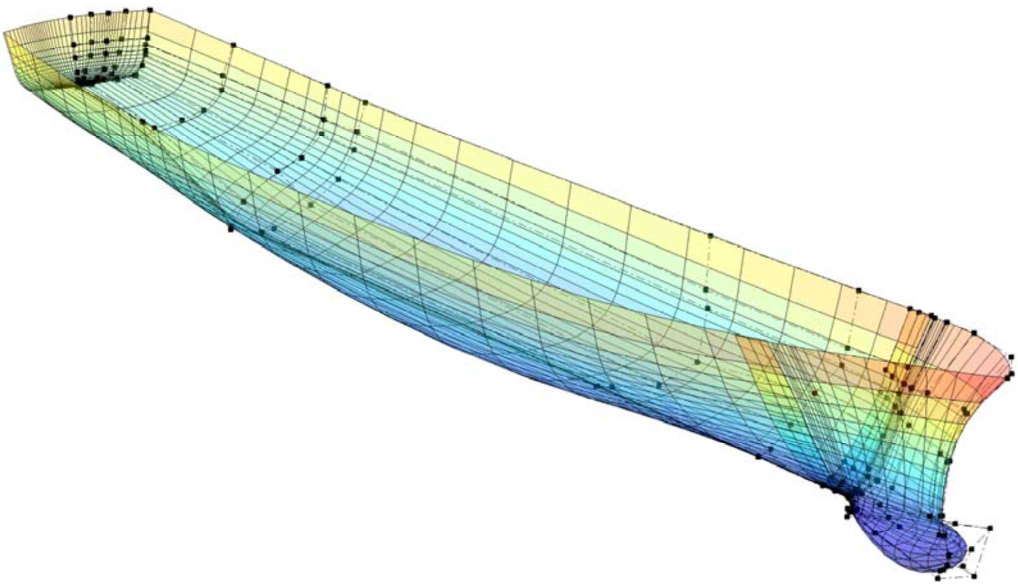

(c) Perspective View

Figure 3.9: US Navy Combatant DTMB 5415 craft

Table 3.1: US Navy DTMB 5415 fitting error

Segment	Error Description	Error Value
Bow	$\bar{\epsilon}_{\text{station}}$ $\bar{\epsilon}_{\text{longitudinal}}$	4.5×10^{-3} 4.3×10^{-3}
Middle body	$\bar{\epsilon}_{\text{station}}$ $\bar{\epsilon}_{\text{longitudinal}}$	4.6×10^{-8} 2.3×10^{-3}
Transom	$\bar{\epsilon}_{\text{station}}$ $\bar{\epsilon}_{\text{longitudinal}}$	5.4214×10^{-7} 5.6330×10^{-7}

3.4.1 Hull Variational Process

A number of different geometry manipulation methods for use in conjunction with optimization algorithms have been proposed in the literature. A set of B-spline control points were directly manipulated by Percival *et al.* [107] while control point perturbation of Bézier polynomial surface patches was demonstrated by Peri and Campana [45]. However, in order to maintain realistic deformations/modifications of the parent hull form, both methods require a significant number of additional constraints on the control points during the course of optimization. Peri and Campana [45] applied the linear parametric transformation proposed by Lackenby [40] followed by further CAD post-processing to improve the surface fairness of the candidate hull produced.

Lackenby's method is advantageous as it requires only the offset data of the ship to modify the lines plan while matching the required values of the

Table 3.2: Catamaran fitting error

Segment	Error Description	Error Value
Bottom hull (outer)	$\bar{\epsilon}_{\text{station}}$ $\bar{\epsilon}_{\text{longitudinal}}$	5.8321×10^{-7} 6.8485×10^{-7}
Bottom hull (inner)	$\bar{\epsilon}_{\text{station}}$ $\bar{\epsilon}_{\text{longitudinal}}$	5.7090×10^{-7} 7.0647×10^{-7}
Upper hull (outer)	$\bar{\epsilon}_{\text{station}}$ $\bar{\epsilon}_{\text{longitudinal}}$	5.4214×10^{-7} 5.6330×10^{-7}
Upper hull (inner)	$\bar{\epsilon}_{\text{station}}$ $\bar{\epsilon}_{\text{longitudinal}}$	4.7329×10^{-7} 4.9864×10^{-7}

longitudinal center of buoyancy (LCB) and prismatic coefficient (c_p). However, this method [40] suffers from surface fairness issues due to the direct manipulation of the sectional area curves. Moving the stations forward and aft creates edges

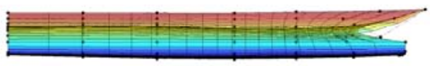

(a) Profile View

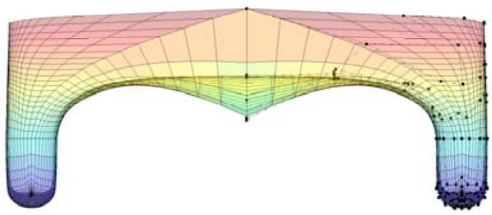

(b) Body Plan View

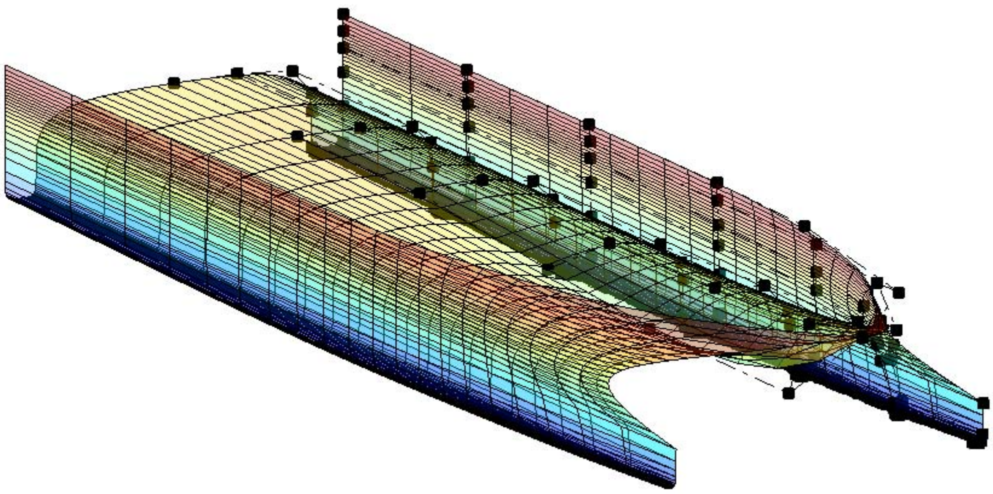

(c) Perspective View

FIGURE 3.10: A WAVE-PIERCING CATAMARAN

along the hull which affect fairness. This issue can be addressed through an interpolation method using B-spline. To improve on Lackenby's method, the use of a non-uniform rational B-spline (NURBS) surface, combined with a modified free-form deformation (FFD) [44], was proposed by Mason and Thomas [43] and has been further adapted in the commercial analysis code Maxsurf [106]. This method is ideal for the basis ship approach employed in this work, in which small adjustments are required to generate new candidate designs instead of gross design modification as in *ab initio* (clean sheet) design.

Shown in Figure 3.12 is an example of manipulating a parent hull through the use of a parametric transformation method in Maxsurf. It can be observed that the hull's surface characteristics are slightly varied when the waterline length

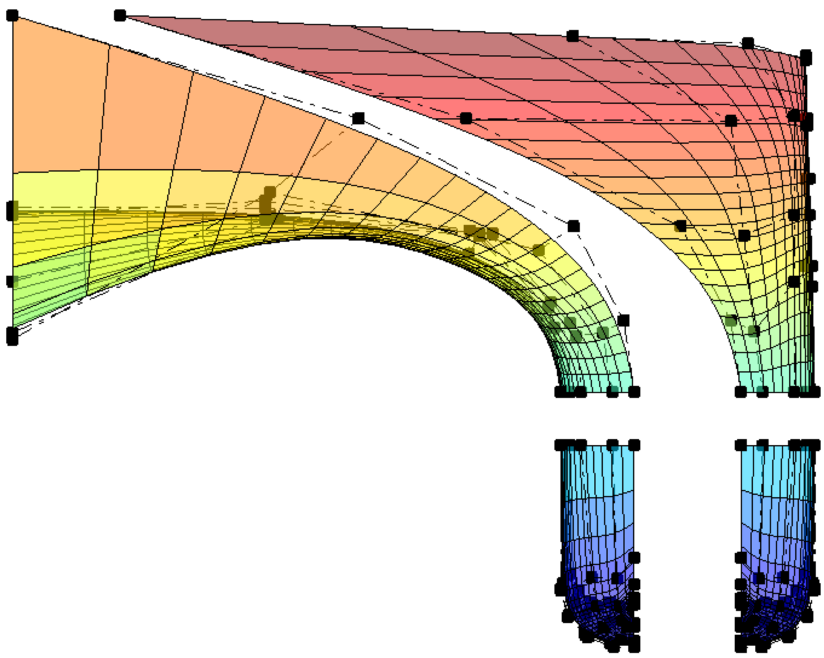

FIGURE 3.11: A WAVE-PIERCING CATAMARAN, BODY PLAN VIEW (EXPLODED)

was changed from 10.04m to 11.04m while maintaining a constant prismatic coefficient, c_p value. In this example, the displacement value was allowed to change during the parametric transformation process. However, large variations of scaling e.g. $\geq \pm 15\%$ of the length, beam and draft values is to be avoided as the resulting candidate hullforms can be expected to distort significantly [106].

This scheme allows for global surface manipulation in which the control points are moved forward, aft and sideways while maintaining the surface fairness. The advantage of global surface manipulation is that it preserves the continuity condition that defines the hard chine of the planing craft. Compared with local control [45], the number of variables and constraints involved during the optimization process are kept to a minimum in order to reduce the complexity of the optimization formulation [108].

3.5 Mathematical Model of the Hydrodynamic Design

The identification of design parameters, such as principal particulars and form coefficients, are described in this section. The performance indicators, which include a set of hydrodynamic characteristics, e.g. calm water resistance, maneuvering performance and response in a seaway, are introduced. Later, the identification of the objective function is described. Several principal assumptions are discussed followed by validation of the mathematical model.

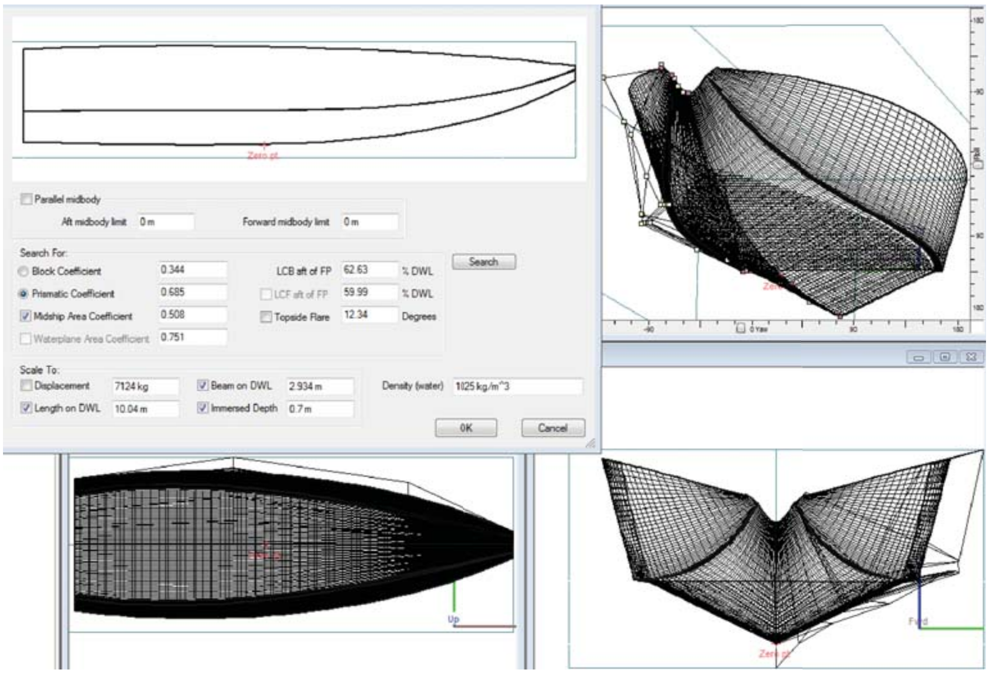

(a) Parent hull

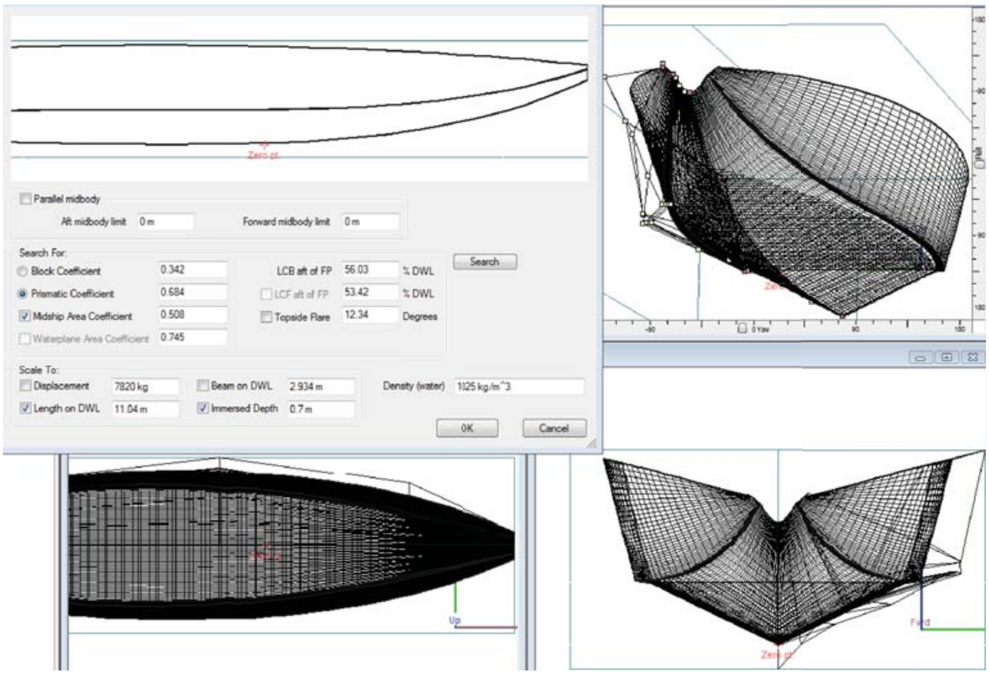

(b) Candidate hull

Figure 3.12: Parametric transformation example of case study craft using Maxsurf

3.5.1 Identification of Design Parameters

Design parameters provide a physical description of a ship [109]. The design parameters incorporated in this work consist of principal parameters and form coefficients, as tabulated in Table 3.3. The principal parameters and form coefficients function as the variables and constraints defined in the optimization process in which some limits-of-applicability constraints are included to ensure the candidate design is valid. Principal parameters and form coefficients such as L, B, T, Δ, c_b and c_p are free to be controlled by the designers (noted as independent). However, validation constraints, such as the minimum and maximum values of $L/\nabla^{1/3}$, Ie, L/B, and B/T need to be adhered to in order to produce valid optimum designs during the optimization exercise [110, 83].

Table 3.3: Design parameters used in the optimization framework

Design parameter	Description	Independent	Dependent
L (m)	Length	√	
B (m)	Beam	√	
T (m)	Draft	√	
Δ (kg)	Displacement	√	
VCG (m)	Vertical center of gravity	√	
c_b	Block coefficient	√	
c_p	Prismatic coefficient	√	
c_m	Midship coefficient		√
c_{wp}	Waterplance coeffiecient		√
WSA (m^2)	Wetted surface area		√
Ie (^{o})	Half angle of entrance at bow		√
GM (m)	Transverse metacentric height		√
LCG (m)	Longitudinal center of gravity		√
Fn	Froude number		√
δ (^{o})	Deadrise angle		√
τ (^{o})	Running trim		√

3.5.2 Descriptions of Performance Indicators

The performance indicators presented in this work consist of a calm water resistance estimation, a maneuvering performance indicator and seakeeping motion predictions. It should be noted that the proposed framework does not limit the use of additional performance indicators if they are available; for example, structural, weight or cost algorithms could be added to the model to improve the design output and explore other issues. The methods employed for high speed planing craft performance prediction are presented below.

Calm water resistance estimation

The resistance estimation used in this study is based on the work of Savitsky [83] and Savitsky and Brown [94] which includes both calm water and added resistance due to a seaway. The planing craft is assumed to be a prismatic craft and the validation ranges published are incorporated as constraints during the course of the optimization process.

In the empirical estimations presented in [83] and [94], there are two important conditions experienced by a planing hull being operated in certain speed ranges that need to be considered. These result in the following different resistance performance estimates.

- At speed coefficients ($c_v = V/\sqrt{g \times B}$) between 0.5 and 1.5, there exist dynamic effects that produce a contribution to lift but are insufficient to result in a significant rise of the center of gravity or emergence of the bow. It has been observed [94] that the flow has only slightly separated from the forward length of the chine and there is significant side wetting. In this speed range, the craft is essentially a high speed semi-displacement or semi-planing hull. Hence, using as an example of the USCG WPB-110 patrol boat [89] with $B = 7.5$m and an economic patrol cruise speed of $V_k =$ 16 knots [111] ($V = 8.23$), the craft at this speed operates in a semi-planing mode where c_v is 0.96.

- At speed coefficients larger than approximately 1.5, a well-designed planing hull should develop dynamic lift forces which will result in a significant rise of the center of gravity, a positive trim with emergence of the bow and separation of the flow from the hard chines. The full planing mode is experienced by the USCG WPB-110 patrol boat during the high speed pursuit scenario at 30 knots where c_v is 1.7.

Maneuvering performance indicator

An empirical estimate for turning circle diameter of planing craft has been derived from experimental data by Denny and Hubble [112]. The maneuvering equation was simplified by Lewandowski [113] and is used in this study. The predicted diameter to length ratio is given as,

$$\begin{aligned} \frac{STD}{L} &\approx \left[1.7 + 0.0222 F_{\nabla}\left(\frac{L}{\nabla^{1/3}}\right)^{2.85}\right]\left(\frac{30}{\delta_r}\right), \\ \text{where} \quad & 0.3 < F_{\nabla} < 4, \qquad 4.5 \leq L/\nabla^{1/3} \leq 7, \\ F_{\nabla} &= \text{volume Froude number}, V/\sqrt{g\nabla^{1/3}} \\ \nabla &= \text{volumetric displacement.} \end{aligned} \tag{3.11}$$

Response in a Seaway

Strip theory [114] has been widely used to compute the seakeeping performance of displacement craft. A study by White and Savitsky [89] suggests that seakeeping estimates for planing boats cannot be generalized from displacement craft. The same has been echoed by others including Lahtiharju *et al.* [90] and Barry *et al.* [91] in which Zarnick's [92, 93] strip theory was used. However, the strip theory can be used to measure the seakeeping response and the added resistance [115] in a seaway experienced by a planing craft operating in a displacement mode where the Froude number, Fn ≤ 0.7 [71]. Regression equations that can be used to evaluate the seakeeping performance of high speed planing craft have been derived by Savitsky and Brown [94] following the work of Fridsma [95]. The seakeeping estimates include added resistance (R_A), average impact acceleration at the craft's centre of gravity (η_{CG}), and the average impact acceleration at the bow[4] (η_{bow}), as shown in Equation (3.12) to (3.16). The added resistance values for $V_k/\sqrt{L} = 2$, $V_k/\sqrt{L} = 4$ and $V_k/\sqrt{L} = 6$ are defined and the intermediate values are obtained using linear interpolation.

The procedures by Savitsky and Brown [94] in 1976 were extended in detail by Savitsky and Koelbel [2] in 1993 that include additional information on the habitability conditions and several design guidelines for hard chine planing craft to operate in a seaway. The convention used by Savitsky and Koelbel that corresponds to the sea-state codes and the significant wave height, $H_{1/3}$ to describe wave environments based on a modified Pierson-Moskovitz [116, 2] spectrum is tabulated in Table 3.4.

Table 3.4: Sea-state Code used in the work of Savitsky and Koelbel [2]

Sea State Code	Sig. Wave Height, $H_{1/3}$ (m)
2	0.67
3	1.40
4	2.10
5	3.04
6	4.57

[4]The derivation of the equations by Savitsky and Brown are based on the imperial system of units. Since the work carried out in this thesis is based on the metric system, care has been taken to ensure correctness by comparing the calculation results with the examples presented in Savitsky and Brown's [94] paper.

Added resistance at $V_k/\sqrt{L} = 2$:

$$R_A = wB^3 \times \left[66 \times 10^{-6} \times \frac{\left(\frac{H_{1/3}}{B} + 0.5\right)\left(\frac{L}{B}\right)^3}{c_\Delta} + 0.0043(\tau - 4) \right] \tag{3.12}$$

Added resistance at $V_k/\sqrt{L} = 4$:

$$R_A = \Delta \times \left[\frac{0.3\frac{H_{1/3}}{B}}{1 + 2\frac{H_{1/3}}{B}} \left(1.76 - \frac{\tau}{6} - 2\tan^3\delta\right) \right] \tag{3.13}$$

Added resistance at $V_k/\sqrt{L} = 6$:

$$R_A = wB^3 \times \left[\frac{0.158\frac{H_{1/3}}{B}}{1 + \left(\frac{H_{1/3}}{B}\right)\left[0.12\delta - 21c_\Delta\left(5.6 - \frac{L}{B}\right) + 7.5\left(6 - \frac{L}{B}\right)\right]} \right] \tag{3.14}$$

Average vertical impact acceleration located at center of gravity:

$$\eta_{CG} = 0.0104\left(\frac{H_{1/3}}{B} + 0.084\right)\frac{\tau}{4}\left(\frac{5}{3} - \frac{\delta}{30}\right)\left(\frac{V_k}{\sqrt{L}}\right)^2 \frac{L/B}{c_\Delta} \tag{3.15}$$

Average vertical impact acceleration located at bow:

$$\eta_{bow} = \eta_{CG}\left[1 + \frac{3.8\left(L/B - 2.25\right)}{\frac{V_k}{\sqrt{L}}}\right] \tag{3.16}$$

Where V_k is speed in knots, $c_\Delta = \frac{\nabla}{B^3}$ is a static beam-loading coefficient and w is water density (kg/m^3). The vertical impact acceleration is measured in 'g', where the value reflects acceleration above static (e.g. 0.7g above static) [2]. While the work by Savitsky and Brown [94] and Savitsky and Koelbel [2] were using imperial system, the values were converted to metric system of units to maintain the consistency of results throughout the thesis. The details on the design guideline for appropriate vertical accelerations are presented in Appendix A.

3.5.3 Identification of the Objective Function

Many formulations with various objective functions such as construction cost [67], tactical maneuver [97], survivability [96], electrical energy usage [99], net present value index (NPVI) [59] and fuel consumption [98], have been proposed. For displacement craft design optimization; examples of work undertaken in this area prior to 1990 can be seen in [117, 118, 57, 119, 120, 54, 121, 122, 52, 123, 124, 53, 125] and during the next decade, to 2000, in [126, 58, 127, 48, 34, 64, 128, 30, 129, 33, 68, 59, 65, 61]. Works published since 2000 include [130, 131, 132, 107, 37, 133, 67, 134, 45, 77, 66, 72, 42, 76, 75, 135, 43, 38]. In the preliminary design stage, when details are minimal, the minimization of resistance has always been a prime objective in ship hull design optimization [33].

During the early design stage, when knowledge of the specifications is incomplete, ship designers seek a hull shape that requires lower power requirements by minimizing the total resistance of the craft. In the field of planing craft design, Nagai and Yoshida [85] focused on minimization of resistance of a planing craft with constraints on the trim angle. Similar studies include those of resistance minimization of the Soviet's BK and MBK hulls by Almeter [78], and multi-objective optimization of resistance and seakeeping by Grigoropoulus and Chalkias [71].

The proposed design framework also supports multidisciplinary design optimization for high speed planing craft. Through the combination of both analytical and empirical estimates, the framework is able to handle both hydrostatic and hydrodynamic performance characteristics in the optimization exercise. It allows for the exploration of constrained, single- and multi-objective optimization problem formulations that would provide ship designers an optimum candidate hull relevant to the mathematical model and a set of trade-off designs respectively.

3.5.4 Principal Assumptions

In the preliminary design stage, ship designers may construct mathematical models of a candidate craft based on key characteristic information available in a relevant database. In doing so, they operate on a number of assumptions in order to evaluate the performance of the candidate ship compared with real-world expectations/requirements. In this section, several principal assumptions in the proposed framework related to hull shape and mass distribution are discussed.

Planing Hull Shape

Following the work of Savitsky [83], the planing hull used throughout this work is assumed to have a prismatic planing surface, that is, a planing hull with constant deadrise and a constant beam for the entire wetted planing area [83]. Although a discussion on including other variations of planing surface exists by modifying the Savitsky's formulation of prismatic planing surface [136], it has been shown in [82] that there is less than a 5 percent difference between the WPB-110ft[5] patrol boat's measured resistance and that of the mathematical model, this error was deemed acceptable in the context of this study.

[5] As has been highlighted by Savitsky and Brown, most planing hulls do not have prismatic forms [94] including the WPB-110ft craft presented by White and Savitsky [89]. Blount and Fox [136] addressed this issue by attempting to identify an effective beam and deadrise which would result in the best prediction in planing range. They indicated that the maximum chine beam and the deadrise at the mid-chine length resulted in best prediction; this is implemented in this work.

Mass Distribution

The proposed planing craft optimization framework can model the bare hull based on the parent offset data. In a stage in which the vertical center of gravity (VCG) location is unknown, the VCG value is given as a function of the draft amidships (Equation (3.17)).

$$VCG = \frac{T}{2} \tag{3.17}$$

3.5.5 Validation of Mathematical Model

The base hull form used in the validation study is a United States Coast Guard (USCG) patrol boat, referred to as USCG 110-ft WPB. Comprehensive performance estimates of this vessel appeared in the work of White and Savitsky [89]. The offsets were obtained through lifting them from the published body plan. Multiple surfaces of the hard chine planing craft are then approximated by the *surface geometry information retrieval* method elaborated in Section 3.3. Shown in Figure 3.13(a) is the original body plan of the hull, and the derived approximations of the hull surfaces are shown in Figure 3.13(b). The published principal characteristics called the 'actual craft' are compared against those of the derived mathematical model in terms of the percentage error of differences. Values are tabulated in Table 3.5 to establish the validity of the mathematical model. Although the block coefficient, c_b, and volumetric displacement, ∇, are not reported in [89], they can be calculated and are included in Table 3.5. It can be observed that between the measured hull and the mathematical model, the geometric values (length, beam and draft) are matched within 1.3% and displacement is matched with a 2.23% of error. A small error in the speed coefficient, c_v, and the calm water resistance, R_c, which is less than 5% is argued to demonstrate the match between the actual vessel and the model is good. Following the basis ship approach method, the numerically optimized candidate designs in later chapters are compared with the modeled craft, hereafter referred to as the 'basis ship'.

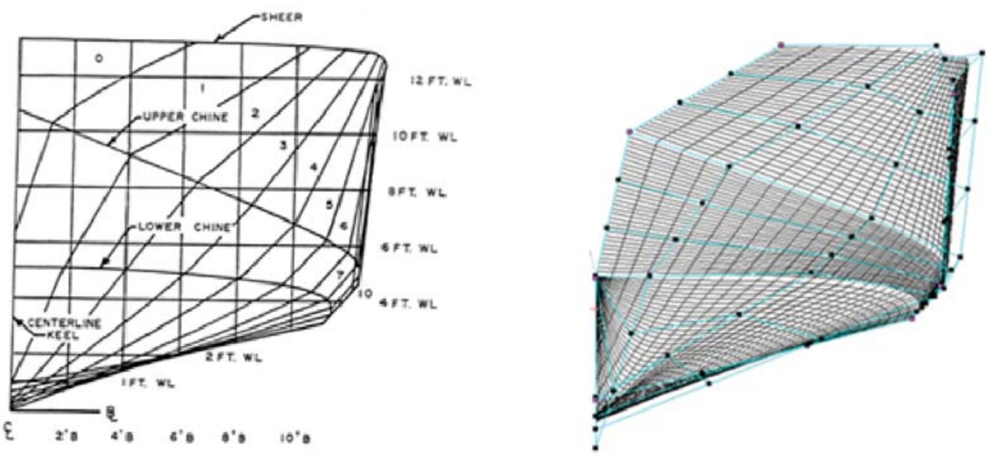

(a) Ship lines [89]   (b) B-spline surfaces defining WPB-110ft

Figure 3.13: Body plan of USCG 110-ft WPB (actual and basis ships)

Table 3.5: Characteristics of USCG 110-ft WPB (actual and basis ship)

Description	Actual ship	Basis ship	% Error
Δ (kg)	120,909	118,217	2.23
∇ (m^3)	-	115	-
L (m)	33	32.93	0.21
B (m)	7.62	7.52	1.33
T (m)	1.58	1.60	1.27
VCG (m)	2.70	2.70	-
V_k (knots)	30	30	-
δ (^{o})	32	32	-
c_v	1.785	1.797	0.67
c_b	-	0.29	-
R_c (kN)	130[1]	135.93[2]	4.56
R_c (kN)	136[2]	135.93[2]	0.05

[1] Tank test data published in [89]
[2] Evaluated using Savitsky 1964 [83] estimation method

3.6 Solution Methodology

In this work, three optimization algorithms are incorporated namely; Non - dominated Sorting Genetic Algorithm (NSGA-II), Infeasibility Driven Evolutionary Algorithm (IDEA) and Surrogate Assisted Evolutionary Algorithm (SA-EA). Summaries of these algorithms are presented in the following subsections.

3.6.1 Non-dominated Sorting Genetic Algorithm (NSGA-II)

Non-dominated Sorting Genetic Algorithm (NSGA-II) [137] is one of the most popular population-based optimization algorithms which has been successfully used in a number of real life applications. Its main steps are outlined in Algorithm 3.1. The algorithm starts with an initial population (P_1) of N candidate solutions initialized by random sampling from the design (variable) space. Each candidate solution of the population is evaluated to yield the corresponding values of the objective and the constraint functions. Based on the objective and constraint function values, the candidate solutions are ranked. The next steps (lines 5-8) are repeated for N_G generations. An offspring population, C_i is created using a recombination operation from the current (or parent) population P_{i-1}. The new offspring solutions are evaluated and the combined set of parents and offspring solutions is ranked. Based on the ranks, the best solutions from the parent population P_{i-1} and the offspring population C_i are retained to form the population for the next generation P_i.

Initialization. All the individuals in the population are initialized by random sampling. A value for each design variable is sampled uniformly between the lower

Algorithm 3.1 Non-dominated Sorting Genetic Algorithm (NSGA-II)

Require: N; {Population size}
Require: N_G; {Number of generations}
Initialize (P_1); {Create an initial populations of solutions}
Evaluate (P_1);
Rank (P_1); {Assign ranks to each solution}
for $i = 2$ to N_G **do**
  C_i = Evolve(P_{i-1}); {Create child solutions from parents of previous generation}
  Evaluate C_i; {Compute the performance of the child solutions}
  Rank ($P_{i-1} + Ci$); {Assign ranks to each solution}
  P_i = Reduce ($P_{i-1} + C_i$); {Identify parents for the next generation}
end for

and upper bounds of the variable, as given in Equation (3.18):

$$x_i = \underline{x_i} + U[0,1](\overline{x_i} - \underline{x_i}); \quad 1 \leq i \leq n \tag{3.18}$$

where x_i denotes the initialized variable, $\underline{x_i}$ and $\overline{x_i}$ are its lower and upper bounds, and $U[0,1]$ is a uniform random number lying between 0 and 1.

Evaluation. For each solution in the population, the values of the objective and constraint functions are evaluated using appropriate simulation or analysis. The fitness of a solution is calculated based on the objective and the constraint values as follows:

1. For a feasible solution, the fitness corresponds to the objective value(s).

2. For an infeasible solution, the fitness corresponds to the value of the largest constraint violation.

Evolution. In NSGA-II, an offspring population is evolved from the current population using selection, crossover and mutation operations. The details of each are provided below.

Selection: In NSGA-II, two parents are selected to create two offspring. The selection of each of these parents is based on a binary tournament. The process of binary tournament is illustrated below to identify a parent and the same needs to be repeated to identify another mating parent.

- Among two potential parents x_1 and x_2, if x_1 is feasible and x_2 is infeasible, x_1 is selected as the parent and vice versa.
- If both x_1 and x_2 are infeasible, the one for which the value of the maximum constraint violation is smaller is selected.
- If both x_1 and x_2 are feasible and x_1 dominates x_2, x_1 is selected and vice versa.
- If both x_1 and x_2 are feasible and neither dominates the other, one of x_1 and x_2 is selected at random.

Crossover: The crossover operation is performed between two parents identified above using simulated binary crossover (SBX) [138]. Two offspring solutions y_1 and y_2 are created from parents x_1 and x_2 by operating on one variable at a time as follows:

$$y_i^1 = 0.5[(1+\beta_{qi})x_i^1 + (1-\beta_{qi})x_i^2] \tag{3.19}$$

$$y_i^2 = 0.5[(1-\beta_{qi})x_i^1 + (1+\beta_{qi})x_i^2] \tag{3.20}$$

where β_{qi} is calculated as,

$$\beta_{qi} = \begin{cases} (2u_i)^{\frac{1}{\eta_c}+1}, & \text{if} \quad u_i \leq 0.5 \\ (\frac{1}{2(1-u_i)})^{\frac{1}{\eta_c}+1}, & \text{if} \quad u_i \geq 0.5 \end{cases} \tag{3.21}$$

and where u_i is the uniform number in the range of [0,1) and η_c is the user defined parameter, *Distributed Index for Crossover*. Probability of crossover (P_c) determines how often the crossover operation is performed.

Mutation: A polynomial mutation operator [139] is used for mutation. In the mutation operation, the value of one or more variables is randomly perturbed as given in Equation 3.23.

$$y_i = x_i + (\overline{x_i} - \underline{x_i})\overline{\delta_i} \tag{3.22}$$

where $\overline{\delta_i}$ is calculated as,

$$\overline{\delta_i} = \begin{cases} (2r_i)^{\frac{1}{\eta_m+1}-1}, & \text{if} \quad r_i \leq 0.5 \\ (1-(2(1-r_i)))^{\frac{1}{\eta_m}+1}, & \text{if} \quad r_i \geq 0.5 \end{cases} \tag{3.23}$$

and where r_i is the uniform random number in the range of [0,1) and η_m is the user defined parameter, *Distribution Index for Mutation*. The numbers of solutions undergoing mutation operation are determined by the probability of mutation (P_m).

Ranking. Individual solutions in a population are ranked based on their fitness value. Feasible solutions are considered better than infeasible solutions and are ranked separately. For single-objective optimization, feasible solutions are sorted based on the objective value while for multi-objective optimization the solutions are ranked based on non-dominance.

NSGA-II uses non-dominated sorting and a crowding distance sorting procedure [137] to rank feasible solutions with multiple objectives. In non-dominated sorting the solutions are arranged in multiple non-dominated fronts. In each non-dominated front, the solutions are non-dominated, whereas the solutions in one front dominate the solutions from the other front. Within a non-dominated front, the solutions are ranked based on a diversity measure and crowding distance [137].

For infeasible solutions the fitness corresponds to the maximum constraint violation. If more than one constraint is violated for a solution, the largest constraint violation value is used for the maximum constraint violation. Infeasible solutions are sorted in increasing order of the maximum constraint violation value.

Reduction. The reduction process is used to retain the N best solutions from a set of 2N solutions (parent and offspring populations) for the next generation. It uses the fitness values or ranks obtained through the above explained procedure.

1. If there are more than N feasible solutions,
   - N feasible solutions are selected in the order of non-dominated fronts and decreasing crowding distance in each front.
2. If the feasible solutions are less than or equal to N,
   - all the feasible solutions are selected in the order of non-dominated fronts and decreasing crowding distance in each front, and
   - the remaining solutions are selected from infeasible solutions in the order of minimum value of maximum constraint violation.

3.6.2 Infeasibility Driven Evolutionary Algorithm (IDEA)

Solutions to real-life constrained optimization problems often lie on constraint boundaries. It is reasonable for a designer to be interested in looking at the solutions that might be marginally infeasible. NSGA-II and most other optimization algorithms intrinsically prefer a feasible solution over an infeasible solution during the search process. However, some recent works [140, 141, 142] suggest that preservation of marginally infeasible solutions during the course of a search can expedite the rate of convergence. The Infeasibility Driven Evolutionary Algorithm (IDEA) which was introduced by Singh *et al.* [143, 144] is used in this study and further elaborated in this section.

A multi-objective optimization problem can be formulated as shown in Equation (3.24).

$$\begin{aligned} \text{Minimize} \quad & f_1(\mathbf{x}), \ldots, f_k(\mathbf{x}) \\ \text{Subject to} \quad & g_i(\mathbf{x}) \geq 0, \quad i = 1, \ldots, m \end{aligned} \tag{3.24}$$

where $\mathbf{x} = (x_1, \ldots, x_n)$ is the design variable vector bounded by lower and upper bounds similarly shown previously in Equation (3.18). A single-objective optimization problem follows the same formulation with $k = 1$.

To effectively explore the search space (including the feasible and infeasible regions), the original k objective constrained optimization problem is reformulated as a $k + 1$ objective unconstrained optimization problem as given in Equation (3.25).

$$\begin{aligned} \text{Minimize} \quad & f'_1(\mathbf{x}) = f_1(\mathbf{x}), \ldots, f'_k(\mathbf{x}) = f_k(\mathbf{x}) \\ & f'_{k+1}(\mathbf{x}) = \text{Violation measure.} \end{aligned} \tag{3.25}$$

The additional objective represents a measure of constraint violation, which is referred to as 'violation measure' [145] in this study. It is based on the amount of relative constraint violation among the population members. Each solution in the population is assigned m ranks, corresponding to m constraints. The ranks are calculated as follows. To obtain the ranks corresponding to the i^{th} constraint, all the solutions are sorted based on the constraint violation value of the i^{th} constraint. Solutions that do not violate the constraint are assigned a rank of 0. The solution with the least constraint violation value is ranked 1, and the rest of the solutions are assigned increasing ranks in the ascending order of their constraint violation value. This process is repeated for all the constraints, and as a result each solution in the population is assigned m ranks. The violation measure is the sum of these m ranks corresponding to m constraints.

The main steps of IDEA are outlined in Algorithm 3.2. IDEA uses simulated binary crossover (SBX) and polynomial mutation operators [137] to generate offspring from a pair of parents selected using binary tournament as in NSGA-II. Individual solutions in the population are evaluated using the original problem definition in Equation (3.24) and infeasible solutions are identified. The solutions in the parent and offspring population are divided into a feasible set, S_f and infeasible set, S_{inf}. The solutions in the feasible set and the infeasible set are both ranked separately using the non-dominated sorting and crowding distance sorting [137] based on $k + 1$ objectives as per the modified problem definition in Equation (3.25). The solutions for the next generation are selected from the sets to maintain feasible solutions in the population. In addition, the infeasible solutions are ranked higher than the feasible solutions (described below) to provide a selection pressure in order to create *better* infeasible solutions which will result in an active search through the infeasible search space.

A user-defined parameter, α, is used to maintain a set of infeasible solutions as a fraction of the size of the population. The numbers N_f and N_{inf} denote the number of feasible and infeasible solutions respectively determined by parameter

Algorithm 3.2 Infeasibility Driven Evolutionary Algorithm (IDEA)

```
Require: N; {Population size}
Require: N_G; {Number of generations}
Require: 0 ≤ α ≤ 1; {Proportion of infeasible solutions}
N_inf = α × N;
N_f = N − N_inf;
Initialize(P_1)
Evaluate (P_1);
for i = 2 to N_G do
    C_{i−1} = Evolve(P_{i−1});
    Evaluate C_{i−1};
    (S_f, S_inf) = Split(P_{i−1} + C_{i−1})
    Rank (S_f);
    Rank (S_inf);
    P_i = S_inf(1 : N_inf + S_f(1 : N_f))
    P_i = Reduce (P_i); {Identify parents for the next generation}
end for
```

α. If the infeasible set, S_{inf}, has more than N_{inf} solutions, the first N_{inf} solutions are selected based on their ranks, otherwise all the solutions from S_{inf} are selected. The rest of the solutions are selected from the feasible set, S_f, provided there are at least N_f feasible solutions. If S_f has fewer solutions, all the feasible solutions are selected and the rest are filled with infeasible solutions from S_{inf}. The solutions are ranked from 1 to N in the order they are selected. Hence, the infeasible solutions selected first will be ranked higher than the feasible solutions selected later.

3.6.3 Surrogate Assisted Evolutionary Algorithm (SA-EA)

While EA's are useful for solving a range of optimization problems, their application in their native forms for computationally expensive optimization problems is restricted. Essentially, as they are population-based methods, EA's require evaluations of numerous solutions before converging to the desired set of solutions. As such an approach is computationally prohibitive for realistic Multidisciplinary Design Optimization (MDO) problems, there is a growing interest in the use of surrogates to reduce the number of actual function evaluations required. Thus, the proposal to incorporate surrogates or approximations within an evolutionary algorithm is attractive and has led to the development of a number of Surrogate Assisted Evolutionary Algorithms (SA-EA) in recent years. The design of a surrogate assisted optimization framework involves a number of challenges, which include the provision of the types of surrogates and their management. It is evident that a function can be better approximated by one type of surrogate than another or even in different parts of the search space. To cater for this flexibility, an evolutionary framework with spatially distributed surrogates of multiple types was developed by Isaacs *et al.* [146]. This SA-EA framework is used in the current study.

The pseudo-code of the Surrogate Assisted Evolutionary Algorithm (SA-EA) is outlined in Algorithm 3.3. The types of surrogate models included in the framework include ordinary response surface method (ORSM), normalized response surface method (RSM), ordinary radial basis function (ORBF), normalized radial basis function (RBF) and kriging method (DACE). All these surrogate models are created for all the objectives and the constraints using a fraction of solutions that have been evaluated using actual analysis. An external archive of solutions evaluated using actual evaluations is maintained and used to periodically train the surrogate models. After every I_{TRAIN} generation, the parent population is evaluated using actual analysis and this information is added to the archive. A new solution is added to the archive only if the normalized distance (using the Euclidean norm) between the new solution and each of the solutions in the archive is more than the user defined distance criterion. This condition avoids the numerical difficulties of building the surrogates if the solutions are too close.

The solutions in the archive are split into multiple partitions using k-means clustering. Using a fraction of the solutions in each partition, the set of surrogate models (ORSM, RSM, ORBF, RBF and DACE) is trained for each of the objective and constraint functions. An 80-20 rule is adopted in which 80% of the solutions in each cluster are used for training while the remaining 20% are used to validate the surrogate models.

In SA-EA, there are two conditions where the surrogate model will not be built or invoked:

1. if there are very few solutions in a partition (insufficient to build the surrogate model), no surrogate models are built for that partition;
2. if the prediction error on the validation data set in the partition is more than the user defined threshold, the surrogate model on that partition is deemed invalid.

A surrogate model with the least prediction error is then used to predict the value of the new candidate solution.

The algorithm uses simulated binary crossover (SBX) and the polynomial mutation operator [137] to generate offspring from a pair of parents selected using binary tournaments as in NSGA-II.

3.7 Module-based Optimization Framework

In this section, the module-based optimization scheme that connects each element in the proposed framework is discussed. The motivation for developing such a

Algorithm 3.3 Surrogate Assisted Evolutionary Algorithm (SA-EA)

```
Require: N; {Population size}
Require: N_G; {Number of generations}
Require: K; {Number of partitions}
Require: I_TRAIN > 0; {Periodic surrogate training interval}
A = φ; {Archive of the solutions}
Initialize(P_1);
Evaluate (P_1);
A = AddToArchive(A, P_1);
S = BuildSurrogates(A, K);
for i = 2 to N_G do
   if modulo(i, I_TRAIN) == 0  then
      Evaluate (P_{i−1}); {Evaluate parent population using the actual analysis}

      A = AddToArchive(A, P_{i−1})
      S = BuildSurrogates(A, K)
   end if
   C_{i−1} = Evolve(P_{i−1}, S)
   EvaluateSurrogate(C_{i−1}, S)
   P_i = Reduce(P_{i−1} + C_{i−1})
end for
```

scheme is elaborated, followed by a discussion on the use of Component Object Model (COM) in Visual Basic for Application (VBA). Finally, the details of the automation scheme are discussed.

3.7.1 Motivation

A naval architect is responsible for producing the best performing candidate ship given specific design requirements/criteria and constraints. In a traditional ship design approach, the naval architect needs to move across different tools to provide the best candidate design while considering aspects such as hydrostatics, hydrodynamics and structural design; for example, in hydrodynamics, a ship designer needs to evaluate various performance measures, such as calm water resistance, maneuvering and response in a seaway. The process can be tedious and involves a high level of know-how to handle various naval architectural tools. Moreover, the information flow between each different aspect is typically sequential.

For instance, commercial tools ‘A’ and ‘B’ might be used for geometry modification and hydrostatics characteristics respectively while in-house codes ‘C’ and ‘D’ are incorporated to evaluate hydrodynamic performance and response in a seaway respectively. Finally, the information is presented in a spreadsheet in order for the data in to be interpreted a reasonable way. Hence, the problem pursued here may read:

> *“Find a good candidate ship given a set of design requirements and constraints, using a set of performance evaluation tools that can be expanded or reduced depending on the task that needs to be undertaken by the candidate ship.”*

An efficient ship design optimization framework has been developed to solve this problem. Contrary to the traditional ship design method outlined above, the performance evaluation tools are integrated within a common framework without any user intervention during execution (Figure 3.1). The framework is populated with a library of optimization algorithms that evaluates the performance of the candidate ship while automatically outputting a set of new variables to a geometry modification module according to the search algorithm used. The proposed framework is expandable/extensible[6] which makes the inclusion of different ship design tools/software easy. Also, the inclusion of commercial or in-house codes is possible without restricting a ship designer to using only one language or design software.

[6] In Computer Science, the term extensible refers to a system/framework that can be modified by changing or adding features [147].

In this work, the Component Object Model (COM) framework is used to integrate and automate each component involved in the planing craft optimization framework. Through COM, commercial codes and softwares are easily integrated with in-house codes using a set of trigger events and data collection methods. This framework is flexible where the ship designer is free to incorporate additional modules and control the complexity of the optimization problem definition.

3.7.2 Component Object Model (COM) and Visual Basic for Application (VBA)

Component Object Model is an interface standard developed by Microsoft to enable interprocess-communication between applications. It provides an interface for applications developed within Microsoft Windows to communicate with each other using several Application Programming Interface (API) calls. In COM, different components are viewed as *objects*, each of which can communicate with the others by query, store information and execute commands.

On top of COM is Visual Basic for Application (VBA) which provides a programming language that allows developers to build custom functions and automate tasks between applications. Implementations of VBA can be seen in several programs/applications, such as Microsoft Excel, AutoCAD and Maxsurf. It allows an application to control other applications using a common interface, thus querying information that can later be stored.

The collection of libraries and classes that represent the applications is called an Object Model. In the example of Excel as a host application, displacement evaluation can be executed inside Maxsurf through calling `Library:Maxsurf`, that contains `Class:Hydrostatics` and `Property:Displacement` [106].

Specifically, the capability to allow a host application to interact with other applications is called *automation*. In the host application, references to other applications need to be created by embedding `Application` objects that interface the host application to the other applications. The `Application` objects can then receive instructions and handle queries from the host application, thus automating the other applications.

3.7.3 Maxsurf Automation

Maxsurf Automation is built on top of a COM framework. It consists of a set of *object models* that allows developers to access the functions inside Maxsurf without user intervention. The object model contains features in a graphic user interface (GUI) that can be invoked using command lines. A set of command lines defines a script/macro that can be run depending on the task at hand. This feature allows a designer to run a set of repetitive actions (*routines*) unattended while automatically extracting the required information/results in spreadsheets, if necessary. While this feature is intended to assist a ship designer to speed up the repetitive design steps such as interactive modification, performance evaluations and data recording, the inter-process nature of COM allows interaction among other softwares. Thus it has been proven to be as a good base for an optimization framework.

Shown in Figure 3.14 is an example of inter-process communication executed between different softwares in the proposed framework. While the optimization codes, surface information retrieval module and a few other performance evaluation modules are written in Matlab, a trigger event is executed through the `xlswrite` command, thus invoking other module calls, such as parametric transformation (resides in Maxsurf) and the calm water resistance (in Hullspeed) calculation module. The queried data are returned in a spreadsheet that is eventually accessed using the `xlsread` command by the optimizer to evaluate the fitness of the objective function.

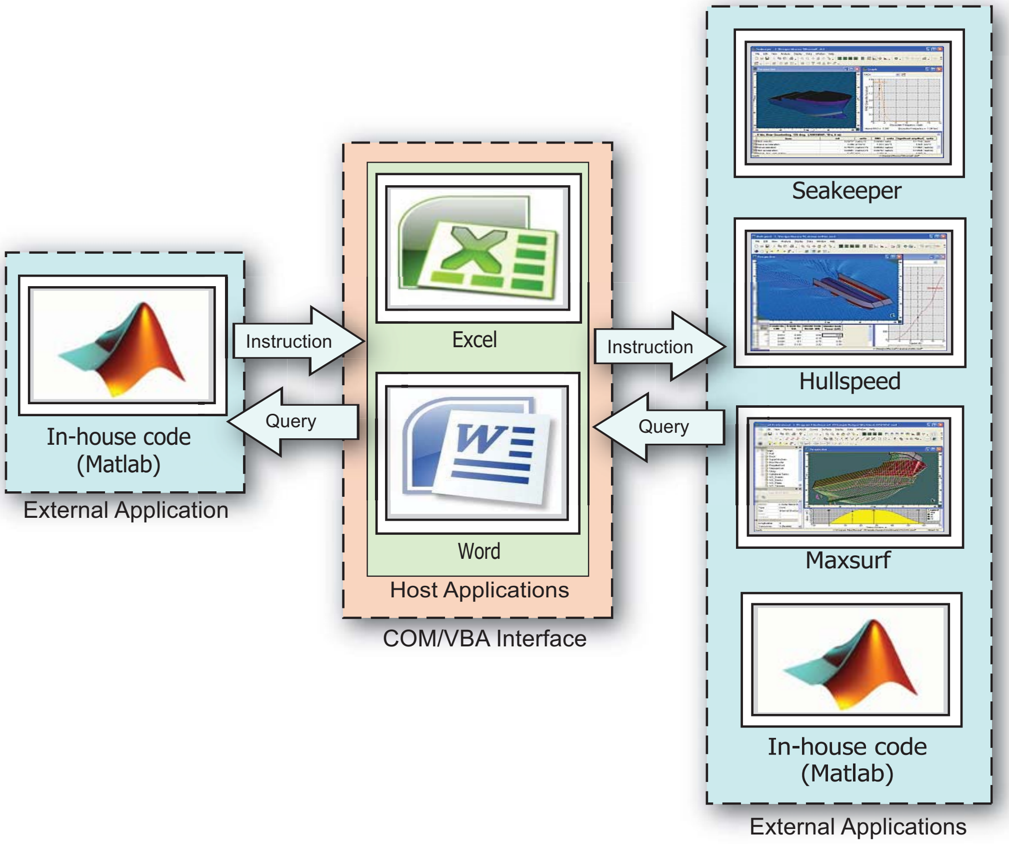

FIGURE 3.14: INTER-PROCESS COMMUNICATION BETWEEN HOST AND EXTERNAL APPLICATIONS THROUGH VBA INTERFACE

3.8 ADVANTAGES AND LIMITATIONS

In this section, the advantages offered by the proposed framework and several known limitations within the scope of this research are presented. The discussion involves the shape representation scheme, hull variational method, mathematical model, solution methodology and COM framework.

(1) Shape Representation

The B-spline curve and surface geometry representation of degree three (cubic B-spline) offered several advantages, such as high flexibility and adequate local influence of the control points towards the curve and surfaces. Furthermore, it gave good levels of accuracy for the surface fitting. However, from the perspective of fully interactive ship design, more creative curves and surfaces could be derived by using a higher degree B-spline.

(2) Hull Variational Method

As the hull variational method presented in Section 3.4.1 did not allow for excessive modifications ($\geq 15\%$) in order to prevent unwanted shape distortion, the candidate ship explicitly inherited the parent ship's shape characteristics. Moreover, as the other features (e.g. single-chine, multi-chine) of the candidate ship were always similar to those of the parent ship, when starting with a planing craft, morphing/evolving to a submarine would be impossible.

(3) Mathematical Model

A mathematical model is not an exact model of reality [59]. The mathematical model presented in this work was heavily dependent on the quality of the empirical estimates. Validation of the performance characteristics is encouraged in order to match the mathematical model and the real ship. Moreover, validation constraints were imposed during optimization (see Section 3.5.1) in order to minimize the risk of optimized candidate designs becoming grossly invalid.

(4) Solution Methodology

Evolutionary algorithms (EAs) are heuristic methods that do not need gradient information and can be easily applied to non-smooth functions involving discrete, integer, real or mixed design variables. They can also find solutions to a multi-objective optimization problem in a single run. However, there is no guarantee of achieving the global minimum from the use of evolutionary algorithm [148]. EAs are population based methods which require evaluations of large numbers of candidate solutions. In this work, the statistical values are presented in the experimental results in order to gain an overview of the convergence of the solutions obtained through optimization.

(5) COM Framework

The architecture of the proposed framework is platform-dependent. As the COM framework is built on top of Microsoft Windows, the COM/VBA approach presented in Section 3.7.2 requires a Microsoft Windows platform for its implementation.

3.9 Summary

In this chapter, an optimization framework for the design of high speed planing craft in the preliminary design stage is presented. The proposed framework supports the design of high speed planing craft though the use of several accepted naval architectural tools that include resistance, seakeeping and maneuvering performance of planing craft and state of the art optimization algorithms. In addition, the optimization framework is constructed with modularity in mind so that a designer would be able to effectively execute the optimization process with different levels of complexity by including additional modules when necessary. The major contributions of the chapter are summarized below.

(1) Surface Information Retrieval and Hull Variational Method

A surface information retrieval method capable of handling hard chine planing craft and a hull form geometry representation based on B-spline curves and surfaces was introduced. Furthermore, a general approach towards hull representation including one-surface hull and multi-surface hull approaches were demonstrated using a few examples, including a yacht, a hard chine planing craft, a Series 60 cargo ship, a U.S. Navy Combatant DTMB 5415 craft, a trawler and a wave-piercing catamaran. Finally, hull variational processes using a parametric transformation method were discussed.

(2) Development of Mathematical Model to Handle High Speed Planing Craft Optimization Problem

A mathematical model has been developed to describe the performance characteristics of a high speed planing craft. In this thesis, the model has been formulated to address displacement, stability, calm water resistance, resistance in a seaway, maneuvering and vertical impact acceleration. Several underlying assumptions based on standard naval architectural practice were discussed . Finally, validation of the mathematical model was presented using the USCG WPB-110ft patrol craft.

(3) Integration with State-of-the-Art Optimization Algorithms

A suite of optimization algorithms is integrated in the proposed framework. In this work, three optimization algorithms are incorporated namely; Non - dominated Sorting Genetic Algorithm (NSGA-II), Infeasibility Driven Evolutionary Algorithm (IDEA) and Surrogate Assisted Evolutionary Algorithm (SA-EA). Apart from NSGA-II (one of the most popular population based optimization algorithms), two other recent algorithms have been introduced withing the framework. Some recent works have suggested that preservation of marginally infeasible solutions during the course of a search can expedite the rate of convergence. Hence, the use of IDEA in the proposed framework is included. A third method, SA-EA, which is capable of reducing the number of function evaluations by incorporating surrogates or approximations is included within this suite of optimization algorithms.

(4) Module-Based Optimization Framework

A module-based optimization framework is described. Primarily driven by the requirements to integrate and automate each component involved in the planing craft optimization framework, the use of a Component Object Model (COM) framework is proposed in this work. The proposal allows for the extension of the framework through its capability to connect in-house codes and commercial codes through a set of trigger events and data collection, thus providing flexibility to ship designers to solve more elaborate optimization problems than demonstrated herein.

Chapter 4

Resistance Minimization of High Speed Planing Craft

Abstract

In this chapter, three resistance minimization case studies are presented. The aim is to demonstrate the capability of the proposed framework to obtain low resistance high speed planing craft designs. Two single-objective problem formulations, for minimizations of calm water resistance and total resistance in a seaway are included. The third is a multi-objective optimization case study that considers total resistance in a seaway, maneuvering and vertical impact acceleration.

4.1 Overview

In the preliminary ship design stage, a naval architect often iterates through several candidate hull designs until a satisfactory hull form is obtained. This process starts with defining a set of requirements which is followed by generating candidate ship lines and then evaluating their displacement, stability, principal parameters and form coefficient characteristics. Later, the hydrodynamic performance characteristics of the candidate ship are evaluated (e.g. resistance, seakeeping and maneuvering). The ship designer iteratively modifies the candidate hull form until the performance characteristic requirements (e.g. adequate displacement and stability, low resistance, good maneuvering) are obtained. Finally, a *feasible* candidate hull form is produced. However, there probably exists a better design, e.g. even lower resistance while satisfying the requirements which could have been identified through optimization. For this reason, optimization is increasingly becoming important in design.

The process discussed above is tedious and time-consuming. With a limited budget, time and human resources, a manual search for the best candidate design might not be performed efficiently. Fortunately, the exercise of searching for an optimum candidate ship given specific design requirements can be translated to an optimization formulation. Optimization methods offer effective search processes which assist ship designers to obtain optimum candidate designs based on the mathematical models constructed.

In this chapter, resistance minimization case studies are presented. The aim is to demonstrate the benefits offered by the proposed design optimization framework. Three state-of-the-art evolutionary optimization algorithms, namely; Non-dominated Sorting Genetic Algorithm (NSGA-II), Infeasibility Driven Evolutionary Algorithm (IDEA) and Surrogate Assisted Evolutionary Algorithm (SA-EA), are incorporated in the case studies. The planing craft used as basis vessels are a 32m USCG WPB-110ft planing boat and a 10m Indian Fast Craft (IFC). The hull forms are hard chine and capable of operating in full planing mode.

In the following sections, single-objective, constrained minimization case studies of calm water resistance and total resistance in a seaway are discussed. Thereafter, a multi-objective, constrained optimization case study that involves minimization of total resistance in a seaway, steady turning diameter and vertical impact acceleration is presented.

4.2 Calm Water Resistance Minimization

The problem definition for this case study is presented in Section 4.2.1, followed by the results in Section 4.2.2 and Section 4.2.3.

4.2.1 Optimization Model

Given a basis hull, the single-objective optimization formulation aimed to identify a candidate design with minimum calm water resistance, R_C, subject to constraints on displacement and metacentric height. Due to the stochastic nature of the employed algorithms, thirty independent runs of each algorithm, NSGA-II, IDEA and SA-EA, were performed. A population size of 40, a crossover probability of 1, a mutation probability of 0.1, a crossover distribution index of 10 and a mutation distribution index of 20 were used by each algorithm. The number of function evaluations used by each algorithm was restricted to 1200. An infeasibility ratio of 0.2 was used by IDEA. The surrogate models employed were restricted to normalized response surface method (RSM), ordinary response surface method (ORSM), normalized radial basis function (RBF), ordinary radial basis function (ORBF) and kriging method (DACE). A training period of 3 and a prediction error of 0.05 were used by SA-EA.

The objective function, variables and constraints are listed below where the subscripts 'B' and 'I' denote the basis ship and candidate ship respectively. The basis ship variable values of length, L, beam, B, draft, T, displacement,

Δ, and metacentric height, GM, are shown in Table 4.1. The procedure for the calm water resistance estimations of the basis and candidate designs are bounded by validation ranges, as suggested by [83] and [106]. These ranges are expressed for half angle of entrance at the bow, I_e, length-cubic root of volumetric displacement ratio, $L/\nabla^{1/3}$, length-beam ratio, L/B, and beam-draft ratio, B/T. The formulation is as follows:

$$
\begin{aligned}
\text{Minimize} \quad & f(L_I, B_I, T_I) = R_C \\
\text{subject to} \quad & g_1 : \Delta_I > \Delta_B \\
& g_2 : GM_I \geq GM_B \\
& g_3 : 3.07 < L_I/\nabla_I^{1/3} < 12.4 \\
& g_4 : 3.7^o < Ie_I < 28.6^o \\
& g_5 : 2.52 < L_I/B_I < 18.28 \\
& g_6 : 1.7 < B_I/T_I < 9.8 \\
\text{Variables (IFC)} \quad & 9.0\text{m} \leq L \leq 11.0\text{m} \\
& 1.8\text{m} \leq B \leq 3.8\text{m} \\
& 0.6\text{m} \leq T \leq 0.8\text{m} \\
\text{Variables (WPB-110ft)} \quad & 29.93\text{m} \leq L \leq 35.93\text{m} \\
& 6.51\text{m} \leq B \leq 8.51\text{m} \\
& 1.50\text{m} \leq T \leq 1.70\text{m}
\end{aligned}
$$

Table 4.1: Respective variables and constraints for IFC and USCG WPB-110ft basis ship

Design	L_B (m)	B_B (m)	T_B (m)	Δ_B (kg)	GM_B (m)
IFC	10.04	2.86	0.70	7,095	1.68
WPB-110ft	32.93	7.51	1.59	118,217	1.64

4.2.2 Numerical Results - IFC

Shown in Figure 4.1(a) are the progress plots of the best run for each of the three algorithms, NSGA-II, IDEA and SA-EA. It can be observed that all three algorithms were able to minimize the calm water resistance to approximately the same value after around 1050 function evaluations. The optimization started with different parameter seeds, thus resulting in different starting points, as shown in Figure 4.1(a). The best candidate designs obtained using NSGA-II, IDEA and SA-EA are tabulated and compared against the basis ship in Table 4.2. The best, mean, median, worst and standard deviation (S.D.) values computed across 30 runs for each algorithm are listed in Table 4.3. A significant reduction in calm water resistance values can be observed when compared with the basis ship. The lengths, beams and drafts of the best designs (presented to two decimal places) were 11.00m, 3.04m and 0.60m for NSGA-II, IDEA and SA-EA respectively. The calm water resistance values of all the optimized candidate designs were approximately 9.58kN for NSGA-II, IDEA and SA-EA, compared to 11.32kN for the basis ship. This reflected the same best hull being identified by each algorithm where a 15.5% reduction in calm water resistance when compared with the basis hull is achieved.

From the progress plots in Figure 4.1(a), it can be observed that NSGA-II was able to find a lower optimized candidate design earlier than IDEA and SA-EA, at around 160 function evaluations. However, both IDEA and SA-EA were able to outperform NSGA-II after 800 function evaluations, hence converging faster to the final solution than NSGA-II. IDEA was able to converge on par with SA-EA at around 1000 function evaluations.

The progress plots for the median designs obtained using NSGA-II, IDEA and SA-EA are shown in Figure 4.1(b). It can be observed that IDEA outperformed both NSGA-II and SA-EA in terms of convergence speed and finding the candidate design with the lowest calm water resistance value. For between 560 and 1040 function evaluations, the performance of SA-EA is similar to NSGA-II. However, SA-EA was able to outperform NSGA-II using 1200 function evaluations.

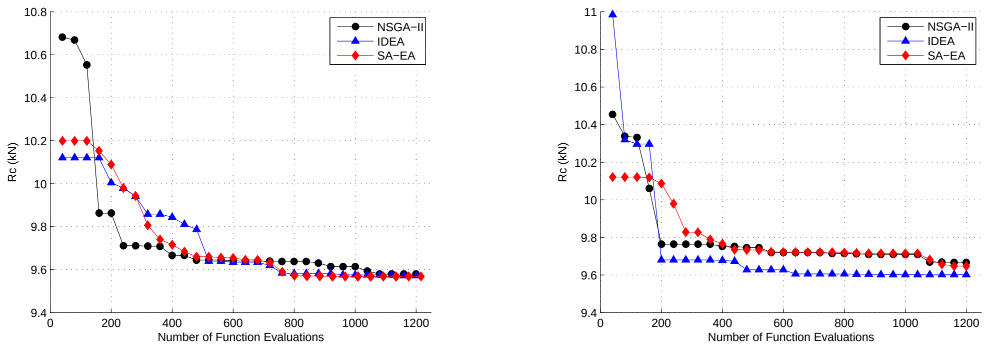

(a) IFC: Progress plots of best designs obtained using NSGA-II, IDEA and SA-EA for R_C minimization problem

(b) IFC: Progress plots of median designs obtained using NSGA-II, IDEA and SA-EA for R_C minimization problem

FIGURE 4.1: IFC: PROGRESS PLOTS FOR BEST AND MEDIAN DESIGNS OBTAINED USING NSGA-II, IDEA AND SA-EA FOR R_C MINIMIZATION PROBLEM

TABLE 4.2: IFC: BEST DESIGNS OBTAINED USING NSGA-II, IDEA AND SA-EA COMPARED AGAINST BASIS SHIP FOR R_C MINIMIZATION PROBLEM

	Basis Ship	NSGA-II	IDEA	SA-EA
Δ (kg)	7095.37	7098.14	7097.20	7095.65
L (m)	10.04	11.00	11.00	11.00
B (m)	2.86	3.04	3.04	3.04
T (m)	0.70	0.60	0.60	0.60
GM (m)	1.679	2.213	2.222	2.222
c_b	0.345	0.345	0.345	0.345
c_m	0.523	0.523	0.523	0.523
c_p	0.664	0.664	0.664	0.664
c_{wp}	0.737	0.737	0.737	0.737
WSA (m^2)	24.08	26.93	26.95	26.95
Fn	1.08	1.03	1.03	1.03
δ (^{o})	28.10	23.31	23.25	23.25
τ (^{o})	6.86	4.87	4.86	4.86
V_k (knots)	20.81	20.81	20.81	20.81
R_C (kN)	11.32	9.58	9.57	9.57
% savings		15.4	15.5	15.5

Table 4.3: IFC: Best, Mean, Median, Worst and S.D. values obtained using NSGA-II, IDEA and SA-EA for R_C minimization problem

Design	NSGA-II	IDEA	SA-EA
Best(kN)	9.58	9.57	9.57
Mean(kN)	9.73	9.61	9.71
Median(kN)	9.67	9.60	9.65
Worst(kN)	10.13	9.70	10.27
S.D.(kN)	0.15	0.03	0.16

4.2.3 Numerical Results - USCG WPB-110ft

The progress plots of the best run for each algorithm, NSGA-II, IDEA and SA-EA are shown in Figure 4.2(a). It can be observed that all three algorithms were able to minimize the calm water resistance at around 800 function evaluations and no better optimized candidate designs were identified within 1200 function evaluations. The optimization started with different parameter seeds, thus resulting in different starting points, as shown in Figure 4.2(a).

The best candidate designs obtained using NSGA-II, IDEA and SA-EA are tabulated and compared against the basis ship in Table 4.4. The best, mean, median, worst and standard deviation (S.D.) values computed across 30 runs for each algorithm are listed in Table 4.5. The low S.D. values indicate the consistency of the converged results obtained by each algorithm.

Significant reductions in calm water resistance values can be observed when compared with the basis ship. The lengths, beams and drafts of the best designs (presented to two decimal places) were approximately at around 35.92m, 7.28m and 1.50m for NSGA-II, IDEA and SA-EA respectively. The calm water resistance values of the best candidate designs are reported at around 122.37kN for all algorithms, compared to 135.93kN for the basis ship. This reflects about 10% reduction in calm water resistance when compared with the basis hull.

It can be observed in Figure 4.2(a) that NSGA-II was able to find lower resistance candidate designs earlier than IDEA and SA-EA (after 160 function evaluations). However, both IDEA and SA-EA were able to marginally outperform NSGA-II after 800 function evaluations, converging faster to the final solution than NSGA-II.

The progress plots for median designs obtained using NSGA-II, IDEA and SA-EA are shown in Figure 4.2(b). It can be observed that both IDEA and SA-EA outperformed NSGA-II in terms of convergence speed and finding candidate designs with lower calm water resistance values using 1200 function evaluations. In this example, the benefit of incorporating surrogate modeling through the use of SA-EA can be observed, in which the convergence of SA-EA is marginally faster than IDEA. Through preservation of infeasible solutions, IDEA was able to converge faster than NSGA-II.

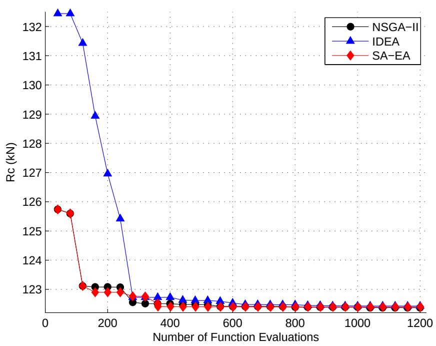

(a) USCG WPB-110ft: Progress plots of best designs obtained using NSGA-II, IDEA and SA-EA for R_C minimization problem

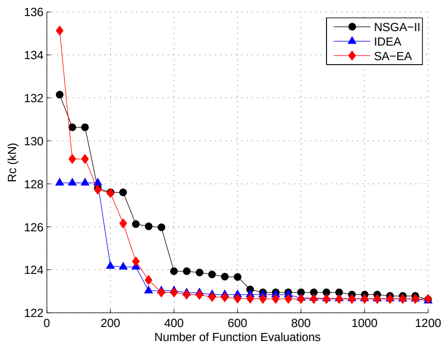

(b) USCG WPB-110ft: Progress plots of median designs obtained using NSGA-II, IDEA and SA-EA for R_C minimization problem

FIGURE 4.2: PROGRESS PLOTS FOR BEST AND MEDIAN DESIGNS OBTAINED USING NSGA-II, IDEA AND SA-EA FOR R_C MINIMIZATION PROBLEM

Table 4.4: USCG WPB-110ft: Best designs obtained using NSGA-II, IDEA and SA-EA compared against basis ship for R_C minimization problem

	Basis Ship	NSGA-II	IDEA	SA-EA
Δ (kg)	118217.78	118218.23	118219.82	118218.09
L (m)	32.93	35.92	35.93	35.93
B (m)	7.52	7.28	7.28	7.27
T (m)	1.60	1.50	1.50	1.50
GM (m)	1.64	1.83	1.83	1.82
c_b	0.292	0.294	0.294	0.294
c_m	0.487	0.488	0.488	0.488
c_p	0.680	0.686	0.686	0.686
c_{wp}	0.614	0.623	0.623	0.623
WSA (m^2)	183.83	194.09	194.15	194.06
Fn	0.86	0.82	0.82	0.82
δ (^{o})	31.86	30.94	30.93	30.98
τ (^{o})	3.76	2.53	2.53	2.53
V_k (knots)	30.00	30.00	30.00	30.00
R_C (kN)	135.93	122.37	122.39	122.39
% savings		9.98	9.96	9.96

Table 4.5: USCG WPB-110ft: Best, Mean, Median, Worst and S.D. designs for R_C minimization problem using NSGA-II, IDEA and SA-EA

Design	NSGA-II	IDEA	SA-EA
Best(kN)	122.37	122.39	122.39
Mean(kN)	123.01	122.76	122.81
Median(kN)	122.73	122.54	122.60
Worst(kN)	125.07	124.49	124.60
S.D.(kN)	0.66	0.54	0.53

4.3 Minimization of Total Resistance in Seaway

The environment in which a high speed planing craft operates is not limited to calm water; for example, the WPB-110ft was designed to conduct coastal patrol and high speed pursuit in relatively high sea-states. While not as versatile, the IFC was designed for coastal patrol and high speed life-saving in conditions up to sea-state 1. Demonstrated in this section is the capability of the proposed framework to apply an optimization approach to improve the basis ship of both the WPB-110ft and IFC through consideration of seakeeping.

4.3.1 Minimization of Resistance in Seaway - IFC

The objective function represents an expansion of the problem definition presented in Section 4.2.1. Essentially, this formulation attempted to identify a candidate design of IFC with a minimum resistance in a seaway, R_T subject to constraints on displacement and stability.

$$\text{Minimize} \quad f(L_I, B_I, T_I) = R_T$$
$$\text{where} \quad R_T = R_C + R_A$$

The seaway operational scenario is defined using a Pierson-Moskovitz [116] energy spectrum in which the vessel is expected to operate in sea-state 1 ($H_{1/3}$=0.4m). Thirty independent runs of each of NSGA-II, IDEA and SA-EA were performed. A population size of 40, a crossover probability of 1, a mutation probability of 0.1, a crossover distribution of 10 and a mutation distribution index of 20 was used by all algorithms. The number of function evaluations used by each algorithm was restricted to 1200. An infeasibility ratio of 0.2 was used by IDEA. The surrogate models employed were restricted to the normalized response surface method (RSM), ordinary response surface method (ORSM), normalized radial basis function (RBF), ordinary radial basis function (ORBF) and kriging method (DACE). A training period of 3 and a prediction error of 0.05 were used by SA-EA.

In Figure 4.3, the best and median progress plots of NSGA-II, IDEA and SA-EA are shown. It can be observed in Figure 4.3(a) that all the algorithms were able to similarly minimize the resistance values in a seaway. SA-EA was able to converge faster than both NSGA-II and IDEA and obtained the optimized candidate design after 400 function evaluations, from which point no further appreciable improvement was achieved. In Figure 4.3(b), one can observe that

NSGA-II was able to find better a candidate design earlier than IDEA and SA-EA but after 400 function evaluations, IDEA and SA-EA performed better.

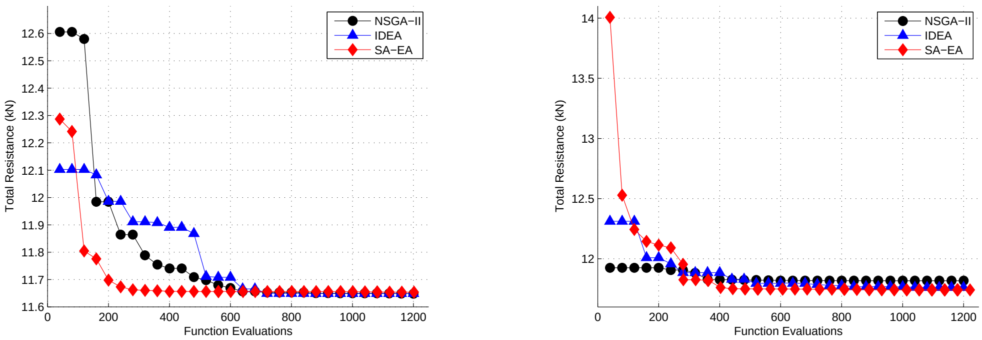

(a) IFC: Progress plots for R_T minimization using NSGA-II, IDEA and SA-EA, best designs

(b) IFC: Progress plots for R_T minimization using NSGA-II, IDEA and SA-EA, median design

Figure 4.3: IFC: Progress plots for R_T minimization using NSGA-II, IDEA and SA-EA

The values of best, mean, median, worst and standard deviation (S.D.) designs obtained are presented in Table 4.6. Presented in Table 4.7 are the best designs obtained using NSGA-II, IDEA and SA-EA. All the algorithms were able to obtain final candidate designs with minimum resistance while operating in a seaway, where effectively similar final designs are observed. Presented to two decimal places, the optimized candidate designs' lengths, beams and drafts were 11.00m, 3.04m and 0.6m respectively which accounted for a reduction of 7.98% compared with those of the basis ship. As observed in Table 4.7, the beam and the length of the optimum candidate are longer compared with the basis ship. With regards to Savitky and Brown's equations shown in Equation (3.14), when the ratio $V_K/\sqrt{L} = 6$, the added resistance value are influenced mostly by product of B^3 (to the power of 3) of the craft. However, the R_T (which equals to $R_C + R_A$) was able to be reduced due to the influence of the large L while maintaining the displacement value during the calculation of R_C.

Table 4.6: IFC: Best, Mean, Median, Worst and S.D. designs obtained using NSGA-II, IDEA and SA-EA for R_T minimization problem

Design	NSGA-II	IDEA	SA-EA
Best(kN)	11.65	11.65	11.65
Mean(kN)	11.84	11.80	11.80
Median(kN)	11.82	11.75	11.74
Worst(kN)	12.12	12.13	12.14
S.D.(kN)	0.138	0.141	0.151

Table 4.7: IFC: Best designs of NSGA-II, IDEA and SA-EA compared against basis ship for R_T minimization problem

	Basis Ship	NSGA-II	IDEA	SA-EA
Δ (kg)	7095.37	7095.70	7095.50	7095.39
L (m)	10.04	10.99	11.00	10.98
B (m)	2.86	3.04	3.04	3.05
T (m)	0.70	0.60	0.60	0.60
GM (m)	1.68	2.22	2.21	2.23
c_b	0.345	0.345	0.345	0.345
c_m	0.523	0.523	0.523	0.523
c_p	0.664	0.664	0.664	0.664
c_{wp}	0.737	0.737	0.737	0.737
WSA (m^2)	24.08	26.94	26.90	26.94
Fn	1.08	1.03	1.03	1.03
δ (^{o})	28.10	23.25	23.36	23.23
τ (^{o})	6.86	4.86	4.87	4.87
V (knots)	20.81	20.81	20.81	20.81
$H_{1/3}$ (m)	0.40	0.40	0.40	0.40
R_C (kN)	11.32	9.57	9.58	9.59
R_A (kN)	1.34	2.08	2.07	2.08
R_T (kN)	12.66	11.65	11.65	11.65
% reduction		7.98	7.98	7.98

4.3.2 Minimization of Resistance in Seaway - USCG WPB-110ft

The resistance minimization in a seaway problem for the USCG WPB-110ft was formulated as the identification of the planing craft's hull form with minimum total resistance in a seaway subject to constraints on displacement, stability and vertical impact acceleration, operating with the speed of 30 knots. The seakeeping scenario for sea-state 3 was modeled using Pierson-Moskovitz energy spectrum with significant wave height $H_{1/3} = 1.34$m. The objective function was similar to that previously defined for IFC shown in Section 4.3.1. Definitions of the variables and constraints were similar to those in Section 4.2.1. An additional constraint that reflected a limit[1] on vertical impact acceleration[2], η, for high speed planing craft of 1.5g [2], $g_7 : \eta \leq 1.5g$ was included.

For each algorithm (NSGA-II, IDEA and SA-EA), ten independent optimization runs were conducted. A population size of 40 was used, with a crossover probability of 1, a mutation probability of 0.1, a crossover distribution index of 10 and a mutation distribution index of 20 respectively for each algorithm. An infeasibility ratio of 0.2 was used by IDEA. SA-EA was executed first in order to obtain the number of function evaluations resulting over 30 generations. The surrogate models used by SA-EA were restricted to RSM, ORSM, RBF, ORBF and DACE, where a training period of 3 and a prediction error of 0.05 were incorporated.

The results across 10 runs for the best, median and worst designs are tabulated in Table 4.8. The low S.D. values indicates the consistency of convergence of the algorithms. Across 10 runs, the average number of function evaluations of SA-EA was 688. Therefore, for comparative purposes, 40 individuals were allowed to evolve in 18 generations, resulting in 720 function evaluations for NSGA-II and IDEA. One can observe that IDEA was able to reduce the total resistance by up to 7.95% followed by SA-EA (7.71%) and NSGA-II (7.35%).

Shown in Figure 4.4(a) are the total resistance values plotted for each algorithm across 10 runs, sorted from the lowest to highest values of total resistance.

[1]The design guidelines for selection of appropriate vertical impact acceleration corresponding to the effects on personnel and structural design for high speed craft are presented in Appendix A.

[2]Savitsky and Brown [94] reported that the vertical impact acceleration at bow, η_{bow}, is always larger than at the center of gravity, η_{bow}. Therefore the inclusion of vertical impact acceleration constraint in this work is referring to the vertical impact acceleration at bow.

It can be observed that, in general, IDEA and SA-EA were able to perform better than NSGA-II in solving the optimization of total resistance in a seaway. The progress plots are shown in Figure 4.4(b) for all algorithms. The best runs provided by SA-EA took only 480 function evaluations to arrive at the 30^{th} generation. It can be observed that SA-EA was faster to converge than NSGA-II for a given number of function evaluations. However, in this example, IDEA outperformed both NSGA-II and SA-EA in delivering a lower total resistance candidate design.

Table 4.8: USCG WPB-110ft: Best, Mean, Median, Worst and S.D. values obtained using NSGA-II, IDEA and SA-EA for R_T minimization problem

Algorithm	Best (kN)	Median (kN)	Worst (kN)	S.D. (kN)	% reduction
NSGA-II	163.65	164.36	166.77	1.250	7.35
IDEA	162.59	163.59	165.41	0.856	7.95
SA-EA	163.01	163.86	166.37	0.965	7.71

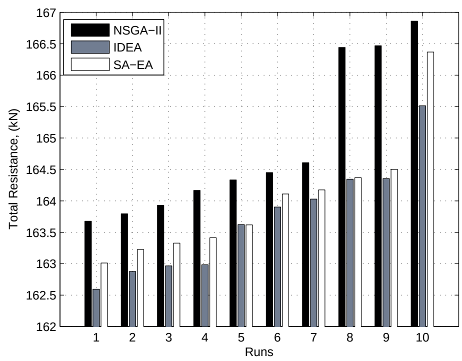

(a) USCG WPB-110ft: Comparison of R_T values obtained by NSGA-II, IDEA and SA-EA across 10 runs

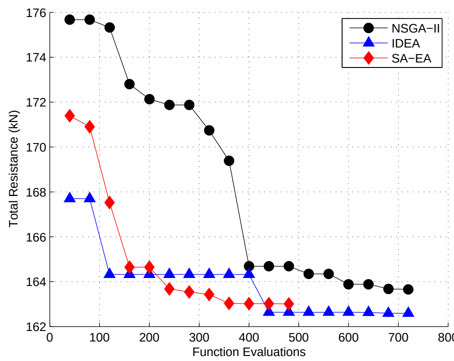

(b) USCG WPB-110ft: Progress plots of R_T minimization problem using NSGA-II, IDEA and SA-EA (best design)

Figure 4.4: USCG WPB-110ft: Progress plots and comparison of best designs obtained using NSGA-II, IDEA and SA-EA for R_T minimization problem

4.4 Multi-objective Optimization Case Study

Demonstrated in this section is the capability of the proposed framework to conduct a multi-objective optimization exercise using the example of WPB-110ft planing craft. The problem formulation is presented in Section 4.4.1 followed by the experimental results in Section 4.4.2.

4.4.1 Optimization Model

The multi-objective optimization problem posed is described as the identification of planing craft hull form geometries with minimum total resistance, R_T, vertical impact acceleration, η, and steady turning diameter, STD, subject to constraints on displacement, Δ, and stability (transverse metacentric height, GM), operating with the speed of 30 knots. The seakeeping scenario for sea-state 3 was modeled using Pierson-Moskovitz energy spectrum with significant wave height $H_{1/3} = 1.34$m. The objective functions are listed below, while the variables and constraints are the same as those in the single-objective model presented in Section 4.2.1.

$$\begin{aligned} \text{Minimize} \quad & f_1, f_2, f_3 \\ \text{where} \quad & f_1(L_I, B_I, T_I) = R_T \\ & f_2(L_I, B_I, T_I) = \eta \\ & f_3(L_I, B_I, T_I) = STD \end{aligned}$$

4.4.2 Numerical Results

The multi-objective optimization i.e. minimization of total resistance, R_T, steady turning diameter, STD and vertical impact acceleration, η is performed using

NSGA-II, IDEA and SA-EA. All the algorithms are able to obtain non-dominated solutions. The non-dominated solutions from all algorithms are then combined to form a pool of non-dominated solutions, as shown in Figure 4.5. It can be observed that the non-dominated set consists of a well-spread solution surface with good diversity which is a desirable outcome [149].

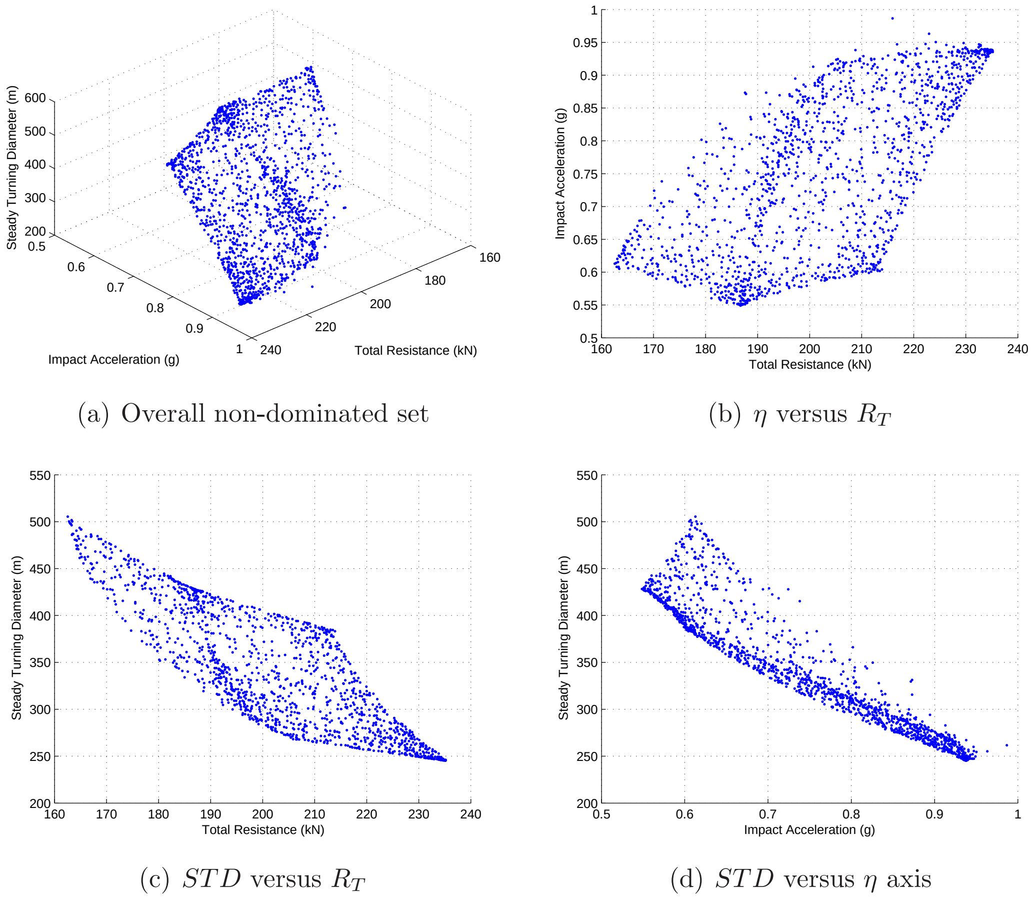

(a) Overall non-dominated set

(b) η versus R_T

(c) STD versus R_T

(d) STD versus η axis

FIGURE 4.5: COLLECTED NON-DOMINATED SET OF MULTI-OBJECTIVE OPTIMIZATION OF R_T, STD AND η USING NSGA-II, IDEA AND SA-EA

The summary of the data obtained from the multi-objective problem formulation is presented in Table 4.9. The results indicate the possibility of designs with R_T varying between 162.58kN and 235.21kN, STD between 245.37m and 505.52m and η between 0.549g and 0.987g. It is worth noting at this stage that the basis hull has a R_T of 176.65kN, STD of 373m and η of 0.75. One can observe that the design with minimum R_T has maximum STD. Similarly the design with minimum STD has maximum R_T.

Table 4.9: Summary data obtained for multi-objective problem formulation

Design	R_T (kN)	η (g)	STD (m)
Basis Ship	**176.65**	**0.75**	**373**
Minimum R_T	162.58	0.613	505.52
Maximum R_T	235.21	0.936	245.83
Minimum η	186.71	0.55	428.19
Maximum η	215.94	0.987	261.58
Minimum STD	235.13	0.938	245.37
Maximum STD	162.58	0.613	505.52

As shown in Figure 4.6, the basis ship is positioned on the non-dominated front of two objectives, R_T and STD. This is an interesting revelation that implies that the basis ship is among the optimum candidate designs. From the figure, what is evident is that the designer chose a good compromise between resistance and steady turning diameter and did not select a design representative of a single-objective analysis (either extreme). Using the proposed framework, demonstrated here is the capability to capture the decision trade-off while at the same time provide an understanding of the design of the USCG WPB-110ft basis ship.

4.5 Summary

In this chapter, three key case studies using two high speed craft examples were presented to demonstrate the capability of the proposed framework. The first two represented the applications of single-objective optimization in calm water and seaway operation. The third was a multi-objective optimization that included R_T, η and STD. The three case studies are summarized as follows.

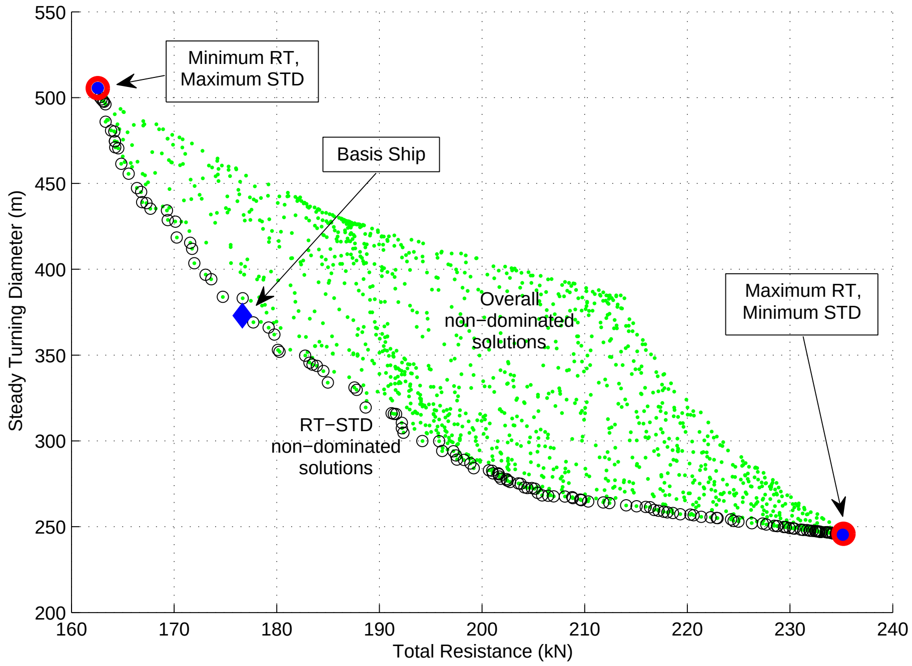

FIGURE 4.6: NON-DOMINATED SET FOR R_T AND STD

1. **Single-objective R_C minimization:** A single-objective calm water resistance minimization case study is demonstrated using IFC and WPB-110ft patrol craft. Up to 15.5% and 9.98% reduction of calm water resistance has been achieved for the IFC and WPB-110ft respectively. Across multiple runs, all the algorithms have small S.D. values indicating their consistency in terms of results and convergence. IDEA and SA-EA consistently exhibited faster rates of convergence as compared with NSGA-II.

2. **Single-objective R_T minimization:** A seaway operational scenario has been introduced in the optimization formulation where the IFC and WPB - 110ft are expected to operate in sea-state 1 ($H_{1/3} = 0.4$m) and sea-state 3 ($H_{1/3} = 1.34$m) respectively. It has been observed in the case study that 7.98% and 7.95% improvements in R_T can be achieved for the IFC and

WPB - 110ft respectively. Similarly, these results have also shown low S.D. values indicating the consistency of the converged solutions. Also, faster rates of convergence and better final solutions were also observed in the optimization results of IDEA and SA-EA than those of NSGA-II.

3. **Multi-objective optimization:** Minimization of total resistance (R_T), steady turning diameter (STD) and vertical impact acceleration (η) is performed using NSGA-II, IDEA and SA-EA. A well-spread solution surface with good diversity in three dimensions has been obtained. Discovered in this case study is the capability of the proposed framework to capture the decision trade-off between total resistance and maneuvering. Furthermore, it has been inferred that the candidate design with relatively low resistance and an acceptable steady turning diameter was seen to be more favorable than the lowest resistance candidate vessel with a large steady turning diameter achieved by the original designers of the basis ship.

The benefits of incorporating a surrogate assisted scheme was shown through the optimization results of SA-EA, while the advantage of preserving a small amount of infeasible solutions for solving high speed planing craft optimization has been presented by IDEA. Both schemes were able to perform better than NSGA-II in terms of the performance of the final candidate designs and convergence speed, thus allowing ship designers to perform useful resistance optimization with a reduced number of function evaluations. An effective means of solving resistance minimization problems for high speed planing craft has been presented in this chapter. The solution methodology has been proven to be useful for providing ship designers with optimum candidate designs while satisfying design requirements.

Chapter 5

Scenario-Based Hydrodynamic Design Optimization

Abstract

Encouraging results were observed for single-speed resistance minimization in the previous chapter. However, in reality, a ship needs to be operated across a varied operational profile (e.g. speed, operational time, sea-states) to satisfy its mission requirements. In this chapter, three hydrodynamic design optimization problems using the WPB-110ft and IFC craft based on their mission requirements are presented. This is referred to as *scenario-based* hydrodynamic design optimization. The scenarios are: (i) multiple speed operation; (ii) multiple sea-state operation; and (iii) operation considering the effects of vertical impact acceleration.

5.1 Introduction

In the previous chapter, optimal single-speed hydrodynamic designs were presented using WPB-110ft and IFC planing craft as examples. The results clearly indicated that significant improvements in terms of reduced resistance can be achieved. The proposed design optimization framework for high speed planing craft was shown to be capable of assisting ship designers by providing candidate hull designs with good performance in the preliminary design stage. In this chapter, the implications of incorporating an *operational profile* in the optimization formulations are explored.

An operational profile is a plan of where and how a ship is to be operated. A vessel's operational profile can be defined based on several aspects, such as the proportion of time spent at each operating speed, the operational environments encountered (e.g. sea-states) and the combinations of speeds and sea-states which depend on the ship's route/mission [30, 150, 151]. More broadly, several aspects that together form a *scenario* can be included in the operational profile such as tactical maneuver, electrical usage/failure and the effect of vertical impact accelerations on operators/mounted equipment.

Three key case studies that deal with scenario-based hydrodynamic design optimization for high speed planing craft are explored in this chapter. The first two utilize WPB-110ft as a basis vessel and address speed variations and multiple sea-states operation, while the third investigates the implications of imposing a vertical impact acceleration constraint on the high speed rescue craft, IFC. Overviews of these cases are presented below.

1. **Single Sea-state, Multiple Speed Operation**: There are six basic speed modes of a USCG patrol vessel outlined by the U.S. Department of Homeland Security [111], namely; idle, tow, patrol, low transit, high transit and intercept. The various times spent at each speed define the *operational tempo*. While most optimization studies in the literature aim to identify the best hull form for a particular speed, in reality such a craft is required to operate over a range of speeds during its lifetime. Therefore, an

optimization of a patrol vessel in a varying operational tempo is explored in Section 5.2.

2. **Multiple Sea-states, Single Speed Operation**: A design optimization case study is conducted, assuming a vessel with a predefined required speed is operating in multiple sea-states. Subsequently the task is to identify the best candidate design that may operate with minimum resistance across varying sea-states. The numerical model and results are presented in Section 5.3.

3. **Effects of η to a Small Craft**: A small high speed planing rescue craft usually arrives at an emergency scene earlier at sea than other support craft in order to perform initial rescue (e.g. from a collision, accident or grounding). In this case study, although the IFC (an equivalent of the USCG 30 foot SRB [152]) was claimed to be designed to operate at speeds of up to 30 knots in high seas, the information on the effect of vertical impact acceleration, η, has not been reported. Therefore, the outcome of imposing a vertical impact acceleration constraint in optimization is examined. The case study is presented in Section 5.4.

Finally, a summary of this chapter is provided in Section 5.5.

5.2 Single Sea-state, Multiple Speed Operation

5.2.1 Introduction

Fuel costs depend on the required engine output and the operating time of a vessel at each speed [126]. In the preliminary design stage, the required power of a vessel can be estimated through the use of resistance regression tools, principal particulars and the design speed. As speed can be decisive for the economic efficiency of a ship, its selection influences the main dimensions of a candidate design.

Shown in Table 5.1 is a set of generic speed guidelines for U.S. Coast Guard patrol vessels [111]. In this work, three operational speeds were chosen to illustrate this concept: patrol (16 knots); transit (25 knots); and intercept (30 knots). Divisions of the predefined times/tempos in which the candidate ship is expected to operate, that is, 60% at 16 knots, 20% at 25 knots and 20% at 30 knots, are shown in Figure 5.1.

Table 5.1: National security patrol craft operational speeds

Mode	Operations	Speed (knots)
Idle	Stopped (e.g. boarding)	0
Tow	Short distance transit/towing/training	5
Patrol	Economical patrol speed	15
Low Transit	Transit to patrol area – rougher seas	18
High Transit	Transit to patrol area – calmer seas	21
Intercept	Top mission speed	≥ 28

For a predetermined operational time of length, t, the total resistance experienced over the lifetime, R_L, with total resistance at 16 knots, 25 knots and 30

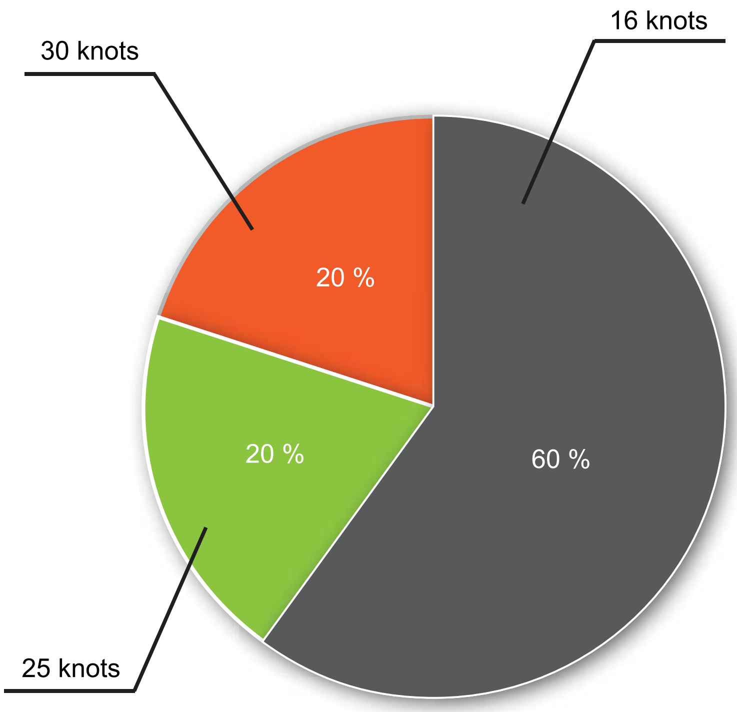

FIGURE 5.1: THE OPERATIONAL PROFILE PIE CHART

knots denoted as R_T^{16}, R_T^{25} and R_T^{30} respectively, can be written as

$$R_L = \sum(R_T^{16} \times 60\% + R_T^{25} \times 20\% + R_T^{30} \times 20\%) \times t \tag{5.1}$$

The value of t can be set as a constant (for example, $t = 1$) when comparing competing optimized candidate designs.

Determined from towing tank experiments at various model speeds, the effective power, P_E, is the power required to move a ship's hull at a given speed in the absence of propeller action. At the concept/preliminary design stage, where the knowledge on the propeller's efficiency is absent, it can be assumed that P_E is approximately equal to the thrust power, P_T, thus

$$P_E \approx P_T$$

where $P_E = R_T\,[\text{kN}] \times V\,\left[\frac{\text{m}}{\text{s}}\right]$.

The fuel consumption, FC, of a hull is proportional to the product of R_T and the speed experienced by the hull. Given the value of the specific fuel consumption, sfc, of its engine, the FC of a candidate ship is written as

$$\begin{aligned} FC &= P_E \times sfc \\ &= R_T\,[\text{kN}] \times V\left[\frac{\text{m}}{\text{s}}\right] \times sfc\left[\frac{\text{grams}}{\text{kW.s}}\right] \end{aligned}$$

Therefore, the lifetime fuel consumptions of competing candidate designs can be compared, assuming that the propulsive efficiency is same for 16, 25 and 30 knots. For a stage in which detailed information is available for ship designers, the high speed planing craft optimization can be executed to minimize the FC. However, given the limited information available in concept/preliminary design, the optimization problem is defined as the minimization of total resistance, R_T, and total resistance over a predefined lifetime, R_L.

5.2.2 Numerical Experimental Setup

The single-objective optimization problem executed is described as the identification of a planing craft hull form with minimum total resistance, R_T, subject to the constraints on displacement, Δ, and stability (transverse metacentric height, GM). A seaway operational scenario with one sea-state conforming to the Pierson-Moskovitz energy spectrum represented by a significant wave height of $H_{1/3} = 1.34$m (sea-state 1) is conducted. The objective function and constraints are listed below where the subscripts 'B', 'I', 'A' and 'C' denote basis ship, candidate ship, added resistance and calm water resistance respectively. The procedure for estimating R_T of the candidate design is bounded the by validation ranges suggested by [94] and [106] for half angle of entrance at the bow, I_e, length-cubic root of volumetric displacement ratio, $L/\nabla^{1/3}$, length-beam ratio, L/B and beam-draft ratio, B/T. These are included in the following formulation. The variable ranges are similar to that presented in Section 4.2.1.

$$
\begin{aligned}
\text{Minimize} \quad & f(L_I, B_I, T_I) = R_T \quad \text{where} \quad R_T = R_C + R_A \\
\text{Subject to} \quad & g_1 : \Delta_I > \Delta_B \\
& g_2 : GM_I \geq GM_B \\
& g_3 : 3.07 < L_I/\nabla_I^{1/3} < 12.4 \\
& g_4 : 3.7^o < Ie_I < 28.6^o \\
& g_5 : 2.52 < L_I/B_I < 18.28 \\
& g_6 : 1.7 < B_I/T_I < 9.8
\end{aligned}
$$

Minimization of total resistance over a set of collective speed is defined as

$$\text{Minimize:} \quad f(L_I, B_I, T_I) = R_L$$

where the constraints and variables are similar to those of the previous formulation.

5.2.3 Numerical Results

Thirty independent runs of IDEA were performed. A population size of 40, a crossover probability of 1, a mutation probability of 0.1, a crossover distribution index of 10, a mutation distribution index of 20 and an infeasibility ratio of 0.2 has been used by the algorithm. The number of function evaluations of the algorithm was restricted to 1200. The best, median, worst and standard deviation values of the objective functions obtained from optimization across 30 runs are reported in Table 5.2. The low values of the standard deviation indicate consistency in convergence of the optimization algorithm across 30 optimization runs.

The R_T values corresponding to the best run of IDEA for each speed are plotted against function evaluations in Figure 5.2(a) to 5.2(d). The algorithm was able to derive savings in R_T compared with the basis hull while satisfying the constraints on displacement and stability. In Table 5.3, the best designs are tabulated and compared against their corresponding basis designs operated at 16 knots (D^{16}), 25 knots (D^{25}), 30 knots (D^{30}) and different percentages of the speed spent lifetime (D^L). Other principal particulars such as the block coefficient, c_b, prismatic coefficient, c_p, waterplane coefficient, c_{wp}, deadrise angle, δ, and wetted surface area, WSA are also presented. The values in 'bold' typeset indicate the speeds for which they were optimized.

Table 5.2: Statistical summary of the objective functions values obtained using IDEA

Opt. Run	Best (kN)	Median (kN)	Worst (kN)	Std. Dev. (kN)
16 knots	41.87	42.26	45.21	1.00
25 knots	135.46	135.8	136.70	0.29
30 knots	161.95	162.96	166.28	1.30
Lifetime	84.31	85.35	87.84	1.35

As shown in Table 5.3, the values of R_T of the basis ship and the corresponding optimized candidate design operating at 16 knots (D^{16}) is 47.23 kN and 41.87 kN respectively, accounting for an 11.34% reduction. For the candidate design at 25 knots (D^{25}), a 10.87% reduction is achieved with the R_T of the basis and optimized candidate designs being 151.97 kN and 135.46 kN respectively. The value of R_T of the basis ship and optimized candidate design operating at 30 knots (D^{30}) is 176.65 kN and 161.95 kN respectively, giving a reduction of 8.32%. It can be observed that the R_T^{16}, R_T^{25} and R_T^{30} for D^L are 41.94 kN, 133.62 kN

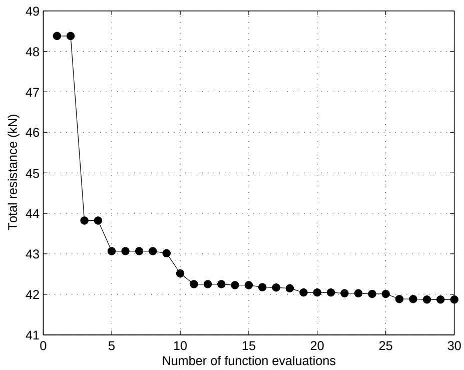

(a) Progress plot of best design for optimization at 16 knots

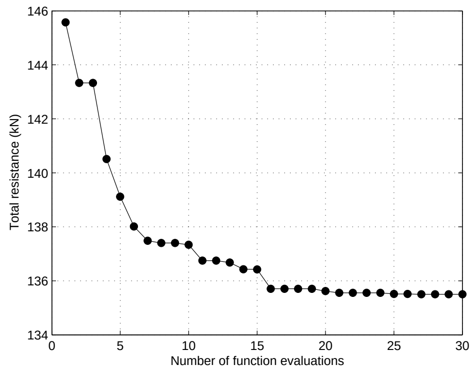

(b) Progress plot of best design for optimization at 25 knots

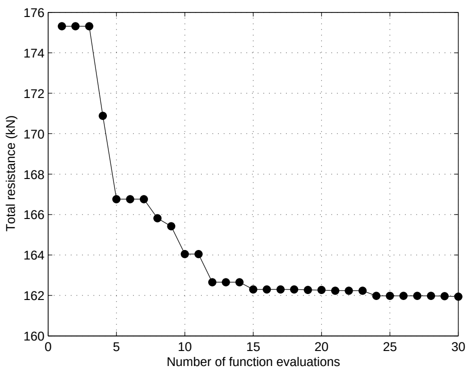

(c) Progress plot of best design for optimization at 30 knots

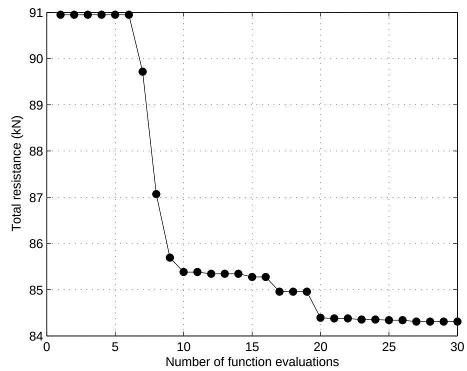

(d) Progress plot of best design for optimization at lifetime operation

FIGURE 5.2: PROGRESS PLOT OF BEST DESIGN FOR WPB-110FT OPTIMIZATION AT 16, 25, 30 KNOTS AND COLLECTIVE SPEEDS IN LIFETIME OPERATION

and 162.10 kN respectively, accounting for the highest savings when operated at 25 knots (12.07%) followed by 16 knots (11.20%) and 30 knots (8.23%). The R_L for basis and D^L is 94.06 kN and 84.31 kN respectively, resulting in a 10.37% of savings across the lifetime scenario.

The above observations suggest that the designs optimized for independent speeds of 16 knots (column D^{16}) and 30 knots (column D^{30}) were marginally better than that optimized for lifetime operations (column D^L). Furthermore, observing the marginal differences in terms of the designs of D^{16}, D^{30} and D^L, it can be implied that effectively similar performing designs were obtained by the three candidates. However, for the design optimized for 25 knots (column D^{25}), no significant improvements were noted compared with the designs observed in columns D^{16}, D^{30} and D^{L}.

Table 5.3: Minimization of R_T for three different speeds of 16, 25 and 30 knots

	Basis	D^{16}	D^{25}	D^{30}	D^{L}
$\nabla(\mathrm{m}^3)$	115.4	115.4	116.54	115.4	115.5
L(m)	32.93	35.92	35.91	35.92	35.93
B(m)	7.52	7.16	7.29	7.16	7.17
T(m)	1.6	1.52	1.51	1.52	1.52
GM(m)	1.64	1.64	1.80	1.65	1.65
c_b	0.291	0.295	0.295	0.295	0.295
c_p	0.680	0.686	0.686	0.686	0.686
$c_w p$	0.614	0.623	0.623	0.623	0.623
$\delta(^o)$	32.09	31.31	30.68	31.29	31.29
$WSA(\mathrm{m}^2)$	193.82	192.75	194.71	192.77	192.91
R_C^{16}(kN)	39.54	**34.33**	35.53	34.34	34.4
R_A^{16}(kN)	7.69	**7.54**	7.69	7.54	7.55
R_T^{16}(kN)	47.23	**41.87**	43.22	41.89	41.94
% savings		**11.34**	8.49	11.31	11.20
R_C^{25}(kN)	113.08	98.39	**99.35**	98.36	98.46
R_A^{25}(kN)	38.89	35.11	**36.11**	35.14	35.16
R_T^{25}(kN)	151.97	133.49	**135.46**	133.5	133.62
% savings		12.16	**10.87**	12.15	12.07
R_C^{30}(kN)	135.93	121.93	123.01	**121.9**	112.02
R_A^{30}(kN)	40.72	40.00	41.29	**40.05**	40.08
R_T^{30}(kN)	176.65	161.94	164.30	**161.95**	162.10
% savings		8.33	6.99	**8.32**	8.32
R_L(kN)	94.06	84.21	85.88	84.22	**84.31**
% savings		10.47	8.69	10.45	**10.37**

5.2.4 Impact on the Savings of Fuel Cost

The total resistance for each candidate design could be used to measure the fuel consumption given the operational definition; for example, from the United States Coast Guard Acquisition Directorate [153] and Karafiath *et. al.* [154], the expected operational tempo, t at sea for USCG WBP-110ft is 3000 hours per year. Therefore the fuel consumption, FC for the candidate designs with R_T^{16}, R_T^{25} and R_T^{30} given the value of specific fuel cost, sfc can be calculated using the expression below:

$$FC = (R_T^{16} \times V_{16} \times 0.6 + R_T^{25} \times V_{25} \times 0.2 + R_T^{30} \times V_{30} \times 0.2) \times sfc \times t \quad (5.2)$$

where V is in $\left[\frac{\mathrm{m}}{\mathrm{s}}\right]$ and the value of sfc is taken as, $sfc = 0.06\frac{\mathrm{grams}}{\mathrm{kW.s}}$ [155].

Shown in Table 5.4 are the fuel consumptions of the optimized candidate designs compared against the basis ship. In agreement to Table 5.3 shown previously, it can be observed that there were similarities among candidate designs D^{16}, D^{30} and D^{L} in terms of performance and principal particulars. It can be implied that the three candidates are effectively the same design, while D^{25} is a different design. It can be pointed out that, in this exercise, no advantage could be observed in terms of defining a set of collective speeds over a predefined lifetime. However, the proposed framework was proven to be capable of identifying the optimum hull form with a significant reduction in resistance against the basis ship, while at the same time enabling a provision for ship designers to evaluate the candidate designs in terms of performance over various operating scenarios.

Table 5.4: Fuel consumption comparisons among candidate and basis designs (t=3000 hours/year)

	FC[kg/hr]	fuel saving (%)
Basis ship	175.39	-
D^{16}	157.48	10.21
D^{25}	160.33	8.58
D^{30}	157.50	10.20
D^{L}	157.66	10.11

5.3 Multiple Sea-states, Single Speed Operation

In this section, the optimization of the WPB-110ft in multiple sea-states with a single speed of operation is presented. At a predefined geographic location, the basis ship is optimized through the minimization of total resistance for three sea-states. The optimized candidate designs obtained from the optimization exercise are then evaluated in terms of performance at the other respective sea-states. Through this case study, the best performing candidate ship across all sea-states is identified.

5.3.1 Introduction

The patrol craft, USCG WPB-110ft, is known to operate at various sea-states to accomplish its mission requirements [154, 89]. In this case study, the scenario-based optimization formulation illustrating a high speed pursuit operation in Northern Australian waters is presented. Upon the attainment of the optimized candidate designs, each of the designs are evaluated in different sea-states to identify the best candidate ship over varying sea conditions.

5.3.2 Numerical Experiments

This case study is defined as the identification of optimized candidate designs of a WPB-110ft patrol craft to operate in the coastal waters of Northern Australia. The patrol craft is required to operate with the speed of 30 knots in three sea-states as shown in Table 5.5, for which the sea-state data was obtained from the work of Peacock [30]. The region of interest around Darwin is shown in

Figure 5.3. The single-objective optimization formulation aimed to identify a coast guard patrol boat with minimum total resistance in a seaway, R_T, subject to constraints on displacement, stability (transverse metacentric height) and average vertical impact acceleration corresponding to the operational sea-states. The seaway scenario with three sea-states conforming to Pierson-Moskovitz energy spectrum represented by a significant wave height of $H_{1/3}$ is chosen, as shown in Table 5.5.

TABLE 5.5: USCG: OPERATIONAL SEA-STATES FOR OPTIMIZATION FORMULATION

Wind speed (ms^{-1})	Sea-state code	Sig. wave height, $H_{1/3}$ (m)
8.12	3	1.34 m
10.40	4	2.32 m
12.74	5	3.62 m

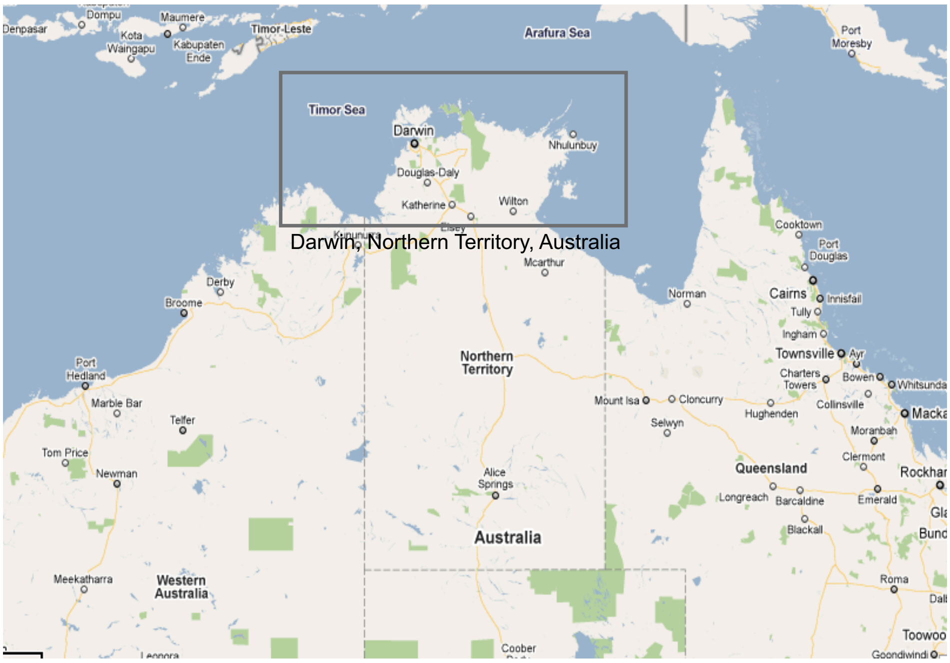

FIGURE 5.3: EXCLUSIVE ECONOMIC ZONE OF NORTHERN AUSTRALIAN WATERS NEAR DARWIN, 200 NAUTICAL MILES FROM COASTAL LINE

5.3.3 Numerical Results

For each algorithm (NSGA-II, IDEA and SA-EA), ten independent runs were executed. A population size of 40 has been used for each algorithm. The optimization parameters used are crossover probability of 1, mutation probability of 0.1, crossover distribution index of 10 and mutation distribution index of 20 respectively for all algorithms. The number of evaluations used by each algorithm is kept approximately equal for fair comparison of performance. An infeasibility ratio of 0.2 is used by IDEA. The surrogate models used were restricted to RSM, ORSM, RBF, ORBF and DACE with a training period of 3 and a prediction error of 0.05 has been used for SA-EA.

The results across 10 runs for best, median and worst designs are tabulated in Table 5.6, 5.7 and 5.8 respectively. This provides an indication of reliability for the three optimization algorithms used in this framework in this case. The details of the best designs obtained by NSGA-II, IDEA and SA-EA are similarly shown in Table 5.9, 5.10 and 5.11.

It can be seen in Table 5.6 that, for sea-states 3 and 4, IDEA and SA-EA were able to perform better than NSGA-II. However, for sea-state 5, IDEA was on par with SA-EA while NSGA-II performed better than the other two. As reflected by its fewer number of function evaluations, SA-EA was able to build surrogate models which reduced the computational effort.

Table 5.6: Summary of best designs across ten runs

		NSGA-II	IDEA	SA-EA
Sea-state 3	Avg. Num. of Fun. Eval.	720	720	688.4
	% Minimized Resistance	7.35	**7.74**	7.71
Sea-state 4	Avg. Num. of Fun. Eval.	880	880	856.8
	% Minimized Resistance	5.69	**6.11**	5.94
Sea-state 5	Avg. Num. of Fun. Eval.	760	760	744.3
	% Minimized Resistance	**4.19**	3.99	4.02

The median designs are reflected in Table 5.7. It can be observed that SA-EA was able to provide a better solution than IDEA and NSGA-II for sea-state 5 with fewer function evaluations and IDEA consistently reported better design solutions than NSGA-II for all sea-states. The same scenario can be observed for the worst designs across 10 runs shown in Table 5.8. Even though SA-EA was able to achieve a better solution for sea-state 5, IDEA consistently outperformed NSGA-II in providing optimized designs for all sea-states.

Table 5.7: Summary of median designs across ten runs

		NSGA-II	IDEA	SA-EA
Sea-state 3	Avg. Num. of Fun. Eval.	720	720	688.4
	% Minimized Resistance	6.96	**7.39**	7.32
Sea-state 4	Avg. Num. of Fun. Eval.	880	880	856.8
	% Minimized Resistance	5.08	**5.53**	4.61
Sea-state 5	Avg. Num. of Fun. Eval.	760	760	744.3
	% Minimized Resistance	3.41	3.63	**3.89**

Table 5.8: Summary of worst designs across ten runs

		NSGA-II	IDEA	SA-EA
Sea-state 3	Avg. Num. of Fun. Eval.	720	720	688.4
	% Minimized Resistance	5.59	**6.35**	5.81
Sea-state 4	Avg. Num. of Fun. Eval.	880	880	856.8
	% Minimized Resistance	2.90	**4.58**	3.88
Sea-state 5	Avg. Num. of Fun. Eval.	760	760	744.3
	% Minimized Resistance	2.51	2.71	**2.77**

5.3.4 Identifying the Overall Best Design

The discussion in Section 5.3.3 is now extended to provide insights for planing craft designers in identifying the overall best design performance of a craft in terms of resistance in a seaway and impact acceleration in a particular sea-state. Each optimized candidate design in its respective sea-state is analyzed in the other sea-states to help uncover the design that would operate well in all conditions. The comparisons of performance were based on the values of total resistance and

Table 5.9: WPB-110ft: Minimization of R_T with η constraint (NSGA-II best design)

	Sea-state 3 (1.32 m)		Sea-state 4 (2.32 m)		Sea-state 5 (3.62 m)	
	Basis	Optimized	Basis	Optimized	Basis	Optimized
Δ(kg)	118246.60	118281.76	118246.60	118250.05	118246.60	118369.30
L (m)	32.93	35.56	32.93	35.80	32.93	35.81
B (m)	7.52	7.24	7.52	7.22	7.52	7.17
T (m)	1.60	1.52	1.60	1.52	1.60	1.53
GM (m)	1.64	1.72	1.64	1.72	1.64	1.64
c_b	0.292	0.294	0.292	0.294	0.292	0.294
c_m	0.487	0.487	0.487	0.487	0.487	0.487
c_p	0.680	0.686	0.680	0.686	0.680	0.686
c_{wp}	0.614	0.623	0.614	0.623	0.614	0.623
WSA (m^2)	183.83	192.25	183.83	192.98	183.83	192.52
δ (^{o})	31.86	31.51	31.86	31.43	31.86	31.8
τ (^{o})	3.76	2.67	3.76	2.58	3.76	2.59
η (g)	0.754	0.632	1.128	0.937	1.625	1.333
R_C (N)	135932.36	123622.26	135932.36	122862.76	135932.36	123071.57
R_A (N)	40700.98	40032.72	52414.03	54762.12	65498.89	69917.93
R_T (N)	176633.34	163654.98	188346.39	177624.89	201431.25	192989.50
% savings	7.35		5.69		4.19	

Table 5.10: WPB-110ft: Minimization of R_T with η constraint (IDEA best design)

	Sea-state 3 (1.32 m)		Sea-state 4 (2.32 m)		Sea-state 5 (3.62 m)	
	Basis	Optimized	Basis	Optimized	Basis	Optimized
Δ(kg)	118246.60	118359.49	118246.60	118257.77	118246.60	118299.45
L (m)	2.93	35.88	32.93	35.92	32.93	35.43
B (m)	7.52	7.18	7.52	7.17	7.52	7.21
T (m)	1.60	1.52	1.60	1.52	1.60	1.54
GM (m)	1.64	1.66	1.64	1.66	1.64	1.66
c_b	0.292	0.294	0.292	0.294	0.292	0.294
c_m	0.487	0.487	0.487	0.487	0.487	0.487
c_p	0.680	0.686	0.680	0.686	0.680	0.686
c_{wp}	0.614	0.623	0.614	0.623	0.614	0.623
WSA (m^2)	183.83	192.88	183.83	192.88	183.83	191.48
δ (^{o})	31.86	31.69	31.86	31.7	31.86	31.77
τ (^{o})	3.76	2.57	3.76	2.55	3.76	2.72
η (g)	0.754	0.613	1.128	0.919	1.625	1.372
R_C (N)	135932.36	122802.66	135932.36	122619.34	135932.36	124149.43
R_A (N)	40700.98	39792.30	52414.03	54217.54	65498.89	69239.49
R_T (N)	176633.34	162594.96	188346.39	176836.88	201431.25	193388.91
% savings	7.95		6.11		3.99	

Table 5.11: WPB-110ft: Minimization of R_T with η constraint (SA-EA best design)

	Sea-state 3 (1.32 m)		Sea-state 4 (2.32 m)		Sea-state 5 (3.62 m)	
	Basis	Optimized	Basis	Optimized	Basis	Optimized
Δ(kg)	118246.60	118247.93	118246.60	118252.25	118246.60	118356.41
L (m)	32.93	35.9214	32.93	35.9103	32.93	35.1667
B (m)	7.52	7.23	7.52	7.19	7.52	7.22
T (m)	1.60	1.51	1.60	1.52	1.60	1.55
GM (m)	1.64	1.75	1.64	1.69	1.64	1.64
c_b	0.292	0.294	0.292	0.294	0.292	0.294
c_m	0.487	0.487	0.487	0.487	0.487	0.487
c_p	0.680	0.686	0.680	0.686	0.680	0.686
c_{wp}	0.614	0.623	0.614	0.623	0.614	0.623
WSA (m^2)	183.83	193.53	183.83	193.08	183.83	190.57
δ (^{o})	31.86	31.29	31.86	31.56	31.86	31.94
τ (^{o})	3.76	2.54	3.76	2.55	3.76	2.82
η (g)	0.754	0.622	1.128	0.925	1.625	1.388
R_C (N)	135932.36	122491.93	135932.36	122600.45	135932.36	125144.27
R_A (N)	40700.98	40519.49	52414.03	54565.43	65498.89	68184.45
R_T (N)	176633.34	163011.42	188346.39	177165.88	201431.25	193328.72
% savings	7.71		5.94		4.02	

impact acceleration at the given sea-state for each optimized candidate hull. For the purpose of clarity, the results obtained using IDEA are used to illustrate the concept.

Each optimized design obtained using IDEA, in sea-states 3, 4 and 5 was allowed to operate in sea-state 3, as shown in Figure 5.4(a). One can observe that the optimum design for sea-state 4 performed better as it had lower total resistance value than the candidate design optimized at sea-state 3. However, the candidate design optimized for sea-state 5 operated in sea-state 3 with the highest resistance and impact acceleration. The same pattern was observed for all optimized designs allowed to operate in sea-state 4, as shown in Figure 5.4(b).

In Figure 5.4(c), the candidate design optimized in sea-state 5 had a lower resistance value than that optimized in sea-state 3, while the candidate design optimized in sea-state 4 had lower resistance and impact acceleration values compared with that optimized at sea-states 3 and 5. Therefore, it can be implied that, with the given number of function evaluations, the design optimized in

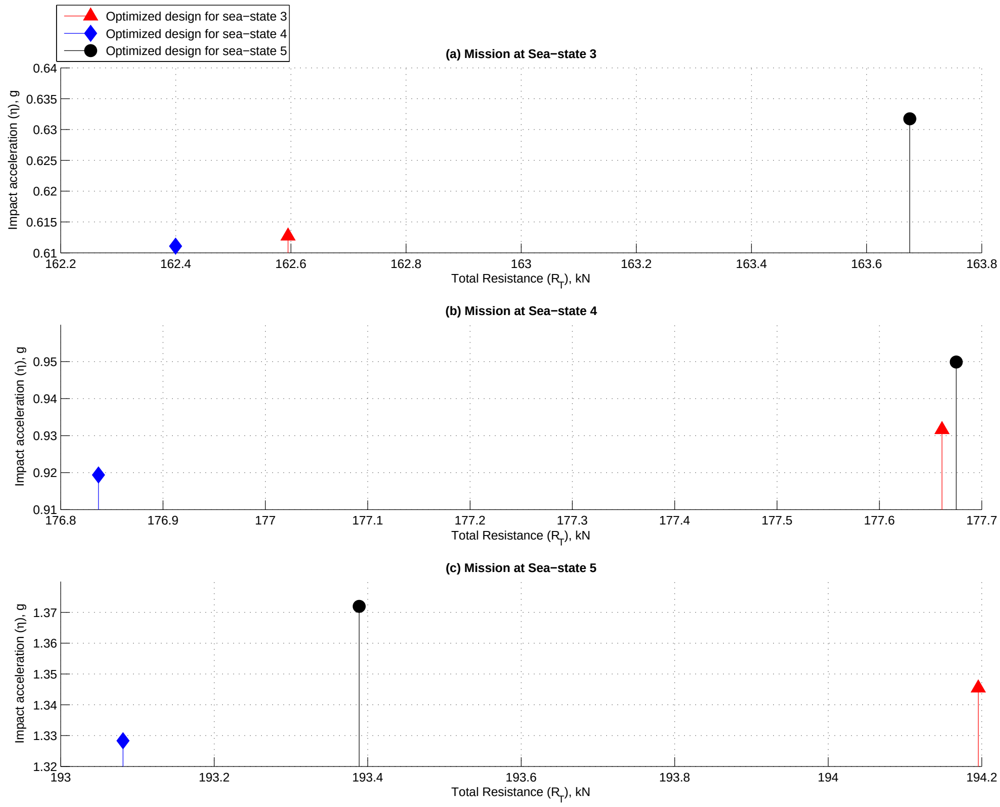

FIGURE 5.4: SEA-STATE OPERATIONAL SCENARIO FOR OPTIMIZED CANDIDATE DESIGN (IDEA)

sea-state 4 was identified as the most well-performing candidate for all sea-state operations (sea-states 3, 4 and 5).

The observations showed that, numerically, there were distinctions among the individual candidate designs optimized for each sea-states. However, from marine engineering point of view, what evident is, there exist only small variations in terms of the resistance and vertical impact acceleration values among the candidate designs optimized at sea-states 3, 4 and 5. For example, in Figure 5.4(a), the difference between the optimized design for sea-state 4 with the R_T value of 162.4 kN and that for sea-state 5 with the R_T value of 163.67 kN is only marginal (0.8%). This small variation indicates that, with additional computing resources, the solutions might converge to similar designs. However, the examples presented here were able to illustrate the identification of the best candidate design among other candidate designs optimized in different sea-states.

5.4 Effects of η to Small Craft

A scenario-based optimization of a fast rescue boat operating in the coastal area of Vishakapatnam in the Bay of Bengal, India is presented using the proposed framework. The problem is formulated through the minimization of R_T in two sea-states, with and without a vertical impact acceleration, η, constraint. The implications of imposing η for small high speed planing craft are described in this section.

5.4.1 Introduction

Small fast boats are primarily used as surveillance vessels near the coast while working in close liaison with law enforcement and emergency services. The IFC is a fast craft similar to the USCG 30 foot SRB [152] in terms of principal dimensions, hull shape and lightweight displacement. Such craft usually arrive at the emergency scene earlier than other support craft in order to perform initial rescue at sea (e.g. in the event of an accident such as, collision or grounding). The IFC was designed to be operated at speeds up to 30 knots in high seas by experienced crews [152]. Although the craft was designed to operate in adverse weather, the effect of vertical impact acceleration on the craft has not been reported.

An optimization problem, which modeled a scenario of a fast rescue boat operating in two different sea-states, was formulated. The outcome of imposing a vertical impact acceleration constraint on the optimization formulation and its effect on the candidate designs when operating in high seas are discussed. Later, it is shown that the basis ship, IFC, violated the safety requirement on vertical impact acceleration. Therefore, the optimization process was *induced* to begin in the infeasible design space. The performances of the optimization algorithms in solving such a problem are also discussed.

5.4.2 Numerical Experiments

This case study refers to the identification of optimized candidate designs to operate at a moderate speed of 21 knots around the coastal waters of Visakhapatnam in the Bay of Bengal, India. The wind speed data for this location which was obtained from the work of ShreeRam and Rao [156] is presented in Table 5.12. This coastal area features an upwelling[1] phenomenon that affects fishery, which is the main economic activity. The season of interest was that of the monsoons in the southwest of the Bay of Bengal where high wind speeds of 5ms^{-1} to 7ms^{-1} are observed from May to September. The values of the significant wave height, $H_{1/3}$ were tabulated for sea-states 2 and 3 assuming Pierson-Moskovitz [2, 116] spectra. The location of interest is shown in Figure 5.5.

Table 5.12: IFC: Operational sea-states for optimization formulation

Wind speed (ms^{-1})	Sea-state code	Sig. wave height, $H_{1/3}$ (m)
6	2	0.8 m
7	3	1.1 m

Two optimization problems are presented in this study, namely; (i) resistance minimization with η constraint, and (ii) minimization of resistance without η constraint. The objective function and constraints are listed in Section 5.2.2.

[1] Upwelling is an oceanographic phenomenon that brings rich nutrients from deep water regions to the coastal area. The nutrients are then utilized by phytoplankton, an increase of which results in increased numbers of fish in the region [157].

FIGURE 5.5: TERRITORIAL WATERS OF VISHAKAPATNAM IN BAY OF BENGAL, INDIA, 12 NAUTICAL MILES FROM THE COASTAL LINE

The seakeeping assessment criteria adopted in this study was the vertical impact acceleration limit for small craft [2] where the maximum vertical impact acceleration chosen at any location of the planing craft for one or two hours of operation had to be less than or equal to 1.5g (Appendix A). Thus, an additional constraint $g_7 : \eta \leq 1.5\text{g}$ was imposed for the first optimization problem.

For each algorithm (NSGA-II, IDEA and SA-EA), ten independent runs were performed. A population size of 40, a crossover probability of 1, a mutation probability of 0.1, a crossover distribution index of 10, and a mutation distribution index of 20 were used for each algorithm. An infeasibility ratio of 0.2 was used by IDEA. The number of function evaluations used by each algorithm was kept approximately equal for a fair comparison. The surrogate models used were restricted to RSM, ORSM, RBF, ORBF and DACE. A training period of 3 and a prediction error of 0.05 was used for SA-EA.

5.4.3 Minimization of R_T in Seaway with η Constraint

The optimization progress plots of IFC with a vertical impact acceleration constraint are presented in Figure 5.6. In general, all the algorithms were able to derive savings in R_T compared with that of the basis hull while satisfying the constraint on vertical impact acceleration for sea-state 2, as shown in Figure 5.6(a). However, for sea-state 3, as shown in Figure 5.6(b), no saving in R_T was achieved. This is supported by the data presented in Table 5.13 to 5.15 which shows that the algorithms searched for feasible solutions at the expense of increased resistance values (denoted with 'upward arrow', ↑ sign). The cause of such results lies in the characteristics of the basis ship itself where its vertical impact acceleration is infeasible (2.11g) in sea-state 3 as it is greater than the imposed vertical impact acceleration limit of 1.5g.

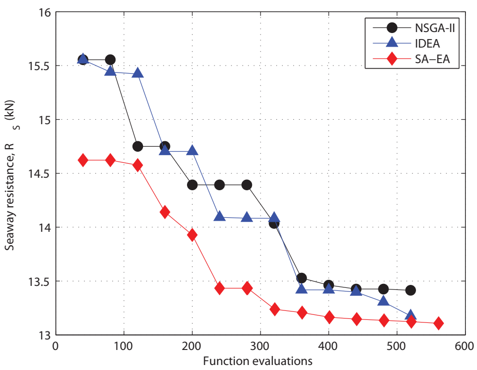

(a) Sea-state 2 ($H_{1/3} = 0.8$m)

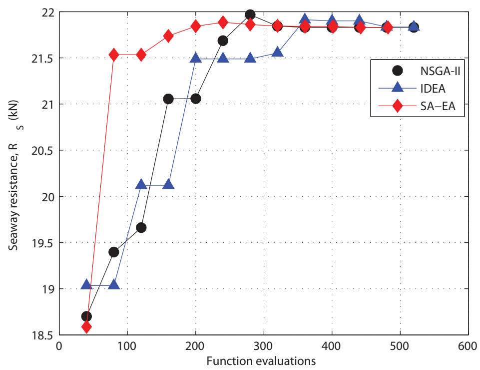

(b) Sea-state 3 ($H_{1/3} = 1.1$m)

Figure 5.6: IFC: Optimization progress plots with vertical impact acceleration constraint

Results for the minimization of R_T with the vertical impact acceleration constraint obtained using NSGA-II, IDEA and SAEA are tabulated in Tables 5.13 to 5.15. It can be observed that, for the IFC design optimized for sea-state 2 ($H_{1/3}$=0.8m), the basis ship exhibited a vertical impact acceleration of 1.64g, which was higher than the constraint imposed in the optimization formulation. NSGA-II was able to obtain feasible designs with a vertical impact acceleration of 1.5g at the expense of an increase in resistance of 0.79%. In contrast, IDEA and SA-EA were not only able to identify feasible designs, but also designs with reduced resistance values of 0.99% and 1.51%. Although both designs were shorter in length, the displacement values were compensated for by larger beam, which caused an increase in GM values.

For sea-state 3 ($H_{1/3}$=1.1m), all the algorithms were able to identify designs that satisfied the vertical impact acceleration constraint at the expense of an increase in R_T compared with that of the basis hull. Shown in Tables 5.13 to 5.15, NSGA-II, IDEA and SA-EA obtained candidate designs with increases in resistance of 61.16%, 61.18% and 61.15% respectively. This was caused by the limit of vertical impact acceleration that could be compensated for by larger principal parameters of length, beam, draft and the displacement. The outcome of these results obtained using EA implies that the vessel had to evolve to the extent of increasing its size in order to obtain lower vertical impact acceleration with the required speed.

Table 5.13: Minimization of R_T with η constraint (NSGA-II best design)

	Sea-state 2 (0.8 m)		Sea-state 3 (1.1m)	
	Basis	Optimized	Basis	Optimized
Δ(kg)	7204.94	7333.90	7204.94	11579.56
L (m)	10.04	9.10	10.04	10.99
B (m)	2.86	3.59	2.86	3.71
T (m)	0.70	0.63	0.70	0.79
GM (m)	2.00	3.22	2.00	2.73
c_b	0.35	0.35	0.35	0.35
c_m	0.53	0.53	0.53	0.53
c_p	0.66	0.66	0.66	0.66
c_{wp}	0.74	0.74	0.74	0.74
WSA (m^2)	24.08	25.87	24.08	33.27
δ (^{o})	27.95	20.57	27.95	24.84
τ (^{o})	6.96	6.60	6.96	6.65
η (g)	1.64	1.50	2.11	1.50
R_C (N)	11547.02	11065.94	11547.02	17466.37
R_A (N)	1761.35	2348.19	1998.88	4364.30
R_T (N)	13308.37	13414.13	13545.90	21830.67
Difference in R_T (%)	0.79 (↑)		61.16 (↑)	

Table 5.14: Minimization of R_T with η constraint (IDEA best design)

	Sea-state 2 (0.8 m)		Sea-state 3 (1.1m)	
	Basis	Optimized	Basis	Optimized
Δ (kg)	7204.94	7260.53	7204.94	11572.02
L (m)	10.04	9.21	10.04	10.97
B (m)	2.86	3.65	2.86	3.72
T (m)	0.70	0.60	0.70	0.79
GM (m)	2.00	3.41	2.00	2.75
c_b	0.35	0.35	0.35	0.35
c_m	0.53	0.53	0.53	0.53
c_p	0.66	0.66	0.66	0.66
c_{wp}	0.74	0.74	0.74	0.74
WSA (m^2)	24.08	26.38	24.08	33.27
δ (^{o})	27.95	19.62	27.95	24.77
τ (^{o})	6.96	6.24	6.96	6.65
η (g)	1.64	1.50	2.11	1.50
R_C (N)	11547.02	10619.00	11547.02	17462.53
R_A (N)	1761.35	2557.62	1998.88	4370.87
R_T (N)	13308.37	13176.62	13545.90	21833.40
Difference in R_T (%)	0.99 (↓)		61.18 (↑)	

5.4.4 Minimization of R_T in Seaway without η Constraint

In this section, the results of resistance optimization without considering vertical impact acceleration of the IFC using NSGA-II, IDEA and SA-EA are presented.

TABLE 5.15: MINIMIZATION OF R_T WITH η CONSTRAINT (SA-EA BEST DESIGN)

	Sea-state 2 (0.8 m)		Sea-state 3 (1.1m)	
	Basis	Optimized	Basis	Optimized
Δ (kg)	7204.94	7229.68	7204.94	11581.66
L (m)	10.04	9.21	10.04	10.99
B (m)	2.86	3.65	2.86	3.72
T (m)	0.70	0.60	0.70	0.79
GM (m)	2.00	3.43	2.00	2.75
c_b	0.35	0.35	0.35	0.35
c_m	0.53	0.53	0.53	0.53
c_p	0.66	0.66	0.66	0.66
c_{wp}	0.74	0.74	0.74	0.74
WSA (m^2)	24.08	26.38	24.08	33.32
δ (^{o})	27.95	19.52	27.95	24.75
τ (^{o})	6.96	6.21	6.96	6.63
η (g)	1.64	1.50	2.11	1.50
R_C (N)	11547.02	10546.33	11547.02	17438.15
R_A (N)	1761.35	2561.58	1998.88	4391.37
R_T (N)	13308.37	13107.91	13545.90	21829.52
Difference in R_T (%)	1.51 ($\downarrow$)		61.15 ($\uparrow$)	

The discussions are geared towards the effect of disabling such a constraint on the performance of the algorithms and its impact on a real-world design for all sea-states.

The results for optimizations without the vertical impact acceleration constraint are shown in Figure 5.7. Total resistance values of the best run of each algorithm are plotted against function evaluations for sea-states 2 and 3 in both of which SA-EA was able to converge faster than IDEA and NSGA-II using its ability to build surrogate models. By comparing Figure 5.6(b) and Figure 5.7(b), one can observe that an increase in R_T as high as 61% was necessary in order to satisfy the impact acceleration constraint. However, a reduction of 2.97% was able to be achieved if the impact acceleration constraint is ignored, as shown in Figure 5.7(b).

Results for minimization of R_T without the vertical impact acceleration constraint obtained using NSGA-II, IDEA and SAEA are tabulated in Table 5.16, 5.17 and 5.18. For the candidate design of IFC optimized for sea-state 2 ($H_{1/3}$=0.8m),

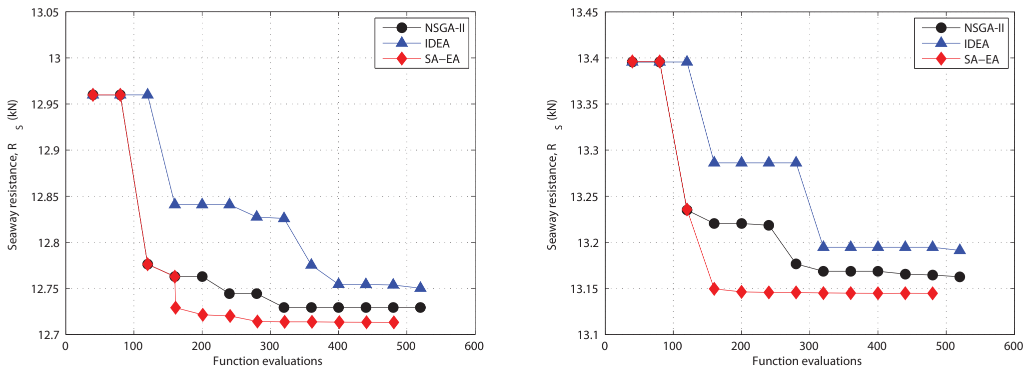

(a) Sea-state 2 ($H_{1/3}$ = 0.8m) (b) Sea-state 3 ($H_{1/3}$ = 1.1m)

FIGURE 5.7: IFC: OPTIMIZATION PROGRESS PLOTS WITHOUT VERTICAL IMPACT ACCELERATION CONSTRAINT

the basis ship experienced a vertical impact acceleration of 1.64g. It is interesting to note that, evolving to longer designs and smaller drafts, the candidate designs obtained were observed to have vertical impact acceleration of 1.58g, 1.59g and 1.58g which were all less than that of the basis ship. The amounts of resistance reduction obtained using NSGA-II, IDEA and SA-EA were 4.35%, 4.19% and 4.47% respectively.

It is also interesting to observe that, for sea-state 3 ($H_{1/3}$=1.1m), although the craft was set to operate in a higher sea-state, all the algorithms were able to reduce the resistance of the basis ship by up to 2.83%, 2.62% and 2.97% using NSGA-II, IDEA and SA-EA respectively. However, across all the candidate designs obtained by NSGA-II, IDEA and SA-EA, one can observe the value of the vertical impact acceleration being 2.06g. This suggests that the optimized candidate designs might only be suitable for unmanned surveillance and ruggedized shock-mounted equipment. In this particular example, it has been shown that:

- reductions in resistance can be realized even when imminent vertical impact acceleration is experienced[2];

- however, although less resistive hulls are able to be identified through the exercise, they are unsuitable for manned operation due to the high vertical impact acceleration value beyond the allowable limit of 1.5g [2]. Therefore, such craft may be useful for unmanned surveillance and ruggedized shock-mounted equipment.

Table 5.16: Minimization of R_T without η constraint (NSGA-II best design)

	Sea-state 2 (0.8 m)		Sea-state 3 (1.1m)	
	Basis	Optimized	Basis	Optimized
Δ (kg)	7204.94	7207.41	7204.94	7206.30
L (m)	10.04	10.98	10.04	10.97
B (m)	2.86	2.80	2.86	2.81
T (m)	0.70	0.65	0.70	0.65
GM (m)	2.00	2.06	2.00	2.07
c_b	0.35	0.35	0.35	0.35
c_m	0.53	0.53	0.53	0.53
c_p	0.66	0.66	0.66	0.66
c_{wp}	0.74	0.74	0.74	0.74
WSA (m^2)	24.08	25.51	24.08	25.53
δ (^{o})	27.95	26.85	27.95	26.77
τ (^{o})	6.96	5.40	6.96	5.39
η (g)	1.64	1.58	2.11	2.05
R_C (N)	11547.02	10172.77	11547.02	10166.02
R_A (N)	1761.35	2556.53	1998.88	2996.65
R_T (N)	13308.37	12729.30	13545.90	13162.67
Difference in R_T (%)	4.35 ($\downarrow$)		2.83 ($\downarrow$)	

5.5 Summary

In this chapter, three scenario-based hydrodynamic design optimizations for high speed planing craft case studies were presented. The first two case studies focused on optimization of the WPB-110ft high speed patrol craft while the third used the

[2]It can be argued that all high speed vessels become slow speed when some environmental threshold is reached. However, the case study indicated that a high speed planing craft with minimum resistance in a seaway could be obtained if high vertical impact acceleration is accepted.

Table 5.17: Minimization of R_T without η constraint (IDEA best design)

	Sea-state 2 (0.8 m)		Sea-state 3 (1.1m)	
	Basis	Optimized	Basis	Optimized
Δ(kg)	7204.94	7210.17	7204.94	7207.62
L (m)	10.04	10.97	10.04	10.99
B (m)	2.86	2.83	2.86	2.84
T (m)	0.70	0.65	0.70	0.64
GM (m)	2.00	2.10	2.00	2.13
cb	0.35	0.35	0.35	0.35
cm	0.53	0.53	0.53	0.53
cp	0.66	0.66	0.66	0.66
cwp	0.74	0.74	0.74	0.74
WSA (m^2)	24.08	25.62	24.08	25.75
δ (^{o})	27.95	26.51	27.95	26.20
τ (^{o})	6.96	5.37	6.96	5.30
η (g)	1.64	1.59	2.11	2.06
R_C (N)	11547.02	10146.15	11547.02	10081.61
R_A (N)	1761.35	2604.18	1998.88	3109.66
R_T (N)	13308.37	12750.33	13545.90	13191.27
Difference in R_T (%)	4.19 (↓)		2.62 (↓)	

Table 5.18: Minimization of R_T without η constraint (SA-EA best design)

	Sea-state 2 (0.8 m)		Sea-state 3 (1.1m)	
	Basis	Optimized	Basis	Optimized
Δ (kg)	7204.94	7206.40	7204.94	7205.98
L (m)	10.04	11.00	10.04	10.98
B (m)	2.86	2.80	2.86	2.79
T (m)	0.70	0.65	0.70	0.66
GM (m)	2.00	2.06	2.00	2.04
c_b	0.35	0.35	0.35	0.35
c_m	0.53	0.53	0.53	0.53
c_p	0.66	0.66	0.66	0.66
c_{wp}	0.74	0.74	0.74	0.74
WSA (m^2)	24.08	25.54	24.08	25.46
δ (^{o})	27.95	26.83	27.95	27.01
τ (^{o})	6.96	5.36	6.96	5.41
η (g)	1.64	1.58	2.11	2.04
R_C (N)	11547.02	10143.50	11547.02	10189.59
R_A (N)	1761.35	2569.75	1998.88	2954.54
R_T (N)	13308.37	12713.24	13545.90	13144.12
Difference in R_T (%)	4.47 (↓)		2.97 (↓)	

high speed IFC rescue craft. The outcomes of the case studies are summarized below.

1. **Single Sea-state, Multiple Speed Operation**: An optimization and analysis of high speed planing craft with a speed and use profile is presented. This scenario-based optimization was demonstrated using an operational

tempo requirement based on the U.S. Department of Homeland Security definitions. Optimized candidate designs identified at 16, 25 and 30 knots were further evaluated at the other respective speeds and their corresponding performances were compared. The study reported that a 10.21% reduction in fuel consumption was achieved over the performance of the basis design. Similar outcomes were observed among the candidate designs D^{16}, D^{30} and D^{L} in terms of performance and principal particulars, implying that they were effectively the same design, while D^{25} was fundamentally a different design. The proposed framework enables the ship designer to identify candidate designs for operations across different speeds with a predefined lifetime operational profile.

2. **Multiple Sea-state, Single Speed Operation**: An optimization exercise involving multiple sea-states was demonstrated in Section 5.3. At a predefined geographic location using ocean data, the basis ship was optimized for three individual sea-states. The resulting optimized candidate designs were then evaluated at the other sea-states and their results compared. Reductions in total resistance of the candidate design were obtained using the proposed framework, with up to 7.74%, 6.11% and 4.19% being identified to operate in sea-states 3, 4 and 5 respectively. For the given number of function evaluations, the formulation of the optimization model identified that across sea-states 3, 4 and 5, the candidate design optimized to operate in sea-state 4 performed better than those optimized to operate in sea-states 3 and 5 in terms of total resistance and vertical impact acceleration characteristics. Such an example illustrates the identification of the best candidate design among other candidate designs that are optimized in different sea-states.

3. **Effects of η to a Small Craft**: In Section 5.4, a scenario-based optimization of a fast rescue boat operating in the coastal area of Bay of Bengal, India was presented using the proposed framework. The problem was formulated through the minimization of R_T in two sea-states, with $H_{1/3}$ of 0.8m and 1.1m, with and without vertical a impact acceleration, η, constraint. Revealed in the first scenario is the capability to design a safe high speed planing craft with R_T reductions of up to 1.51%. Shown in the latter scenario is the capability of the proposed framework to produce candidate designs that may be suitable for unmanned operations and shock-mounted equipment with reductions in R_T of up to 4.47%.

Three case studies have been discussed in this chapter. The proposed framework provides the capability for ship designers to explore several candidate designs through the inclusion of operational profiles in the preliminary stage. Overall, the proposed optimization framework for high speed planing craft shows promise for solving and understanding scenario-based hydrodynamic design optimization problems.

Chapter 6

Beyond Hydrodynamic Design Optimization

Abstract

In the previous chapters, solutions to several optimization problems using the proposed framework were presented. The results showed the framework's capability to assist ship designers in designing optimal high speed planing craft. In this chapter, the question of "what is beyond hydrodynamic design optimization?" is addressed. A method for uncovering variable relationships, described as *innovization* is presented using optimization results of single-objective minimization of calm water resistance. The variable relationship in the form of a mathematical equation is then used as a low-cost performance approximation scheme for solving resistance minimization problems. This highlights the benefits of incorporating an innovization method in the high speed planing craft design optimization study.

6.1 Introduction

In the previous chapters, several optimization problems of varying complexity have been presented using the proposed framework. The demonstrations included single-objective calm water resistance minimization, design optimization for a seaway operation, scenario-based design optimization and multi-objective optimization of resistance in a seaway, maneuvering and vertical impact acceleration. The proposed framework was shown to be capable of providing superior candidate designs in the concept/preliminary design stage. Now, one might ask, what is there beyond hydrodynamic design optimization?

To answer such a question, the perspectives of both an optimization algorithm and a ship designer are considered. For optimization, the determination of an optimum design using an evolutionary algorithm involves several processes (e.g. evaluation, selection, mutation and recombination) across generations [158]. From a ship designer's perspective, Barnum and Mattson [159] highlighted that the process for determining good designs through an evolutionary process is akin to a traditional iterative manual process of combining and recombining features from an initial set of concept designs. Using an optimization algorithm, the determination of good designs is achieved through the definition of the *objective* function while the intuitive and innovative elements accumulated by a human (i.e. a ship designer) from years of design practice, that are imperative for determining good designs, are called *subjective* functions [158]. Therefore, the pursuit of obtaining good designs that begins with the determination of a suitable objective function, the variables and the constraints do not stop at the optimization algorithm level. The next step for the designer is to understand and manipulate the relationships that lie beneath the optimum designs.

The rationale[1] behind a set of optimized candidate ship designs obtained has not been widely discussed, although there are vast amounts of published literature on the development of mathematical models (e.g. regression models, computational fluid dynamics (CFD), finite element analysis (FEA)), faster algorithms and comparisons of the candidate designs' performance in solving ship design problems. The capability to uncover secrets behind optimum designs bring forth two advantages. Firstly, it provides for a deeper understanding of the characteristics of optimum designs and, secondly, allows for the derivation of a low-cost approximation scheme (henceforth referred to as a *pseudo-performance* indicator) for solving ship design optimization problems in the concept design stage (Figure 6.1). This process is called *innovization*.

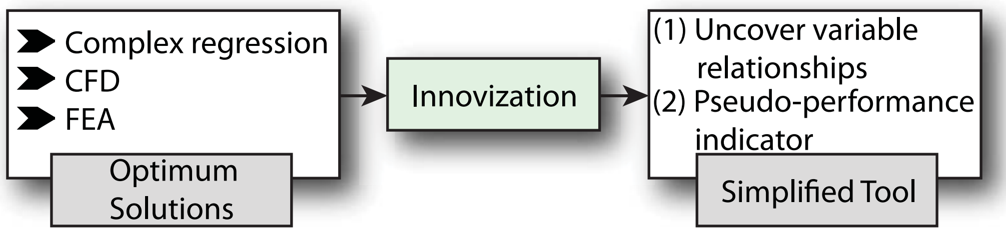

FIGURE 6.1: OVERVIEW OF INNOVIZATION CONCEPT

Deb and Srinivasan [161] defined *innovization* as "a method of finding new and innovative design principles by means of optimization techniques". Simply put, innovization is a combination of innovation and optimization methods. The process of discovering innovative design principles through optimization techniques allows ship designers to understand what lies beneath an optimized candidate ship design. Armed with this knowledge, meaningful reasoning can be extracted from a well-designed ship that has been obtained through optimization. The

[1]Rationale, is defined as 'an explanation of the fundamental reasons (especially an explanation of the working of some device in terms of laws of nature)' [160].

concept of innovization has been presented through various engineering design examples [161, 162, 163] involving a well-studied truss design problem, gear train design, multiple-disc clutch brake design and spring design. In real world design optimization problems, this concept has been demonstrated for optimal machining parameters [164], revealing some relationships that are not visible in a mathematical model. In turn, knowing such relationships may help designers to pinpoint and manipulate the variable(s) that lead to optimum designs.

Recently in [162], the principle of innovization was extended and compared with multi-adaptive regression splines (MARS) [165]. In principle, MARS does not assume a predetermined form for the fitting function and is sufficiently accurate to predict the value of an objective function given the independent variables but it lacks the provision of a meaningful and informing relationship in a design context. Although it is able to produce a set of piece-wise linear equations, the MARS model approach remains abstract in its expression. In contrast, the innovization method that assumes a form of fitting function, is able to find and deliver a meaningful and easy to interpret relationship between objective functions, variables and constraints. In this section, an attempt is made to generate relationships following the generic[2] form of Equation (6.1) [162].

$$\Pi_{j=1}^{N} \phi_j^{b_{ij}} = c_i \tag{6.1}$$

A designer establishes N design rules, ϕ_j, using post-optimization data (e.g. variables, objective functions and constraints), where c_i is the proportionality constant for the i-th design rule and the b_{ij}'s are the corresponding powers of the design rules. This form of equation can be readily computed and used by designers

[2]The generic form used in [162]'s work assumes a product of several variables.

unlike other forms such as neural networks or MARS models. Its utilization is further explained in Section 6.2 and the validity of the derived relationships are established through rigorous analysis.

The remaining parts of this chapter are organized as follows. In Section 6.2, an attempt to uncover the relationship between variables using post-optimization results is made. The relationships obtained are then used in a *pseudo-resistance* formulation and demonstrated in Section 6.3. Discussed in Section 6.4 are several proposals for future work, and Section 6.5 concludes the chapter.

6.2 Uncovering Variable Relationships

The results of the single-objective calm water resistance, R_C minimization problem for the WPB-110ft were presented in Section 4.2.3. For convenience, the summary of the best designs is presented in Table 6.1. The best designs obtained from 30 independent runs of NSGA-II, IDEA and SA-EA were accumulated to form a pool of optimized candidate solutions, as shown in Figure 6.2. The discovery of the relationships among the variables of the optimized candidate solution is in the form of solving a single-objective optimization problem, as shown in Equation (6.2) to (6.5), following the form of Equation (6.1).

Table 6.1: Single-objective calm water resistance optimization results

	NSGA-II	IDEA	SA-EA
R_C (kN)	122.37	122.39	122.39
L, B, T (m)	35.92, 7.28, 1.5	35.93, 7.28, 1.5	35.93, 7.27, 1.5

The single-objective optimization problem is defined by the minimization of the mean squared error (MSE) among the principal characteristics (L,B,T) of the optimized candidate solutions operating at 30 knots and the predicted principal characteristics (depicted by subscript 'p') as defined in Equation (6.2) to (6.5). The optimization problems are solved using NSGA-II with a population size of 100 evolving over 100 generations with a random seed of 10, a crossover probability of 1, a mutation probability of 0.1, a crossover distribution index of 10 and a mutation distribution of 20. These formulations effectively aimed to discover characteristic length-beam (r_{LB}), length-draft (r_{LT}), beam-draft (r_{BT}) and length-beam-draft (r_{LBT}) relationships among the set of promising solutions.

$$\text{For } r_{LB} \text{ relationship:} \quad B_p = x_1 L^{x_2}, \tag{6.2}$$

$$\text{minimize:} \quad f(x) = MSE(B - B_p)$$

$$\text{For } r_{LT} \text{ relationship:} \quad T_p = x_1 L^{x_2}, \tag{6.3}$$

$$\text{minimize:} \quad f(x) = MSE(T - T_p)$$

$$\text{For } r_{BT} \text{ relationship:} \quad T_p = x_1 B^{x_2}, \tag{6.4}$$

$$\text{minimize:} \quad f(x) = MSE(T - T_p)$$

$$\text{For } r_{LBT} \text{ relationship:} \quad T_p = x_1 B^{x_2} L^{x_3}, \tag{6.5}$$

$$\text{minimize:} \quad f(x) = MSE(T - T_p)$$

The variable bounds used for the discovery were set as $0 \leq x_1 \leq 100$, $-1 \leq x_2 \leq 1$ and $-100 \leq x_3 \leq 100$.

As stated previously, the innovization method assumes a form of fitting function to deliver meaningful and easy to interpret variable relationships for use by ship designers; for example, as shown in r_{LBT} (Equation 6.5), the formulation tries to find the MSE between the predicted draft, T_p, and the draft obtained from the pool of optimized candidate solutions, T. It is assumed that there exists a product relationship that fits the pool of the optimized candidate solutions. Following the form of Equation (6.1), the relationship is written as $x_1 = T_p B^{x_2} L^{x_1}$. Therefore, for the purpose of optimization, the form is written as $T_p = x_1 B^{-x_2} L^{-x_3}$. The negative sign is reflected later in the variable set where x_2 and x_3 are allowed to vary in the ranges $-1 \leq x_2 \leq 1$ and $-100 \leq x_3 \leq 100$, respectively.

Presented in Table 6.2 are the resulting derived relationships together with their corresponding MSE values. The progress plots of the constants of the four equations over the number of generations listed in Table 6.2 are presented in Figure 6.3. It can be observed that the resistance minimization induced the variables to align themselves in accordance with the relationships. The hypothesis at this stage is that low resistance designs would follow the relationships listed in Table 6.2. A closer look at Figure 6.2(a), 6.2(b) and 6.2(d) reveal that the candidate designs with lower R_C had large Ls and small Bs and vice-versa which similarly echoed by Shneekluth and Bertram [126]. The behaviour of variables L and B towards R_C highlighted in this work is also supported by Jons *et al.* [79] based on a database of planing patrol vessels. As shown in Figure 6.2(c), although the innovization formulation was able to derive a relationship for B and T, a weak correlation was observed in determining low/high resistance designs as compared with the observations made for Figure 6.2(a), 6.2(b) and 6.2(d).

Table 6.2: Derived relationship based on accumulated final design solutions of NSGA-II, IDEA and SA-EA

Description	Derived relationship	MSE
Length-beam relationship, r_{LB}	$77.8 = BL^{0.663}$	0.253
Length-draft relationship, r_{LT}	$5.66 = L^{0.37}T$	0.052
Beam-draft relationship, r_{BT}	$7.24 = B^{0.792}T$	0.016
Length-beam-draft relationship, r_{LBT}	$36.04 = L^{0.395}B^{0.89}T$	0.002

Shown in Table 6.3 are the characteristics of several classes of U.S. Coast

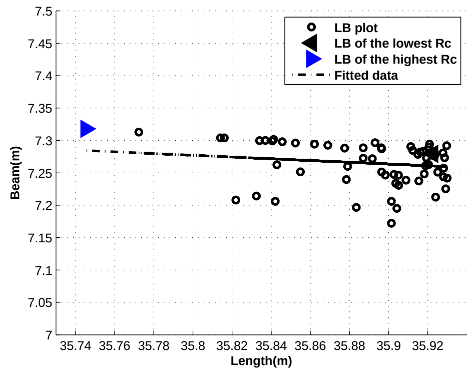

(a) r_{LB} relationship

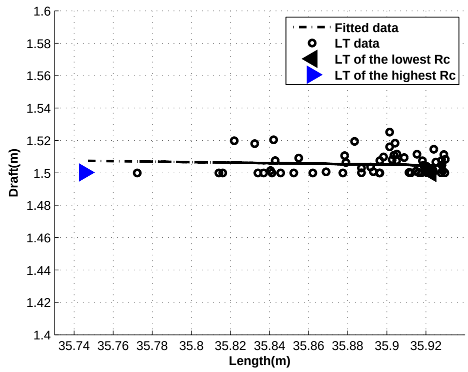

(b) r_{LT} relationship

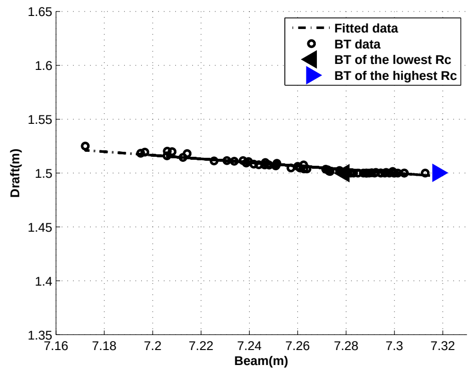

(c) r_{BT} relationship

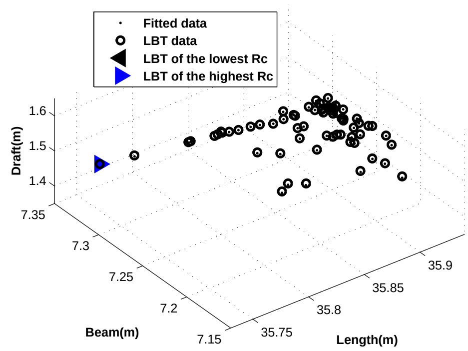

(d) r_{LBT} relationship

FIGURE 6.2: ACCUMULATED SINGLE-OBJECTIVE OPTIMIZATION FINAL DESIGNS OF ALL ALGORITHMS (NSGA-II, IDEA AND SA-EA) AND DISCOVERY OF DESIGN PRINCIPLES OF USCG WPB-110 PATROL CRAFT

Guard patrol boats: the 87-ft Marine Protector, 95-ft Cape and 110-ft Island. During the preliminary design stage, it is common for ship designers to calculate ratios, such as the length-to-beam (L/B) in order to indicate the slenderness (thus predicting the resistance characteristics) and stability of the vessel. The same procedure could be applied with the derived relationship where the values of L, B and T were substituted to obtain values for the ship. It can be observed in Table 6.3 that, although the L/B ratio values were almost similar, the r_{LBT} values varied significantly across the different classes. This indicates that further

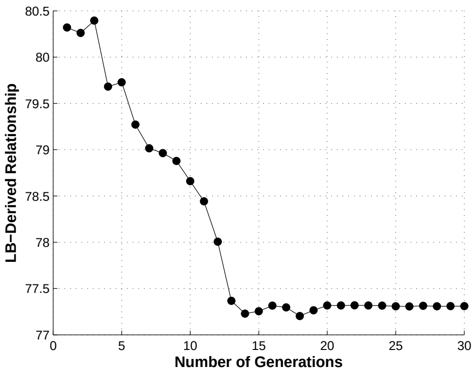

(a) r_{LB} relationship across generations

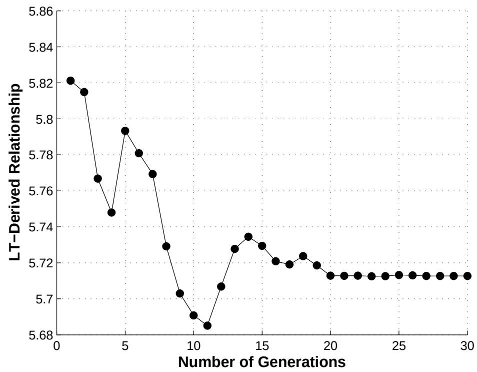

(b) r_{LT} relationship across generations

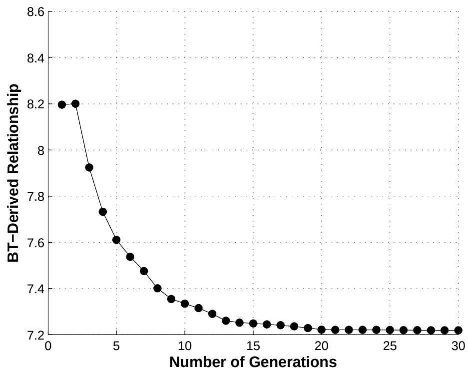

(c) r_{BT} relationship across generations

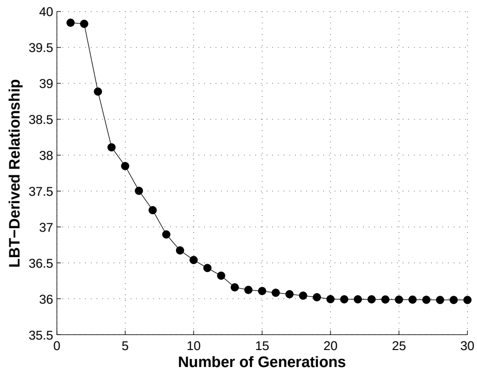

(d) r_{LBT} relationship across generations

FIGURE 6.3: CONVERGENCE BEHAVIOUR OF THE DEFINING DERIVED RELATIONSHIPS OF r_{LB}, r_{LT}, r_{BT} AND r_{LBT} ACROSS GENERATIONS USING DATA OF NSGA-II (RUN-1) AS AN EXAMPLE

studies must be conducted in order to consider the applicability of the derived expression for different classes of planing vessels. Deriving from a specific class, it was the interest of this preliminary study to observe the performance of the r_{LB}, r_{LT}, r_{BT} and r_{LBT} relationships using the example of WPB 110-ft patrol craft.

Examples of the calculated values based on the derived r_{LB}, r_{LT}, r_{BT} and r_{LBT} relationships plotted against resistance for a single optimization run are shown in Figure 6.4. It can be observed that a single value calculated using the derived r_{LB}

and r_{LT} relationship might return a wide range of different values of resistance as shown in Figure 6.4(a) and Figure 6.4(b). In contrast, the values calculated using the r_{BT} and r_{LBT} relationships show good correlation with resistance, as illustrated in Figure 6.4(c) and Figure 6.4(d). However, this is not supported for r_{BT} (shown in Figure 6.2(c)) as weak correlation were observed for determining high-low resistance designs. Thus the hypothesis at this stage is that the r_{LBT} relationship could be used as a basis for identifying low-resistance designs. In order to test this hypothesis, the resistance computation was replaced by the r_{LBT} relationship equation and the optimization problem solved using NSGA-II.

Table 6.3: USCG patrol craft design trend across classes

Class	87-ft Marine Protector	95-ft Cape	110-ft Island
L (m)	26.5	28.5	33.5
B (m)	5.8	6	7.5
T (m)	1.5	1.6	1.6
Δ (kg)	*-	102,000	116,000
v (knots)	26	25	30
C_v	1.773	1.676	1.799
Fn	0.822	0.762	0.845
L/B	4.57	4.75	4.47
B/T	3.41	3.00	3.75
L/T	17.67	17.81	20.94
r_{LB}	53.33	57.95	80.82
r_{BT}	3.58	3.88	4.34
r_{LT}	34.64	39.62	46.25
r_{LBT}	24.54	27.72	35.63

*Data unavailable in the literatures

6.3 Pseudo-resistance Minimization

The single-objective optimization problem posed is defined by the minimization of the pseudo-resistance derived from the r_{LBT} relationship shown in Table 6.2, subject to constraints on displacement (Δ) and stability (transverse metacentric height GM). The objective function and constraints are listed below where the subscripts 'B' and 'I' denote basis hull and candidate hull respectively. The optimization algorithm used is NSGA-II with a population size of 80, evolving

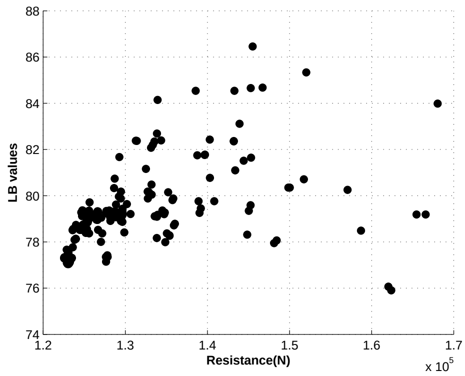

(a) Calculated LB values vs. Resistance

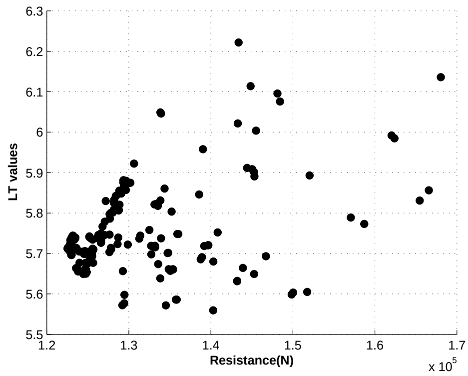

(b) Calculated LT values vs. Resistance

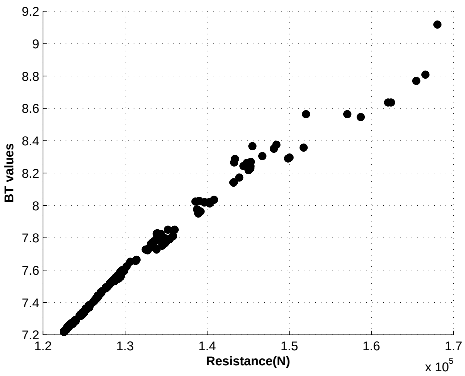

(c) Calculated BT values vs. Resistance

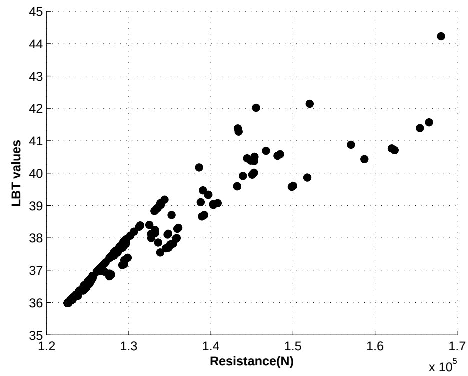

(d) Calculated LBT values vs. Resistance

FIGURE 6.4: OVERVIEW OF THE CALCULATED r_{LB}, r_{LT}, r_{BT} AND r_{LBT} VALUES AGAINST RESISTANCE ACROSS ONE OPTIMIZATION RUNS

over 60 generations with a random seed of 10, a crossover probability of 1, a mutation probability of 0.1, a crossover distribution index of 10 and a mutation distribution index of 20.

In addition to the variable bounds of L, B and T presented in the formulation, two new variable bounds were introduced to gain insight into the effect of larger variable ranges on the derived relationship. In total, three variable ranges for L, B and T which were included in the pseudo-resistance minimization problem are tabulated in Table 6.4. Variable Range 1 is defined by ±10% of the basis hull's length, beam and draft which is the same range as that applied in the actual

R_C minimization problem presented in Section 4.2. Variable Range 2 and Range 3 were defined by ±20% and ±50% of the basis hull's length, beam and draft, thereby serving to span a larger design space. Savitsky's validation constraints g_3, g_4, g_5 and g_6 as shown in Section 4.2.1 were included in the formulation to preserve the same feasible search domain of the pseudo-resistance as of the original resistance minimization formulation.

$$
\begin{aligned}
\text{Minimize} \quad & f(L_I, B_I, T_I) = L_I^{0.395} B_I^{0.89} T_I - 36.04 \\
\text{Subject to} \quad & g_1 : \Delta_I \geq \Delta_B \\
& g_2 : GM_I \geq GM_B \\
& g_3 : 3.07 \leq L_I/\nabla_I^{1/3} \leq 12.4 \\
& g_4 : 3.7^o \leq Ie_I \leq 28.6^o \\
& g_5 : 2.52 \leq L_I/B_I \leq 18.28 \\
& g_6 : 1.7 \leq B_I/T_I \leq 9.8 \\
\text{Variable bounds} \quad & 29.93m \leq L_I \leq 35.93m \quad (L_B = 32.93m) \\
& 6.51m \leq B_I \leq 8.51m \quad (B_B = 7.51m) \\
& 1.50m \leq T_I \leq 1.70m \quad (T_B = 1.59m)
\end{aligned}
$$

TABLE 6.4: DIFFERENT VARIABLE DEFINITIONS FOR PSEUDO-RESISTANCE OPTIMIZATION PROBLEM

	Var. Range 1		Var. Range 2		Var. Range 3	
	Low	High	Low	High	Low	High
L (m)	29.93	35.93	26.30	39.50	16.50	49.40
B (m)	6.51	8.51	6.00	9.00	3.76	11.28
T (m)	1.50	1.70	1.28	1.92	0.80	2.40

Shown in Figure 6.5 are the progress plots of the minimization of the r_{LBT} equation using three variable ranges across 60 generations. The objective function values and the corresponding variables L, B and T of the optimized candidate designs operating at 30 knots are presented to two decimal places in Table 6.5. It can be observed that all three formulations resulted in low objective function values with the lowest being is achieved by variable Range 1 with 2.202×10^{-8}, followed by variable Range 2 and Range 3 with values of 1.946×10^{-6} and 8.543×10^{-6} respectively. It is important to highlight that, for problems with extended variable ranges, the optimization algorithm needs to be run for a larger number of evaluations. For both variable Range 2 and Range 3 instances, there are still significant over satisfactions of the constraints due to their larger variable ranges. However, it could be observed that variable Range 1 reported values of L, B and T with close similarity to those observed in Section 4.2.3 (repeated in Table 6.1). The pseudo-minimization R_C values reported for variable Range 1, Range 2 and Range 3 were 122.55 kN, 122.57 kN and 122.37 kN respectively. While the pseudo-minimization R_C values using variable Range 3 resulted in a close value to the actual R_C minimization using Savitsky's [83] method reported in Table 6.1, the overall R_C minimization results using the pseudo-resistance equation reported in Table 6.5 is comparable with the actual R_C minimization results using Savitsky's [83] method. It is clear from this exercise, given the data of the optimized designs for a specific ship class, that the r_{LBT} equation can be derived and subsequently used in lieu of a full resistance computation. It is a computationally cheap indicator that can be used by designers to identify low-resistance hull form designs.

Table 6.5: Optimization results using pseudo-resistance equation

Variable Range	Objective Function, f	L(m)	B(m)	T(m)	R_C(kN)
Range 1	2.202×10^{-8}	35.87	7.24	1.51	122.55
Range 2	1.946×10^{-6}	39.36	7.08	1.48	122.57
Range 3	8.543×10^{-6}	36.42	7.80	1.40	122.37

In comparing with the optimization results obtained using Savitsky's regression model, it can be observed in Figure 6.5 that the optimization process converged and stabilized around the 20^{th} generation, accounting for 160 function evaluations, while in the R_C minimization presented in Chapter 4 (Figure 4.2(a)), the solutions converged at around 800 function evaluations. It can be concluded that the use of a pseudo-resistance formulation provides the advantage of faster convergence for optimization in the concept and preliminary design stages.

6.4 Future Work

In this chapter, a preliminary study that attempted to explore beyond hydrodynamic design optimization was presented. This work is known to be among the first to implement and contribute in the field of innovization for optimum high speed planing craft design. Encouraging observations have been made that lead

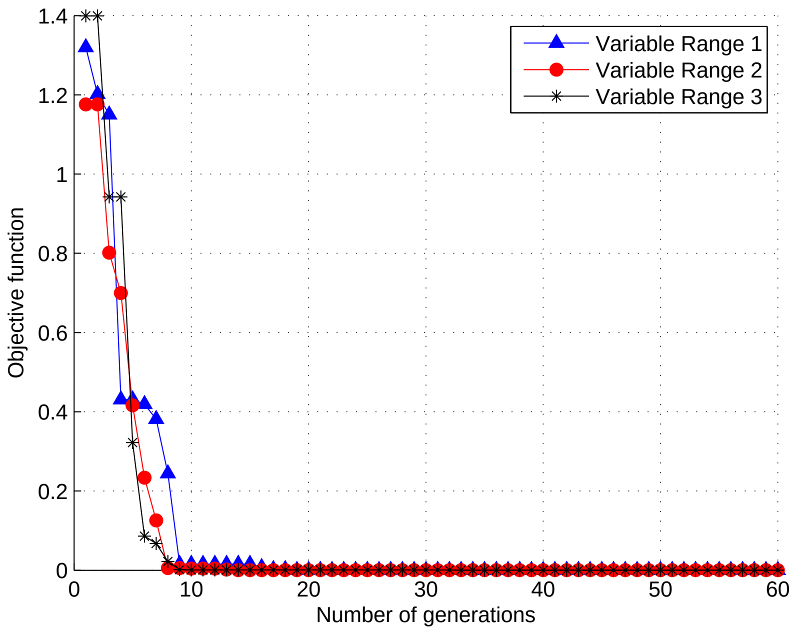

Figure 6.5: Progress plot of three single-objective optimization using different variable bound ranges

to suggestions for possible future work.

- The demonstration of the innovization concept has been applied to calm water resistance. This work can be extended to derive computationally cheap indicators for other performance measures such as seakeeping or maneuvering.

- Ship designers often use some form of relationship as design rules, such as the L/B ratio, prior to performance evaluations. Through the use of an innovization approach, the derivation of pseudo-performance indicators across different ranges of ships has been made possible. Interesting and valuable insights can be gained through the analysis of optimum designs, leading to the generation of new design rules for various classes of vessels.

- An innovization approach offers intuitive relationships among the variables in the pool of optimum designs. Post-optimization results obtained using higher fidelity tools (e.g. CFD and FEA) can be used to derive pseudo - performance indicators that are applied for optimization in concept design stage.

6.5 Summary

The principle of uncovering a variable relationship for low-resistance hard chine planing craft hull form designs was presented in this chapter. The optimization results obtained from single-objective calm water resistance minimization of WBP-110ft craft reported in Chapter 4 (Section 4.2.3) were used for the purpose of innovization. The accumulated optimization results were analyzed to uncover meaningful relationships that can be subsequently used to identify promising designs. The validity of such relationships were analyzed to derive a computationally cheap indicator that can be used in lieu of full resistance computation. It is interesting to observe that a pseudo-resistance minimization, i.e. use of the uncovered relationship equation instead of the computationally expensive resistance estimation, leads to a similar set of superior candidate designs. Although such expressions can be derived from a pool of optimized candidate designs for a particular ship class, their applicability for other classes needs to be investigated prior to its use. Proposals for future work include the derivation of pseudo-performance indicators across different ships. While, in this preliminary study both uncovering a relationship between variables and pseudo-resistance optimization was demonstrated using calm water resistance, the principle can be applied to derive computationally cheap indicators for other performance measures such as seakeeping or maneuvering. While the final design obtained from an optimization exercise is useful, interesting and valuable insights can be gained through an analysis of designs evaluated during the course of search, leading to the generation of new design rules for various classes of vessels.

Chapter 7

Conclusion

Presented in this thesis is a framework for optimum design of high speed planing craft. The framework incorporates a flexible geometry modeler, several experimentally derived naval architectural analysis tools and a suite of optimization algorithms to assist designers in the conceptual and preliminary design stages. The geometry modeler and the underlying analysis was validated using experimental data of the USCG WPB-110ft patrol craft. Thereafter, the framework was used to solve various single- and multi-objective formulations of high speed craft design problem. This thesis is one of the early works that investigates the use of optimization methods for the design of high speed planing craft engaged in various operational scenarios, rather than optimizing it for calm water and a single-speed operation. Furthermore, it provides an insight into the recipe behind superior designs identified using the principles of innovization.

7.1 Summary and Outcomes

The aim of this study was to develop a framework for optimum design of high speed planing craft in conceptual and preliminary design stages. To achieve this, a flexible geometry modeler and several experimentally derived naval architectural analysis tools were combined with state-of-the-art optimization algorithms. This optimization framework utilized a full geometric representation of hard chine planing craft, where the optimum design was identified based on the operational requirements.

The first step was the identification of a suitable mathematical model to represent the geometry of hard chine planing craft. The geometry representation and the analysis tools were then validated through the use of published experimental results. Measured validation errors of within 5% were observed between the published values and those of the generated model. Therefore, the identified mathematical model was deemed appropriate for its use within the optimization framework, particularly in the early stages of design.

The need for flexibility i.e. easy incorporation of analysis tools of varying fidelity and source (in-house or commercial) and the capability of representing various forms of the optimization problem is of paramount importance in any design tool supporting concept and preliminary design stages. An extensible, module-based optimization framework was developed that allowed customization of problem formulations, and utilized Component Object Model (COM) for a seamless integration between different analysis softwares. Furthermore, three state-of-the-art evolutionary algorithms was incorporated in the proposed framework, namely Non-dominated Sorting Genetic Algorithm (NSGA-II), Infeasibility Driven Evolutionary Algorithm (IDEA) and Surrogate Assisted Evolutionary Algorithm (SA-EA) to assist efficient solution of the optimization problems. The performance of the candidate designs obtained from these different optimization algorithms were compared to illustrate the benefits.

The first case study considered in this thesis related to the minimization of calm water resistance. Investigations were carried out using a well-known

USCG patrol craft, WPB-110ft, and a small fast rescue boat, IFC which is equivalent to the USCG 30-ft SRB craft. Reductions in calm water resistance of 10% and 15.5% were achieved for WBP-110ft and IFC respectively. These case studies were then extended to investigate resistance minimization in a seaway operation, in which both craft were optimized and reductions in R_T of up to 8% was achieved when compared with their respective basis designs. Following the success of single objective optimization studies, a multi-objective optimization case study was conducted using the WPB-110ft craft, wherein the objectives included the minimization of resistance in a seaway, vertical impact acceleration and steady turning diameter. It was revealed that the basis ship itself was one of the non-dominated solutions. The findings suggest that the designer chose the basis ship as a good compromise between resistance and maneuvering, and did not select a design representative of a single-objective analysis (either extreme). The proposed framework demonstrated the capability of capturing decision trade-offs.

Following the success of single- and multi-objective optimization case studies, a scenario-based hydrodynamic design optimization problem was attempted, wherein the craft was optimized for the following cases (i) multiple speeds operation and (ii) multiple sea-states operation. The effects of vertical impact acceleration constraint was also studied in the context of a small craft operation. The results illustrated the capabilities of the framework to deal with operational profiles in the preliminary design stage. It allows unique designs to emerge, based on specialized missions required to be accomplished by the candidate craft.

Finally, a preliminary case study aimed at investigating beyond hydrodynamic design optimization was presented. The concept of innovization, which combines the best of both design optimization tools and the ship designer's innovative skills, was introduced. This principle helps ship designers uncover the variable relationship that leads to low resistance hard chine planing craft hull form designs. Furthermore, the variable relationship expressed as a mathematical equation obtained from innovization was demonstrated to be able to serve as a pseudo-performance indicator. The optimization results were compared with those obtained using the original regression model (Savitsky) and resulted in a good match. The proposed use of the innovization principle shows promise for reducing computational load, especially in conjunction with higher fidelity tools e.g. CFD and FEA in the concept and preliminary design stages.

7.2 Achievements

This thesis has laid a foundation for a state-of-the-art optimization framework for the design of high speed planing craft. Its proposals, experimental results and findings complement those of ship designers for producing optimum planing craft for use in the recreational, commercial and military domains. In summary, the achievements evidenced in this thesis are grouped into the following five areas.

1. The first achievement is related to the identification of a validated 3D geometric model of a high speed planing craft. Through the use of the proposed planing craft geometry representation method, combined with experimentally derived naval architectural tools, a validated 3D mathematical model to represent the complete geometry of a high speed planing craft was identified and compared favorably with experimental data published in the literature. Such a capability is valuable for ship designers for the visualization. Furthermore, it provides for valid model generation capability within an optimization framework.

2. A modular design framework has been presented in this work. The proposal

focused on the use of the COM interface within a design framework. A workflow example using a number of analysis tools that were seamlessly coupled within the proposed framework was incorporated. It provides ship designers with the flexibility to include analysis tools of varying fidelity. Through a modular design framework, a ship designer is free to add/replace the modules.

3. The possible areas of optimization for high speed planing craft were thoroughly explored. The investigation started with the minimization of calm water resistance and resistance in a seaway, followed by a multi-objective optimization case study of total resistance, vertical impact acceleration and steady turning diameter. Later, optimization problems based on operational scenarios were explored. The capability offered by the proposed framework provides unlimited possibilities for creating designs for specialized missions of high speed planing craft.

4. Since it is known that there is no 'one-size-fits-all' algorithm for solving optimization problems [9], a real-coded evolutionary algorithm, an infeasibility-driven evolutionary algorithm and a surrogate-assisted evolutionary algorithm were incorporated in the proposed framework and the performance of the candidate designs obtained from different optimization algorithms were compared. All three algorithms were capable of solving the forms of the optimization problems posed with adequate efficiency.

5. A preliminary insight into what is beyond hydrodynamic design optimization was investigated. The "secrets" behind optimum planing craft designs were uncovered using the example of the WPB-110ft craft. A relationship in the form of a easily computable mathematical expression, was shown to be

an effective performance measure in concept and preliminary design stages. This finding opens up the possibility of developing of optimum design rules for any particular ship class.

7.3 Future Areas of Research

Following are suggestions for future areas of related research.

1. **Other Aspects of Ship Design:** The framework proposed in this thesis was constructed using experimentally validated empirical naval architectural tools and its capabilities were demonstrated through rigorous numerical experiments. Expanding beyond calm water resistance, this work featured the inclusion of added resistance in a seaway, vertical impact acceleration and maneuvering performance in the optimization formulation which could be extended to cater for other analysis, such as those of dynamic stability, cost and structural adequacy etc.

2. **Other Ship Forms and Types** (e.g. planing catamarans): The work presented in this thesis focused on monohull high speed planing craft. However, the capability of the proposed framework to represent a multihull craft such as a catamaran was demonstrated in Chapter 3. With modularity in mind, the inclusion of a multihull analysis would be possible.

3. **Higher-Fidelity Tools:** In this thesis, empirical regression models were used in the case studies. However, as the empirical tools were restricted in terms of their range of applicability and the hull type being interrogated, it was not possible to discover truly innovative designs (designs with unusual looks). However, this could be possible through the use of more first

principle-based analytical methods, such as computational fluid dynamics (CFD).

4. **Beyond Hydrodynamic Design Optimization:** Distilling design rationales from a pool of optimized candidate ship designs is an area largely unexplored as of today. Since vast amount of data is generated during numerical/physical experiments, the approach offers a mechanism to uncover useful relations which in turn could be used as cheap performance indicators. In this work, innovization principles were demonstrated using the well known USCG WPB-110ft craft. New design rules for other ship types could be developed using the method proposed in this thesis.

Bibliography

[1] Access Science McGraw-Hill. Ship Design Spiral. Webpage, 2011.

[2] D. Savitsky and J. G. Koelbel, Jr. Seakeeping of Hard Chine Planing Hull. Technical report, Society of Naval Architects and Marine Engineers, 1993.

[3] J. H. Evans. Basic Design Concepts. *Naval Engineers Journal*, 71:671–678, 1959.

[4] T. D. Lyon and F. Mistree. A Computer Based Method for Preliminary Design of Ships. *Journal of Ship Research*, 29:251–269, 1985.

[5] L. Lord. *Naval Architecture of Planing Hulls*. Cornell Maritime Press, 3rd edition edition, 1963.

[6] G. Rottman. *US Patrol Torpedo Boats, World War II*. Osprey Publishing, 2008.

[7] D. J. Clark, W. M. Ellsworth, and Meyer J. R. The Quest for Speed at Sea. Technical report, Naval Surface Warfare Center, Carderock Division, 2004.

[8] L. Jones. Emergency Vessels not 'Equipped' for High Seas. Canberra Times, May 2011.

[9] R. M. Lewis, V. Torczon, and Trosset M. W. Direct Search Methods: Then and Now. *Journal of Computational and Applied Mathematics*, 124(1-2):191 – 207, 2000.

[10] USCG. Coast Guard History. Electronic Web page, 12 2008.

[11] M. Bole. *A Hull Surface Generation Technique Based on a Form Topology and Geometric Constraint Approach*. PhD thesis, University of Strathclyde, Glasgow, UK, 2003.

[12] F. Chapman. *Tractat om Skepps-Byggeriet ("Treatise on Shipbuilding")*. 1778.

[13] D. W. Taylor. Calculations for Ships' Forms and the Light Thrown by Model Experiments upon Resistance, Propulsion, and Rolling of Ships. In *Transactions of the International Engineering Congress, San Francisco*, 1915.

[14] F. W. Benson. Mathematical Ships' Lines. *Transactions of the Institution of Naval Architects (INA)*, 82, 1940.

[15] A. Reed and H. Nowacki. Interactive Creation of Fair Ship Lines. *Journal of Ship Research*, 18, 1972.

[16] F. de Casteljau. Outillage Methodes Calcul. Technical report, Andre Citroen Automobilies SA, Paris, 1959.

[17] P. Bézier. *Numerical Control, Mathematics and Applications.* John Wiley and Sons, 1972.

[18] P. Bézier. Mathematical and Practical Possibilities of UNISURF. In *Computer Aided Geometric Design*, 1974.

[19] W. Gordon and R. Riesenfield. B-spline Curves and Surfaces. In Barnhill and Riesefield, editors, *Computer Aided Geometric Design.* Academic Press, 1974.

[20] L. Piegl and W. Tiller. *The NURBS Book.* Springer-Verlag Berlin / Heidelberg / New York, 1997.

[21] D. F. Rogers and S. G. Satterfield. B-spline Surfaces for Ship Hull Design. *ACM SIGGRAPH Computer Graphics*, 14(3):211–217, 1980.

[22] D. F. Rogers, S. Satterfield, and F. Rodriguez. Ship Hulls, B-spline Surfaces, and CAD/CAM. *IEEE Computer Graphics and Applications*, 3:37–45, 1983.

[23] S. Harries, C. Abt, and K. Hochkirch. Modeling Meets Simulation - Process Integration to Improve Design. In *Honorary Colloquium for Professor Hagen, Schluter and Thiel*, 2004.

[24] C. Abt and S. Harries. A New Approach to Integration of CAD and CFD for Naval Architects. In *Proceedings of the 6th International Conference on Computer Applications and Information Technology in the Maritime Industries (COMPIT2007)*, April 2007.

[25] H. Voelcker. Modeling in the Design Process. In *Design and Analysis of lntegrated Manufacturing Systems*, pages 167–199, Washington, DC, 1988. National Academy Press.

[26] R. Taggart and E. F. Magnusson. Mathematical Derivation of Destroyer-Type Hulls. *Naval Engineers Journal*, 79:19–28, 1967.

[27] M. Bole. Parametric Generation of Yacht Hulls. Master's thesis, Naval Architecture and Small Craft Design, University of Strathclyde, 1997.

[28] M. Bole and C. Forrest. Early Stage Integrated Parametric Ship Design. In *Proceedings of the 12th International Conference on Computer Applications in Shipbuilding (ICCAS 2005)*, Busan, South Korea, August 2005.

[29] S.L. Cooper, D. P. G. Burger, and T. P. McDonald. Concepts for a Fleet Tanker: An Exploration into Options and Pricing. In *Proceedings of the RINA Support Ships Conference*, 2007.

[30] D. A. Peacock. *Decision-Based Hydrodynamic Design of Displacement Monohulls*. PhD thesis, School of Mechanical and Manufacturing Engineering, July 1998.

[31] V. Shapiro. *Solid Modeling*. Elsevier Science Publishers, 2002.

[32] F. Perez-Aribas and J. Suarez. Quasi-developable B-spline Surfaces in Ship Hull Design. *Computer-Aided Design*, 39:853–862, 2007.

[33] S. Harries. *Parametric Design and Hydrodynamic Optimization of Ship Hull Forms*. PhD thesis, Institute of Naval Architecture and Ocean Engineering, Technische Universitt Berlin, 1998.

[34] F. Mistree, W. F. Smith, B. A. Bras, J.K. Allen, and D. Muster. Decision-Based Design: A Contemporary Paradigm in Ship Design. *Transactions of the Society of Naval Architects and Marine Engineers (SNAME)*, 98:565597, 1990.

[35] G. Creautz and C. Schubert. An Interactive Line Creation Method using B-splines. *Computer and Graphics*, 5:71–78, 1980.

[36] L. Bardis and M. Vafiadou. Ship-hull Geometry Representation with B-spline Surface Patches. *Computer-Aided Design*, 24(4):217 – 222, 1992.

[37] E. F. Campana, D. Peri, and U. P. Bulgarelli. Optimal Shape Design of a Surface Combatant with Reduced Wave Pattern. In *Reduction of Military Vehicle Acquisition Time and Cost through Advanced Modelling and Virtual Simulation*, 2002.

[38] A. Pinto, D. Peri, and E. F. Campana. Multi-objective Optimization of a Containership using Deterministic Particle Swarm Optimization. *Journal of Ship Research*, 51:217–228, 2007.

[39] L. J Doctors. A Versatile Hull-Generator Program. In *Proceedings of the Twenty-First Century Shipping Symposium*, pages 140–158, University of New South Wales, Sydney, Australia, 1995.

[40] H. Lackenby. On the Systematic Geometrical Variation of Ship Forms. *Transactions of the Institution of Naval Architects (INA)*, 92:289–315, 1950.

[41] H. Soding and U. Rabien. Hull Surface Design by Modifying an Existing Hull. In *Proceedings of the First International Symposium on Computer-Aided Hull Surface Definition Symposium (SCAHD '77)*, pages 19–29, 1977.

[42] M. Hoekstra and H.C. Raven. An Approach to Constrained Hydrodynamic Optimization of Ships. In *Marine Propulsion Conference*, 2004.

[43] A. Mason and G. Thomas. Stochastic Optimisation of IACC Yachts. In *Proceedings of the 6th International Conference on Computer and IT Application in the Maritime Industries (Compit 2007)*, pages 122–141, Cortona, 2007.

[44] T. W. Sederberg and S. R. Parry. Free-form Deformation of Solid Geometric Models. In *ACM SIGGRAPH Computer Graphics*, volume 20, pages 151–160, 1986.

[45] D. Peri and E. F. Campana. Multidisciplinary Design Optimization of Naval Surface Combatant. *Journal of Ship Research*, 47:1–12, 2003.

[46] I.L. Buxton. Engineering Economics Applied to Ship Design. *Transactions of the Royal Institution of Naval Architects (RINA)*, 114:409–428, 1972.

[47] D. Andrews. Creative Ship Design. *Transactions of the Royal Institution of Naval Architects (RINA)*, 123:447–458, 1981.

[48] A. J. Keane, W. G. Price, and R. D. Schachter. Optimization Techniques in Ship Concept Design. *Transactions of the Society of Naval Architects and Marine Engineers (SNAME)*, 133:123–140, 1991.

[49] C. Smith and R. G. Woodhead. A Design Scheme for Ship Structures. *Transactions of the Royal Institution of Naval Architects (RINA)*, 116:47–66, 1974.

[50] J. Moe and K. M. Gisvold. Optimization and Automated Design of Structures. Technical report, Division of Ship Structures, University of Trondheim, 1968.

[51] J. Moe and S. Lund. Cost and Weight Minimization of Structures with Special Emphasis on Longitudinal Strength Members of Tankers. *Transaction of the Royal Institution of Naval Architects (RINA)*, 110:43–70, 1968.

[52] H. Nowacki, F. Brusis, and P. M. Swift. Tanker Preliminary Design - An Optimization Problem with Constraints. *Transactions of the Society of Naval Architects and Marine Engineers (SNAME)*, 78:357–390, 1970.

[53] P.K. Pal. *Optimum Design of Trawlers*. PhD thesis, Indian Institure of Technology, Kharagpur, India, 1981.

[54] A. J. Lutkus, G. G. Piche, and K. E. Wagner. Sequential Optimization Technique for Trawler Design. Technical report, College of Engineering, University of Michingan, 1970.

[55] R. Hooke and T. A. Jeeves. Direct Search Solution of Numerical and Statistical Problems. *Journal of ACM*, 8:212–229, 1961.

[56] A. Z. Fiacco and G. P. McCormick. *Non-linear Programming: Sequential Unconstrained Minimization Technique*. Wiley, 1968.

[57] J. H. Evans and D. Khoushy. Optimized Design of Midship Section Structure. *Transaction of the Society of Naval Architects and Marine Engineers (SNAME)*, 71:144–191, 1975.

[58] A. H. Day. The Optimization of Aerodynamic Lift Distribution for a Heeled Yacht in a Wind Gradient. *Transaction of the Royal Institution of Naval Architects (RINA)*, 134:91–108, 1991.

[59] T. Ray. *Preliminary Ship Design in the Multiple Criteria Decision Making Framework*. PhD thesis, Indian Institute of Technology, Kharagpur, 1995.

[60] R. Leopold. Mathematical Optimization Methods Applied to Ship Design. Technical report, Department of Naval Architecture and Marine Engineering, Massachusetts Institute of Technology, 1965.

[61] C. E. Janson. Shape Optimization of a Simple Hull Fom with Respect to Total Resistance as Computed by SHIPFLOW system. Technical report, FLOWTECH Int. AB., Gothenburg, Sweden, 1992.

[62] C. E. Janson, K. J. Kim, L. Larsson, D. Holm, and B. Esping. Optimization of the Series 60 Hull from a Resistance Point of View. In *Prooceedings of the CFD Workshop Tokyo 1994*, 1994.

[63] J. J. Maisonneuve. Optimization Tools for Ship Resistance and Seakeeping Problems. In *Proceedings of the FAST93 - 2nd International Conference on Fast Sea Transportation*, 1993.

[64] V. Ganesan. *A Model for Multidisciplinary Design Optimization of Containership*. PhD thesis, Virginia Polytechnic Institute and State University, Blacksburg, Virginia, 1999.

[65] W. F. Smith. *The Modeling and Exploration of Ship Systems in the Early Stages of Decision-based Design*. PhD thesis, University of Houston, 1992.

[66] M. A. Gammon. *Ship Hull Form Optimization by Evolutionary Algorithm*. PhD thesis, Institute for Graduate Studies in Science and Engineering, Yildiz Technical University, Istanbul, 2004.

[67] M. Majumder, A. Akinturk, and S. M. Calisal. Optimized Design of Small Craft. *Marine Technology*, 39:67–76, 2002.

[68] A. H. Day and L. J. Doctors. Resistance Optimization of Displacement Vessels on the Basis of Principal Parameters. *Journal of Ship Research*, 41:249–259, 1997.

[69] R. Dejhalla, Z. Mrsa, and S. Vukovic. Application of Genetic Algorithm for Ship Hull Form Optimization. *International Shipbuilding Progress*, 48:117–133, 2001.

[70] R. Dejhalla, Z. Mrsa, and S. Vukovic. A Genetic Algorithm Approach to the Problem of Minimum Ship Wave Resistance. *Marine Technology*, 39:187–195, 2002.

[71] G. J. Grigoropoulos and D. S. Chalkias. Hull-Form Optimization in Calm and Rough Water. *Computer-Aided Design*, 42(11):977 – 984, 2010.

[72] G. J. Grigoropoulos. Hull Form Optimization for Hydrodynamic Performance. *Marine Technology*, 41:167–182, 2004.

[73] J. M. Vasconcellos. Optimization Procedure as Decision Tool for Ship Design. In *Proceedings of the Pacific 2010 International Maritime Conference (Pacific 2010)*, Sydney, Australia, 2010.

[74] R. Wolf, J. Dickmann, and R. Boas. Ship Design using Heuristic Optimization Methods. In *Proceedings of the 46th AIAA/ASME/ASCE/AHS/ASC Structures, Structural Dynamics and Materials Conference*, Austin, Texas, 2005. Massachusetts Institute of Technology.

[75] S. N. Neti. Ship Design Optimization using Asset. Master's thesis, Virginia Polytechnic Institute and State University, Blacksburg, Virginia, 2005.

[76] L. Koh, M. Atlar, E. Mesbahi, C-E. Janson, L. Larsson, and C Abt. Novel Design and Hydrodynamic Optimisation of a High-speed Hull Form. In *Proceedings of the 5th International Conference on High Performance Marine Vessels*, Shanghai, China, 2005.

[77] G. Zaraphonitis, A. Papanikolaou, and D. Mourkoyannis. Hull-form Optimization of High Speed Vessel with Respect to Wash and Powering. In *Proceeding of the 8th International Marine Design Conference*, pages 43–54, Athens, 2003.

[78] J. M. Almeter. Resistance Prediction and Optimization of Low Deadrise, Hard Chine, Stepless Planing Hulls. In *Proceedings of the Ship Technology and Research Symposium (STAR)*, 1995.

[79] O. P. Jons, J. Koelbel, and R. Sheldon. A New Generation of High-performance Planing Craft. *Naval Engineers Journal*, pages 234–247, 1985.

[80] A. F. Mohamad Ayob, T. Ray, and W. Smith. An Optimization Framework for the Design of Planing Craft. In *Proceedings of the International Conference on Computer Applications in Shipbuilding 2009 (ICCAS09)*, pages 181–186, Shanghai, 2009.

[81] A. F. Mohamad Ayob, T. Ray, and W. F. Smith. A Framework for Scenario-Based Hydrodynamic Design Optimization of Hard Chine Planing Craft. In *Proceedings of the 9th International Conference in Computer and IT Applications in the Maritime Industries (COMPIT'10)*. Technische Universitat Hamburg-Harburg, 2010.

[82] A. F. Mohamad Ayob, T. Ray, and W. F. Smith. Hydrodynamic Design Optimization of a Hard Chine Planing Craft for Coastal Surveillance. In *Proceedings of the Pacific 2010 International Maritime Conference (Pacific 2010)*, Sydney, Australia, 2010.

[83] D. Savitsky. Hydrodynamic Design of Planing Hull. *Marine Technology*, 1:71–95, 1964.

[84] V. Bertram. Appropriate Tools for Flow Analyses for Fast Ships. In *Proceedings of the 4th International Conference of High Performance Marine Vehicles (HIPER)*, Naples, Italy, 2008.

[85] T. Nagai and Y. Yoshida. Minimum Resistance Hull Form of Planing Craft with Controlled Trim Angle. In *Proceedings of the Sixth (1996) - International Offshore and Polar Engineering Conference (1996)*, 1996.

[86] P. D. Herrington and R. G. Latorre. Development of an Aluminum Hull Panel for High Speed Craft. *Marine Structures*, 11:47–71, 1998.

[87] O. Faltinsen and T. Svensen. Incorporation of Seakeeping Theories in CAD. In *Proceedings of the International Symposium on CFD and CAD in Ship Design*, 1990.

[88] J.M.J. Journee. Quick Strip Theory Calculations in Ship Design. In *Proceedings of the Conference on Practical Design of Ships and Mobile Structures (PRADS'92)*, 1992.

[89] J. A. White and D. Savitsky. Seakeeping Predictions for U.S.C.G Hard Chine Patrol Boats. In *Proceedings of the N.Y. Metropolitan Section of SNAME*, 1988.

[90] E. Lahtiharju, T. Karppined, M. Hellevaara, and T. Aitta. Resistance and Seakeeping Characteristics of Fast Transom Stern Hulls with Systematically Varied Form. *Transactions of the Society of Naval Architects and Marine Engineers (SNAME)*, 99:85–118, 1991.

[91] C. D. Barry, D. Gosh, R. Akers, and A. Ulak. Implementation, Application and Validation of the Zarnick Strip Theory Analysis Technique for Planing Boats. In *Proceedings of the High Performance Yacht Design Conference*, 2002.

[92] E. Zarnick. A Non-linear Mathematical Model of Motions of a Planing Boat in Regular Waves. Technical report, David W Taylor Naval Ship Research and Development Center, 1978.

[93] E. Zarnick. A Non-linear Mathematical Model of Motions of Planing Boat in Irregular Waves. Technical report, 1979.

[94] D. Savitsky and P. W. Brown. Procedures for Hydrodynamic Evaluation of Planing Hulls in Smooth and Rough Water. *Marine Technology*, 13:381–400, 1976.

[95] G. Fridsma. A Systematic Study of the Rough-water Performance of Planing Boats (Irregular waves - Part II). Technical report, 1971.

[96] E. Boulougouris and A Papanikolaou. Optimisation of the Survivability of Naval Ships by Genetic Algorithm. In *Proceedings of the 3rd Conference on Computer Applications and Information Technologies in the Maritime Industries (COMPIT'04)*, Siguenza, Spain, 2004.

[97] K. R. Akhil, D. Ghose, and R. S. Koteswara. Optimization Deployment of Multiple Decoys to Enhance Ship Survivability. In *Proceedings of the 2008 American Control Conference*, 2008.

[98] D. Radan, T.A. Sorensen, A.J.and Johansen, and A.K. Adnanes. Probability Based Generator Commitment Optimization in Ship Power System Design. In *WSEAS Transactions on Systems*, 2006.

[99] NAVSEA. Report to Congress on Alternative Propulsion Methods for Surface Combatants and Amphibious Warfare Ships. Technical report, Naval Sea Systems Command, United States Navy, 2007.

[100] N. H. Doerry. Sizing Power Generation and Fuel Capacity of the All-Electric Warship. In *Proceedings of the IEEE Electric Ship Technologies*, 2007.

[101] R. M. Birna, M. Dastani, J. C. Meyer, and F. S. de Boer. Goal-oriented Modularity in Agent Programming. In *Proceedings of the Fifth*

International Joint Conference on Autonomous Agents and Multiagent Systems, AAMAS '06, pages 1271–1278, New York, NY, USA, 2006. ACM.

[102] MSDN. Microsoft Developer Network Resources. Electronic Webpage Manual, 2011.

[103] M. Bole and B. S. Lee. Integrating Parametric Hull Generation into Early Design Stage. *Shiffstechnik / Ship Technology Research*, 53:115–137, 2006.

[104] D. F. Rogers and J. A. Adams. *Mathematical Elements of Computer Graphics*. McGraw-Hill Publishing Company, 1990.

[105] T. Pajdla and V. Hlavac. Surface Discontinuities in Range Images. In *Proceedings of the Fourth International Conference on Computer Vision*, pages 524 –528, may 1993.

[106] Maxsurf. Maxsurf User Manual Version 13. Technical report, Formation Design Systems, 2007.

[107] S. Percival, D. Hendrix, and F. Noblesse. Hydrodynamic Optimization of Ship Hull Forms. *Applied Ocean Research*, 23(6):337 – 355, 2001.

[108] K. Deb. *Optimization for Engineneering Design: Algorithm and Examples*. Prentice-Hall of India, 1995.

[109] A. Brown and M. Thomas. Reengineering the Naval Ship Concept Design Process. In *In Ship Systems Engineering Symposium, ASNE*, 1998.

[110] Maxsurf. Hullspeed User Manual Version 13. Technical report, Formation Design Systems, 2007.

[111] Commandant (CG-934). *Homeporting of Four National Security Cutters at Coast Guard Island, Alameda, California - Environmental Assessment*. U.S. Department of Homeland Security, 2007.

[112] S. B. Denny and N. E. Hubble. Prediction of Craft Turning Characteristics. *Marine Technology*, 28:1–13, 1991.

[113] E. M. Lewandowski. *The Dynamics of Marine Craft: Maneuvering and Seakeeping*. World Scientific Publishing Company, 2004.

[114] N. Salvesen, E. O. Tuck, and O. M. Faltinsen. Ship Motions and Sea Loads. *Transaction of Society of Naval Architects and Marine Engineers*, 78:250–287, 1970.

[115] N. Salvesen. Added Resistance of Ships in Waves. *Journal of Hydronautics*, 1(12):24–34, 1978.

[116] W. J. Pierson and L. Moskowitz. A Proposed Spectral Form for Fully Developed Wind Seas Based on the Similarity Theory of S. A. Kitaigorodskii. *Journal of Geophysical Research*, 69(24):51815190, 1964.

[117] K. P. Beier, H. Nowacki, C. Schubert, and A. Weichbrodt. A General Purpose Software System for Optimization in Ship Design. In *Proceedings of the ICCAS 76, A Scandinavian Joint Conference on Computer Applications in the Automation of Shipyard Operation and Ship Design*, pages 111–116, Gothenburg, Sweden, June 1976.

[118] A. Bosnic. *Optimization of Ship Design in Consideration of Technical and Economical Problems.* PhD thesis, Faculty of Mechanical Engineering and Naval Architecture, University of Zagreb, 1975.

[119] K.W. Fisher. Economic Optimization Procedure in Preliminary Ship Design. *Transactions of the Royal Institute of Naval Architects (RINA)*, 114, 1972.

[120] T. Kuniyasu. Application of Computer to Optimization of Principal Dimensions of Ships by Parametric Study. *Japan Shipbuilding and Marine Engineering*, 1968.

[121] P. Mandel and R. Leopold. Optimization Methods Applied to Ship Design. *Transactions of the Society of Naval Architects and Marine Engineers (SNAME)*, 74:477–521, 1966.

[122] R. Murphy, D.J. Sabat, and R.J. Taylor. Least Cost Ship Characteristics by Computer Techniques. *Marine Technology*, 2:174–202, 1965.

[123] M. G. Parsons. Optimization Methods for Use in Computer-Aided Ship Design. In *Proceedings of the First Technology and Research (STAR) Symposium, SNAME*, 1975.

[124] D. S. Somekh. Optimum Oil-Tankship by a Convergent Random Search Technique. Master's thesis, Massachusetts Institute of Technology (MIT), 1967.

[125] I. Grubisic, V. Zanic, and G. Trincas. Concept Design System for Interactive Optimization of Specialized Vessels. In *Proceedings of the Marine and Offshore Computer Applications*, 1988.

[126] H. Schneekluth and V. Bertram. *Ship Design for Efficiency and Economy.* Butterworth-Heinemann, 1998.

[127] I. Grubisic, V. Zanic, and G. Trincas. Concept Design System for Interactive Optimization of Fishing Vessels. In *Proceedings of the International Conference of Engineering Design*, 1990.

[128] A. Zborowski and S. R. Sainsbury. Small Vessel Hull Form Optimization for Heave and Pitch Performance. *Marine Technology*, 25, 1998.

[129] C. H. Huang, C. C. Chiang, and S. K. Chou. An Inverse Geometry Design Problem in Optimizing Hull Surfaces. *Journal of Ship Research*, 42:79–85, 1998.

[130] W. L. Neu, O. Hughes, W. H. Mason, S. Ni, Y. Chen, V. Ganesan, Z. Lin, and S. Tumma. A Prototype Tool for Multidisciplinary Design Optimization of Ships. In *Proceedings of the Ninth Congress of the International Maritime Association of the Mediterranean*, Naples, Italy, 2000.

[131] S. Harries, F. Valdenazzi, C. Abt, and U. Viviani. Investigation on Optimization Strategies for the Hydrodynamic Design of Fast Ferries. In *Proceedings of the International Conference on Fast Sea Transportation*, 2001.

[132] D. Hendrix, S. Percival, and F. Noblesse. Practical Hydrodynamic Optimization of Monohull. Technical report, David Taylor Model Basin, NSWC-CD, West Bethesda, Maryland, ETATS-UNIS, 2001.

[133] P. F. Chen and C. H. Huang. An Inverse Hull Design Problem in Optimizing the Desired Wake of Ship. *Journal of Ship Research*, 46:138–147, 2002.

[134] J. Heimann and S. Harries. Optimization of the Wave-Making Characteristics of Fast Ferries. In *Proceedings of the 7th International Conference on Fast Sea Transportation (FAST 2003)*, Ischia, October 2003.

[135] C. Koechert. Automatic CFD Optimizing of Hull Forms Using Strategy-Driven Transformation Functions. In *Proceeding of the 6th International Conference on Computer Applications and Information Technology in the Maritime Industries (COMPIT'07)*, 2007.

[136] D. L. Blount and D. L. Fox. Small-Craft Power Prediction. *Marine Technology*, 13(1):14–45, 1976.

[137] K. Deb, A. Pratap, S. Agarwal, and T. Meyarivan. A Fast and Elitist Multiobjective Genetic Algorithm: NSGA-II. *IEEE Transactions on Evolutionary Computation*, 6:182–197, 2002.

[138] K. Deb and R. B. Agrawal. Simulated Binary Crossover for Continuous Search Space. Technical report, Department of Mechanical Enginering, Indian Institute of Technology, Kanpur, India, 1994.

[139] K. Deb and M. Goyal. A Combined Genetic Adaptive Search (GeneAS) for Engineering Design. *Computer Science and Informatics*, 26:30–45, 1996.

[140] S.B. Hamida and M. Schoenauer. An Adaptive Algorithm for Constrained Optimization Problems. In *Proceedings of the 6th International Conference on Parallel Problem Solving from Nature*, PPSN VI, pages 529–538, London, UK, 2000. Springer-Verlag.

[141] S.B. Hamida and M. Schoenauer. ASCHEA: New Results using Adaptive Segregational Constraint Handling. In *Proceedings of the 2002 Congress on Evolutionary Computation, 2002. CEC '02.*, volume 1, pages 884 –889, may 2002.

[142] E. Mezura-Montes and C.A.C. Coello. A Simple Multimembered Evolution Strategy to Solve Constrained Optimization Problems. *IEEE Transactions on Evolutionary Computation*, 9(1):1 – 17, feb. 2005.

[143] H. K. Singh, A. Isaacs, T. Ray, and W. F. Smith. Infeasibility Driven Evolutionary Algorithm (IDEA) for Engineering Design Optimization. In *Proceedings of the 21st Australasian Joint Conference on Artificial Intelligence (AI'08)*, pages 104–115, Berlin, Heidelberg, 2008. Springer-Verlag.

[144] H. K. Singh, A. Isaacs, T. T. Nguyen, T. Ray, and X. Yao. Performance of Infeasibility Driven Evolutionary Algorithm (IDEA) on Constrained Dynamic Single Objective Optimization Problems. In *Proceedings of the Eleventh conference on Congress on Evolutionary Computation (CEC'09)*, pages 3127–3134, Piscataway, NJ, USA, 2009. IEEE Press.

[145] H. K. Singh. *Development of Optimization Methods to Deal with Current Challenges in Engineering Design Optimization.* PhD thesis, School of Engineering and Information Technology, University of New South Wales @ Australian Defence Force Academy, Canberra, Australia, 2011.

[146] A. Isaacs, T. Ray, and W. F. Smith. An Evolutionary Algorithm with Spatially Distributed Surrogates for Multiobjective Optimization. In *Progress in Artificial Life*, volume 4828/2007, pages 257–268. Springer Berlin / Heidelberg, 2007.

[147] G. V. Wilson. Extensible Programming for the 21st Century. *ACM Queue - Programming Languages*, 2:48–57, December 2004.

[148] K. A. De Jong. *Evolutionary Computation: A Unified Approach.* The MIT Press, 1st edition, March 2002.

[149] K. Deb. *Multi-objective Optimization using Evolutionary Algorithm.* John Wiley & Sons, LTD, 2001.

[150] G. Guzsvany, C. Flockhart, and S.M. Cannon. Operational Profile of Naval Surface Ships and Lifetime Structural Load Analysis. In *Proceedings of the Pacific 2006 International Maritime Conference*, Sydney, Australia, 2006.

[151] X. Xie, D. L. Xu, J. B. Yang, J. Wang, J. Ren, and S. Yu. Ship Selection using a Multiple-criteria Synthesis Approach. *Journal of Marine Science and Technology*, 13:50–62, 2008. 10.1007/s00773-007-0259-4.

[152] H. Halberstadt. *USCG–Always Ready*. Presidio Press, 1987.

[153] USCG. United States Coast Guard Acquisition Directorate. Electronic Web page.

[154] G. Karafiath, D. S. Cusanelli, S. D. Jessup, and C. Barry. Hydrodynamic Efficiency Improvements to the USCG 110 ft WPB ISLAND Class Patrol Boats. *Transaction of Society of Naval Architects and Marine Engineers*, 109:197–220, 2001.

[155] EPA. Commercial Marine Emission Inventory Development - Final Report. Technical report, United States Environmental Protection Agency, July 2002.

[156] P. ShreeRam and L.V.G Rao. Upwelling Features Near Sri Lanka in the Bay of Bengal. In K.V.S.R. Prasad, editor, *Proceedings of the National Symposium on Half A Century Progress in Oceanographic studies of North Indian Ocean since Prof. La Fond's Contributions (HACPO)*, pages 30–33. Andhra University, 2005.

[157] K. Mann and J. Lazier. *Dynamics of Marine Ecosystems: Biological-Physical Interactions in the Oceans*. Wiley-Blackwell, 3rd edition edition, November 2005.

[158] D. E. Goldberg. *The Design of Innovation: Lessons from and for Competent Genetic Algorithms*. Kluwer Academic Publishers, Norwell, MA, USA, 2002.

[159] G. J. Barnum and C. A. Mattson. A Computationally Assisted Methodology for Preference-Guided Conceptual Design. *Journal of Mechanical Design*, 132(12):121003, 2010.

[160] Princeton. Electronic Dictionary, 2011.

[161] K. Deb and A. Srinivasan. Innovization: Innovating Design Principles Through Optimization. In *Proceedings of the 8th Annual Conference on Genetic and Evolutionary Computation (GECCO '06)*, pages 1629–1636, New York, NY, USA, 2006. ACM.

[162] S. Bandaru and K. Deb. Automating Discovery of innovative design principles through optimization. Technical report, Indian Institute of Technology Kanpur, 2010.

[163] S. Bandaru and K. Deb. Towards Automating the Discovery of Certain Innovative Design Principles Through a Clustering-based Optimization Technique. *Engineering Optimization*, pages 1–31, 2011.

[164] R. Datta and K. Deb. A Classical-cum-Evolutionary Multi-objective Optimization for Optimal Machining Parameters. In *Proceedings of the World Congress on Nature Biologically Inspired Computing (NaBIC 2009)*, pages 607–612, 2009.

[165] J. Friedman. Multivariate Adaptive Regression Splines. *The Annals of Statistics*, 19(1):1–67, 1991.

[166] R. Gehling. Uniform Operating Limitations for High-speed Craft. In *Proceedings of the Pacific 2010 International Maritime Conference (Pacific 2010)*, Sydney, Australia, 2010.

Appendix A

Design Guidelines for Selection of Vertical Acceleration

In 1993, Savitky and Koelbel [2] presented a design guideline for selection of appropriate vertical impact acceleration for hard chine planing craft. The guideline is still relevant and used in determining uniform operating limitations for high speed craft by the International Code of Safety for High-Speed Craft (HSC Code) 2006 committee [166]. Shown in Table A.1 is the general design guidelines for selection of vertical impact acceleration reproduced from the work of Savitsky and Koelbel [2].

Table A.1: Design guidelines for selection of vertical acceleration

Vertical Acceleration (g)	Effects on Personnel	Application for Structural Design
0.6	Minor discomfort	Craft for fare paying passenger transport
1.0	Maximum for military function, long term (over 4 hours)	
1.5	Maximum for military function, short duration (1-2 hours)	
2.0	Test discontinued	Patrol boat crews and average owners
3.0	Extreme discomfort	Test crews, tournament sportfishermen, long races
4.0		Medium length races
5.0	Physical injury	Race boat drivers, short races
6.0		Military crew under fire